R-600 (Volume I of IV)

CONTROL, GUIDANCE, AND NAVIGATION FOR ADVANCED MANNED MISSIONS

(Final Report on Task II of Contract NAS-9-6823)

VOL I   SYSTEMS

JANUARY 1968

INSTRUMENTATION LABORATORY

MASSACHUSETTS   INSTITUTE   OF   TECHNOLOGY

Cambridge   39,   Mass.

R-600

CONTROL, GUIDANCE, AND NAVIGATION FOR ADVANCED MANNED MISSIONS

(Final Report on Task II of Contract NAS-9-6523)

VOL. I SYSTEMS

JANUARY 1968

INSTRUMENTATION LABORATORY
MASSACHUSETTS INSTITUTE OF TECHNOLOGY
CAMBRIDGE, MASSACHUSETTS

Approved: _____ Date: 16 Jan '68
JAMES H. FLANDERS, DIRECTOR, ADVANCED CG&N
APOLLO GUIDANCE AND NAVIGATION PROGRAM

Approved: _____ Date: 18 Jan 68
DAVID G. HOAG, DIRECTOR
APOLLO GUIDANCE AND NAVIGATION PROGRAM

Approved: _____ Date: 18 Jan 68
RALPH R. RAGAN, DEPUTY DIRECTOR
INSTRUMENTATION LABORATORY

ACKNOWLEDGEMENT

Systems, Volume I, is the work of the following authors:

Chapter I   James H. Flanders
                 Dr. Donald C. Fraser
                 Frederic D. Grant
                 John R. Lawson
                 Raymond H. Morth

Chapter 2   Philip N. Bowditch
                 Robert Crisp
                 James Corrigan
                 Jerold P. Gilmore
                 Dr. Albert L. Hopkins
                 Warren Jenkins
                 John Lawson
                 Dr. James S. Miller

Chapter 3   James H. Flanders, et. al.

The publication of this report does not constitute approval by the National Aeronautics and Space Administration of the findings or the conclusions contained therein. It is published only for the exchange and stimulation of ideas.

R-600

CONTROL, GUIDANCE AND NAVIGATION FOR ADVANCED MANNED MISSIONS

(Final Report on Task II of Contract NAS-9-6823)

ABSTRACT

This is a study of Navigation, Guidance, and Control for Advanced Manned Space Missions. It is divided into the areas of systems, computer subsystems, radiation subsystems, and inertial subsystems. From a system aspect a study is made of guidance and navigation requirements imposed by the different phases of interplanetary missions. A representative system is described as a design model. Detailed descriptions are provided of analytical and development work on advanced concepts in computer, radiation, and inertial subsystems.

It is shown that required system performance advances are well within reason but that the requirements for reliability will demand new standards in design concepts, quality assurance, maintainability, and quiescent failure rates.

Guidelines for further developments in this direction are set forth.

January 1968

TABLE OF CONTENTS

TABLE OF CONTENTS (Cont'd)

INTRODUCTION

This is a Final Report on Advanced Manned Missions Guidance and Control Systems Study, NASA Contract NAS 9-6823. This contract was let to the Instrumentation Laboratory of MIT on February 20, 1967. As set forth in the work statement, the study objective was summarized in the following sentence:

> The objective of this study is to develop and demonstrate via laboratory tests, advanced guidance and control techniques which, for future manned missions, will minimize spacecraft constraints, enhance mission flexibility, and eliminate the mission-time dependency of guidance and control system reliability, while maintaining adequate performance to accomplish the required missions.

To approach this objective, the study was organized into four major task areas: Systems integration, Computer Design, Optical Systems, and Inertial Sensors.

This study effort has been conducted in an environment of emerging mission and system requirements definition. For example, concurrent work on manned flyby missions was conducted by the Space Division of North American Rockwell under contract No. NAS 8-18025. The final report resulting from this study became available in August, 1967. A study of a manned Mars landing mission was undertaken by the Boeing Co., Aerospace Group under a similar NASA contract. These studies were in progress during the period covered by the MIT/IL contract.

It was the objective of the study and development to achieve a general enhancement of subsystems needed to meet the demands of advanced manned missions. But a definition of these demands had to be related to the emerging results of such studies as are cited above, without becoming keyed to a particular mission or class of missions. Consequently, work on the contract in its early phases concentrated on aspects of computer, inertial and optical sybsystem characteristics which seemed obviously important based on the general problems of advanced manned missions. These aspects were highlighted in the Work Statement and included:

a. longer operational reliable lifetime

b. greater operational flexibility

c. lower demand on electrical and thermal sybsystems

d. minimum constraints on spacecraft maneuvers or attitudes.

Selection of important problems was immeasurably aided by the experience of the MIT Instrumentation Laboratory in the design and development of the Control, Guidance, and Navigation System for NASA's Apollo Mission. This experience has covered both hardware and software responsibilities. As a result, MIT/IL personnel working on this task were able to bring to it a fund of applicable experience and knowledge which proved to be very beneficial.

Later in the contract period, more definition of mission and system requirements became available. At this stage, it became possible to approach consideration of the systems integration problem by a study of requirements for navigation, guidance, and control systems. This study attempted to evaluate required navigation and guidance performance levels without being tied too closely to one mission concept. Analysis of requirements, then, expanded its scope as a better understanding of overall mission became available. However, a definitive statement of requirements can come only after a specific mission and spacecraft system has been adopted. Such a statement is not a part of this report.

In summary then, this report includes a first section, Analysis of Requirements and a second on Design Studies and Development Hardware. The first will establish broad guidelines for the requirements task, and the second will present a system design model, and a detailed exposition of design and development accomplishments in the specific computer, optical, and inertial subsystem areas.

The computer, optical, and inertial subsystem portions have been bound separately to provide specialized documents for those with specialized interests.

1. ANALYSIS OF REQUIREMENTS

The requirements placed upon control, guidance, and navigation systems for advanced manned missions can be generated only as fast as the missions themselves are defined. The present contractual effort covered a study effort of approximately ten months. During this short period, it was possible to investigate only certain highlights of proposed manned missions that may be part of the national space program in the last third of this century. These highlights are reported on in this Chapter, and are limited to manned exploration of the inner planets of our Solar System. It will be apparent from the following material, that the studies basically covered many different mission phases briefly, in order to get a general picture of the nature of the problem. Detailed phase-by-phase analysis of specific missions is yet to come.

1.1 Orbital Operations - The Space Station and the Logistics Vehicles

One next step in advanced manned missions will certainly be long duration earth orbital operations culminating in the establishment of a space station. The space station's mission will not have demanding guidance and navigation requirements. Modest attention will have to be paid to the maintenance of the desired equilibrium orbit and to attitude control of the space station with respect to the earth and to the sun.

The space station can be mentioned here principally for the contributions it can make to checkout of advanced hardware and software. Inertial subsystems would benefit from extended checkout in a space station, not from the standpoint of performance evaluation, but from the data gained about reliability, maintainability, and ability to cope with environmental conditions of prolonged free fall. Computer subsystem elements could go through a similar qualification program in a space station and "pay their passage" by containing operational software for onboard operations such as attitude control and data processing. Finally, advanced optical subsystems would benefit tremendously from an installation period on a space station. Besides gaining data on reliability, maintainability and environmental design from such an installation, it would be possible to conduct a program of performance evaluation even though the earth atmosphere below would have different characteristics than planetary atmospheres. In conclusion, the earth orbital space station is viewed as a mandatory qualification facility for the type of hardware and software discussed in the four volumes of this report.

Earth orbital operations of interplanetary mission modules will also play a significant role as qualification missions for system and vehicle elements of future manned missions. The ability of crew and systems to function for months

on end in a free-fall environment will be tested in earth orbit. In this situation many problems of environmental and operational stress on men and systems can be investigated in relative safety. Emergency return to earth will be provided for. Repair and resupply can be arranged for in a few days.

The role of earth orbital operations in advanced manned missions and the use of logistics vehicles are discussed here for the sake of completeness. The size of vehicles required for interplanetary missions is so great that currently conceived boosters cannot launch a complete interplanetary vehicle into a trans-planetary orbit from a ground launch. The necessary mass in earth orbit is obtained by multiple launches of vehicle elements from the ground using boosters of the up-rated Saturn V capability. The interplanetary departure vehicle is then assembled and checked out in Earth orbit by a crew which may be different from the crew which will go on the mission itself. Obviously, such a plan of operations depends on multiple launches of boosters into orbit and multiple trips of orbital logistics vehicles shuttling men and materials back and forth from the scene of assembly and checkout operations.

These logistics missions do not represent a major challenge in navigation, guidance, or control beyond what has been demonstrated today. The logistics vehicle mission consists of orbital insertion, rendezvous and docking, deboost, atmospheric entry, and landing. Orbital insertion is currently a guidance function of the booster stage. The logistics vehicle system could be designed to perform the boost guidance function. If future developments prodice an orbital supply system where the boosters are not re-usable, then economic factors might well justify providing primary booster guidance from the logistics vehicle system. Such capability exists potentially in the early Apollo systems, although this capability is presently used only as a boost phase monitor.

The other mission phases of the logistics vehicle duplicate substantially what was proven in the Gemini missions and what now exist as Apollo mission requirements on navigation, guidance, and control. Rendezvous- and-docking and deboost and atmospheric entry are capabilities that have been thoroughly demonstrated already. Entry velocities from earth orbit are less critical than the lunar return velocities of the Apollo Mission which were successfully simulated on the Apollo 4 (AS-501) Flight in November, 1967.

The landing phase of the orbital logistics vehicle may/will place additional requirements on the on-board system, if a touchdown at pre-pared sites on land is desired. These additional requirements start to merge

with those of aircraft inertial systems. Basic to such a requirement is a specif-
ication on the required inertial accuracy in the terminal area, the weather min-
imums postulated, and the willingness to equip the orbital logistics vehicle with
sensor systems for external navigation and landing aids.

The next section discusses requirements for manned interplanetary mis-
sions which, unlike earth orbital operations, create a new magnitude of technolog-
ical problems in the area of control, guidance and navigation.

1.2 Manned Interplanetary Mission

1.2.1 Study Intent and Scope

This section describes the analytical effort which was undertaken
with the objective of defining the navigation and guidance requirements for
a manned interplanetary mission. The basic ground rules for this study
were that the navigation and guidance would be performed by an entirely
self-contained stellar-inertial system and that no very-low-thrust engines
(e.g. ion engines) would be used. Within this framework a statistical
error analysis was performed in order to identify the critical parameters
and to evaluate the requirements which must be placed upon the various op-
tical and inertial components.

The interplanetary mission was studied in four phases: transplane-
tary injection from earth orbit, interplanetary or midcourse phase, oper-
ation within the sphere of influence of a near planet, and earth entry after
returning from an interplanetary mission. Each of these phases is dis-
cussed separately below. A description of the methods used to perform the
error analysis in each phase is presented, followed in each case by a dis-
cussion of the results obtained.

In all phases, the error analysis was performed by considering the
statistics of first order deviations from a reference trajectory; thus all
the convenient techniques of linear filter theory could be applied to the
problem. Mission opportunities were selected from those discussed in
references 1 to 3. Launch dates and leg duration information were ex-
tracted from these sources and used as input to a digital computer program
which generated reference trajectory data in sufficient detail for use in the
error analysis programs. The procedure here was to use the launch data
and time of flight information together with a Fourier-Bessel series ex-
pansion of the planetary orbits[4] to obtain the position and velocity vectors
of the departure and destination planets for each leg of the interplanetary trip.

This provided the input necessary to solve Lambert's problem for each leg of the trip using a universal variable technique formulated by Battin [5]. The solution to this two-body problem (sun-spacecraft) provided conic sections to be used as reference trajectories for the interplanetary legs. For the flyby trips, near-planet hyperbolae were determined from the inbound and outbound relative velocity vectors (obtained from the solution to the interplanetary legs) using the near planet as the primary gravitational source. If any trip involved a negative minimum passing distance at any planet it was automatically rejected and an iteration on passing distance was begun to remedy this situation.

1.2.2 Mission Phases

1.2.2.1 Transplanetary Injection

A statistical error analysis of the injection into an interplanetary path from an earth orbit was performed in order to defire the demands upon the inertial subsystem during this phase of operation. A strapped down inertial measurement unit was assumed and no externally derived information was used during the turn.

The reference trajectory was generated in each case using the required velocity concept together with a cross product steering law [4, 6]. This was implemented with a modified version of a computer program which was originally written for the Apollo translunar injection by Mr. Peter Philliou of the MIT Instrumentation Laboratory [7]. The required velocity is defined as that velocity which will cause the vehicle to arrive at a specified time at a preselected inertial target and is computed as a solution to a Lambert problem.

No effort was made in this study to optimize either the guidance or targeting schemes. The criterion for an acceptable scheme was that the resulting burn time should be reasonable and that the objective of defining the sensitivity of position and velocity errors to individual inertial component errors should not be affected to first order by minor changes in the reference trajectory. All data necessary to characterize the vehicle and engine was extracted from references 1 and 2.

The inertial component error model used is described in detail in Volume IV, Chapter 2 of this report. The basic error sources in this model combine to cause two types of error. One is the angular misalignment of the computed inertial reference frame with respect to the desired

reference and the other is the error in indicated specific force which would result even if the two frames were perfectly aligned. Specifically, each component is described by:

$$\epsilon(t) = \epsilon_{opt} + \epsilon_{mech} + NBD\ (t_p + t)$$
$$+ ADOA \int_0^t a(\tau)\ d\tau$$

$$a_I(t) - a(t) = a_b + \Delta SF\ a(t) \qquad (\text{ thrust axis })$$

$$a_I(t) - a(t) = a_b + \epsilon\ a(t) \qquad (\text{ cross axes })$$

where:

$\epsilon(t)$	=	angular misalignment of the two inertial coordinate frames
ϵ_{opt}	=	angular error introduced when optically aligning the accelerometers with respect to the inertial reference frame
ϵ_{mech}	=	angular error introduced by improper mechanical alignment of the accelerometers on the body
NBD	=	non-compensated bias drift of the appropriate gyro
t_p	=	time before t=0 the unit was aligned
ADOA	=	acceleration sensitive drift about the output axis of the appropriate gyro
$a(t)$	=	actual acceleration
$a_I(t)$	=	indicated acceleration
a_b	=	accelerometer bias
ΔSF	=	accelerometer scale factor error

We can write the three dimensional error model in a more convenient form by assuming that the X body axis is along the thrust direction and by making the following definitions:

$$\underline{\gamma}^T = \left[\underline{\gamma}_{AL}^T,\ \underline{\gamma}_{DR}^T,\ \underline{\gamma}_B^T,\ \underline{\gamma}_{SF}^T,\ \underline{\gamma}_{ADOA}^T \right]$$

$$M_I = \left[M_{AL},\ M_{DR},\ M_B,\ M_{SF},\ M_{ADOA} \right]$$

$$M_{AL} = \begin{bmatrix} 0 & 0 & 0 \\ 0 & 0 & a(t) \\ 0 & -a(t) & 0 \end{bmatrix} \qquad M_{DR} = (t + t_p) \, M_{AL}$$

$$M_B = 3 \times 3 \quad \text{Identity Matrix} \qquad M_{SF} = \begin{bmatrix} a(t) & 0 & 0 \\ 0 & 0 & 0 \\ 0 & 0 & 0 \end{bmatrix}$$

$$M_{ADOA} = M_{AL}(t) \int_0^t a(t) \, dt$$

where:

$\mathcal{X}_{AL}$ = a vector of the sum of the values of ϵ_{opt} and ϵ_{mech} for each axis

$\mathcal{X}_{DR}$ = 3 vector consisting of the NBD value for each axis

$\mathcal{X}_B$ = 3 vector consisting of the a_b value for each axis

$\mathcal{X}_{SF}$ = 3 vector consisting of the ΔSF value for each axis

$\mathcal{X}_{ADOA}$ = 3 vector consisting of the ADOA value for each axis

In these terms the error in indicated specific force is given by the product of the 3x15 rotation matrix M with the 15 vector $\mathcal{X}$:

$$\underline{e}_I = M_I \underline{\mathcal{X}}$$

It can be shown[8] that the 6x6 covariance matrix of position and velocity estimation errors (P) for this case obeys the differential equation.

$$\dot{P} = FP + PF^T + MC^T + CM^T$$

where M is a 6x15 matrix whose first 3 rows are zero and whose last three rows contain the elements of M_I. The 6x15 correlation matrix C, which arises because the inertial component errors at one time are correlated with themselves at other times*, obeys the differential equation:

$$\dot{C} = FC + M \Gamma$$

where $\Gamma = \overline{\mathcal{X} \, \mathcal{X}^T}$

The 6x6 matrix F is the fundamental matrix of the linear perturbation equation which describes the position and velocity estimation errors. The computation of this matrix is discussed in detail by Battin[4]. The initial value of P is set by the uncertainties in position and velocity which exist in earth orbit just prior to engine ignition. If one assumes that the initial state vector for injection has been supplied solely from ground tracking such that the initial error vector is uncorrelated with IMU errors,

---

*They have the form of a time varying bias, hence are a correlated or colored driving noise.

C is the null matrix initially.

Table 1.2-1 and figures 1.2-1 through 1.2-6 summarize the results of a survey of the errors which result during an injection of a vehicle characterized by:

Exhaust Velocity	=	27,400 feet per second
Thrust	=	600,000 pounds
Initial Weight	=	2,313,760 pounds
Mass Flow Rate	=	705 pounds per second

The total velocity change was 19149 feet per second and the burn time was 2302 seconds.

The position and velocity errors which result at any given time due to any of the inertial component parameters are essentially a linear function of that parameter. Table 1.2-1 presents the slopes of these straight lines at the end of the burn for each of the error sources in the IMU model. This same linear property applies to the trace of the initial covariance matrix. An initial isotropic RMS position error of 0.04 miles combined with an initial isotropic RMS velocity error of 0.17 feet per second leads to an RMS position error of 0.18 miles and an RMS velocity error of 0.59 feet per second at burnout with a perfect IMU. Ten times these initial values leads to an RMS error which is ten times larger; one tenth smaller initial conditions lead to one tenth smaller error at burnout. Figures 1.2-1 through 1.2-6 illustrate the growth curves of the RMS position and velocity errors for each of the sources. Figure 1.2-7 presents the growth curves for the model injection under study.

The following is a best guess at the instrument performance that may be anticipated in the mid-1970 time frame.

Initial RMS Postion Error	=	0.04 miles
Initial RMS Velocity Error	=	0.18 fps
Accelerometer Bias	=	0.1 cm/sec^2
Accelerometer Scale Factor Error	=	50 ppm
NBD	=	1.5 meru
Prealign Time	=	1 hour
ADOA	=	1 meru/g
Optical Misalignment	=	60 arc seconds
Mechanical Misalignment	=	20 arc seconds

RMS VELOCITY UNCERTAINTY (FT/SEC PER CM/SEC²)

RMS POSITION UNCERTAINTY (MILES PER CM/SEC²)

BURN TIME (SECONDS)

POSITION

VELOCITY
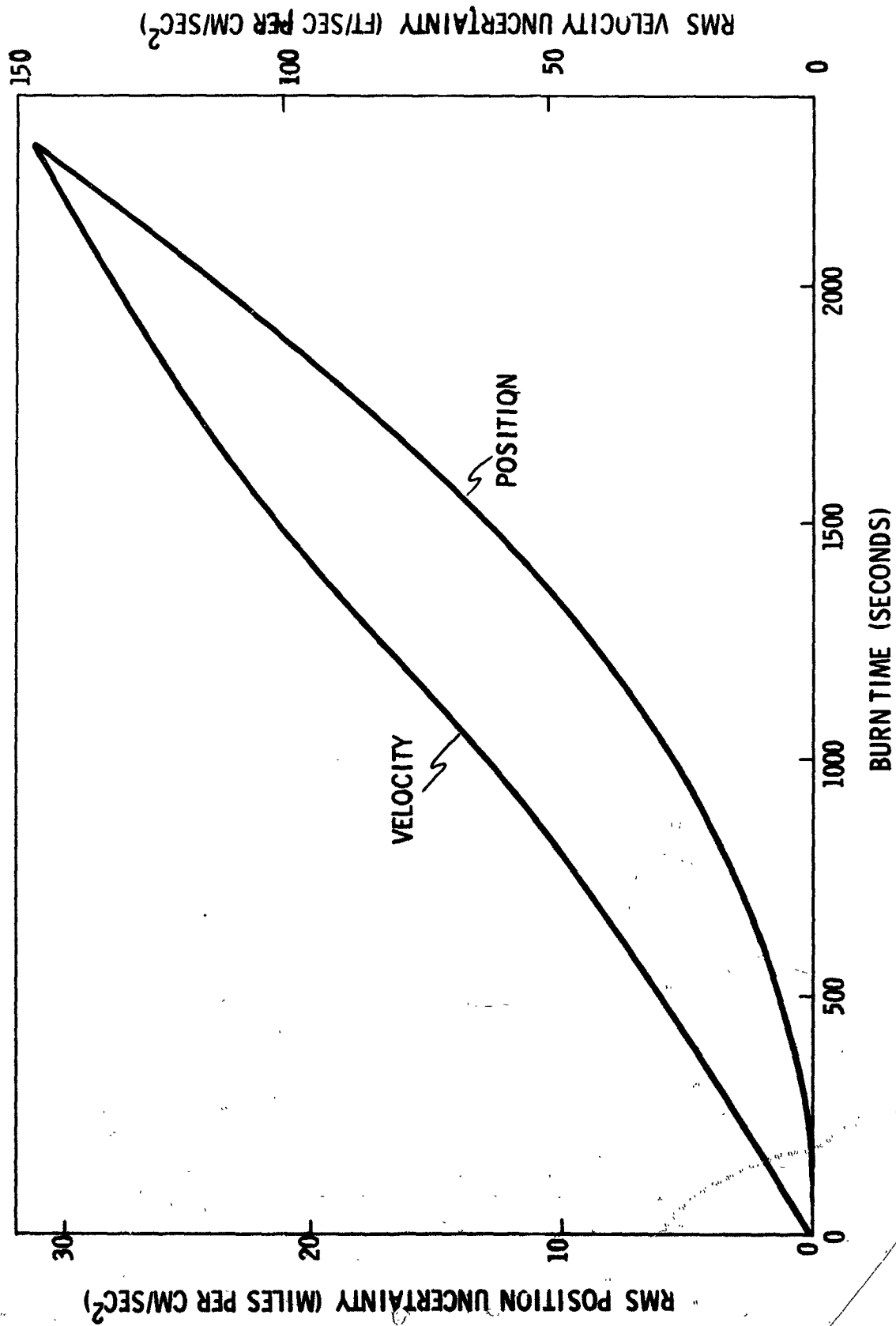
Fig. 1.2-1 Sensitivity To Accelerometer Bias.
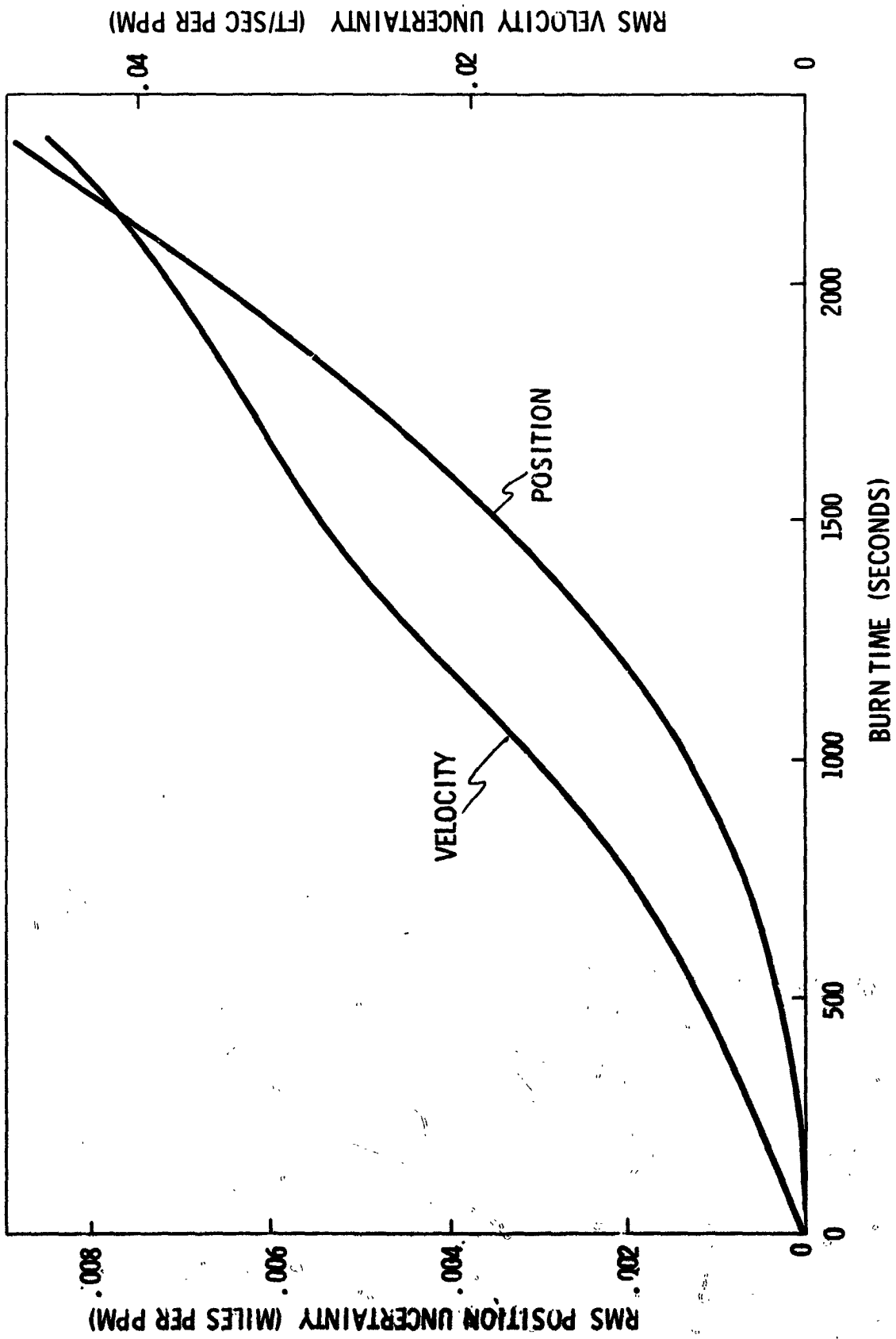
Fig. 1.2-2 Sensitivity to Accelerometer Scale Factor Errors

RMS VELOCITY UNCERTAINTY (FT/SEC PER PPM)

BURN TIME (SECONDS)

RMS POSITION UNCERTAINTY (MILES PER PPM)

POSITION

VELOCITY

RMS VELOCITY UNCERTAINTY (FT/SEC PER MERU)

RMS POSITION UNCERTAINTY (MILES PER MERU)

BURN TIME (SECONDS)
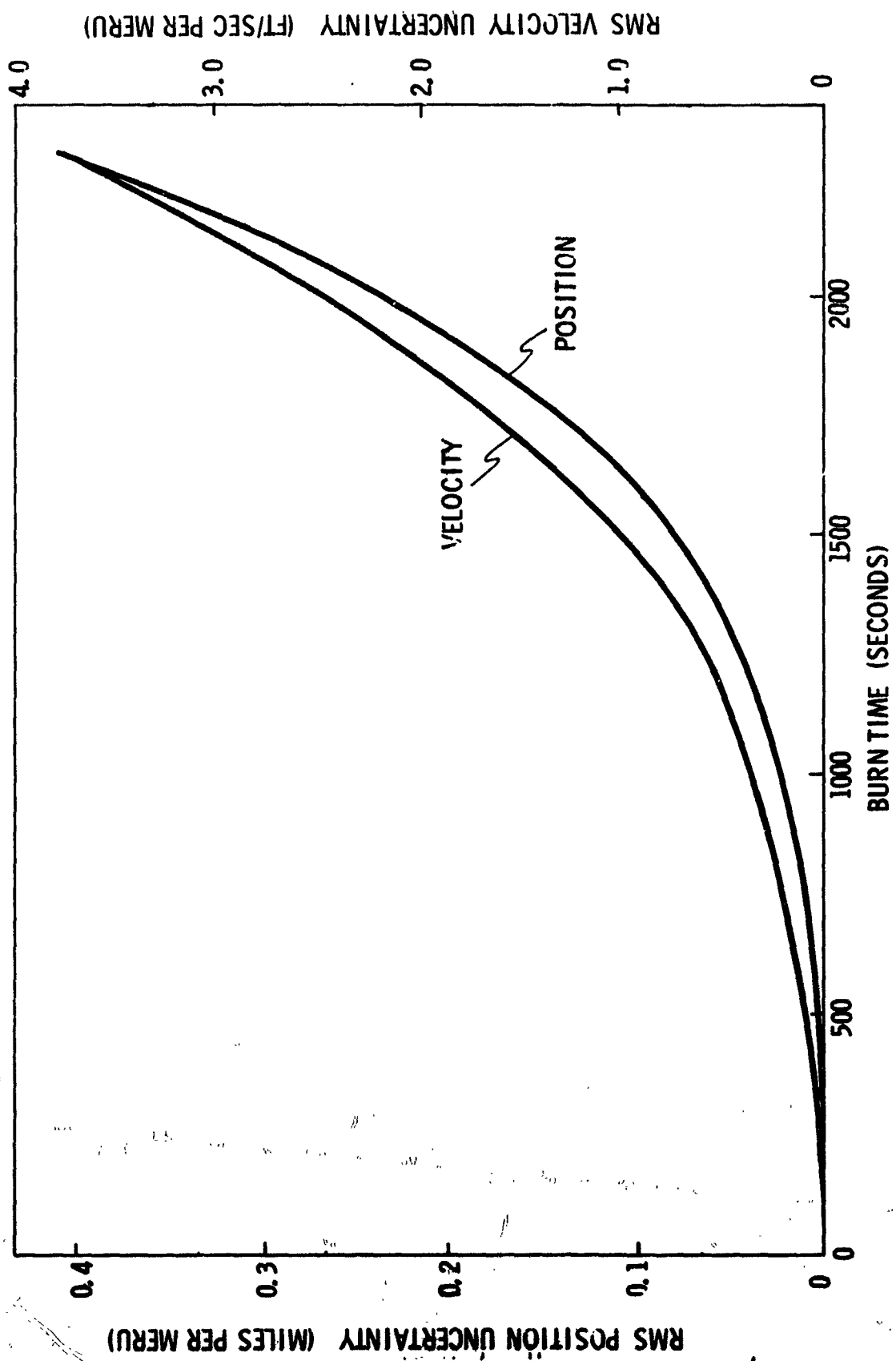
POSITION

VELOCITY

Fig. 1.2-3 Sensitivity to NBD; Prealign Time = 0

RMS VELOCITY UNCERTAINTY (MILES/MERU)

RMS POSITION UNCERTAINTY (MILES/MERU)

BURN TIME (SECONDS)
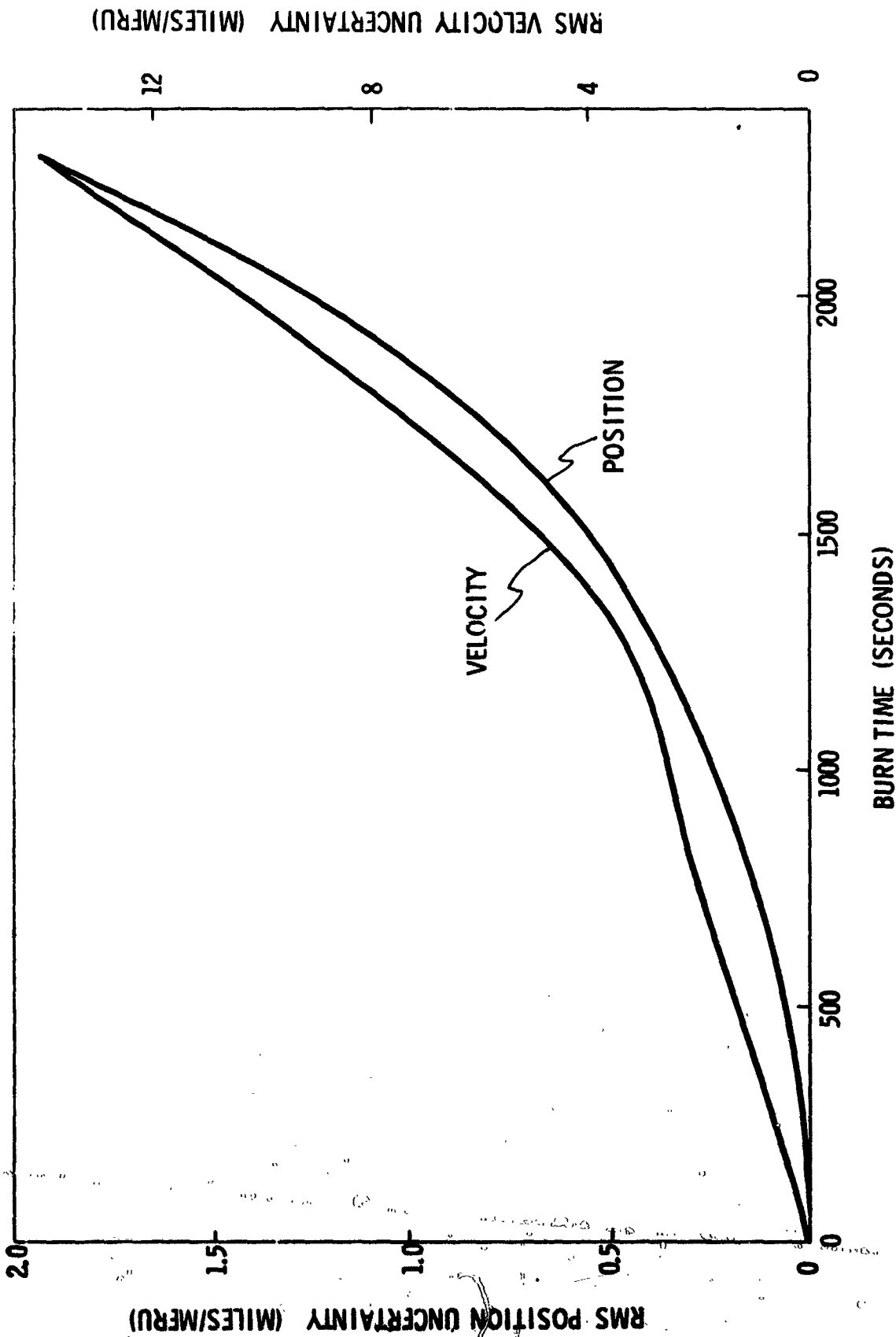
POSITION

VELOCITY

Fig. 1.2-4   Sensitivity to NBD: Prealign Time = 1 Hour.
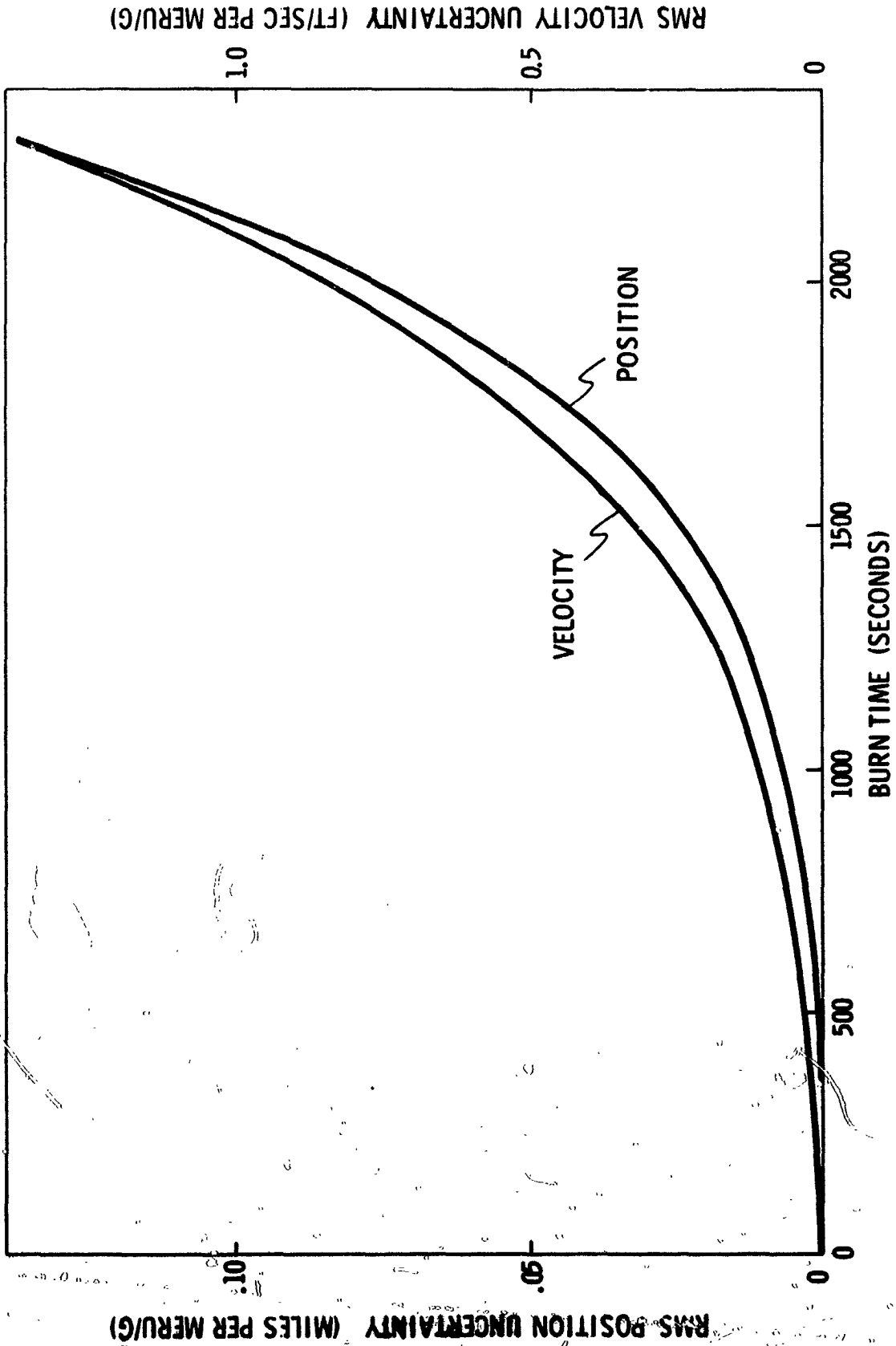
Fig. 1.2-5 Sensitivity to ADOA
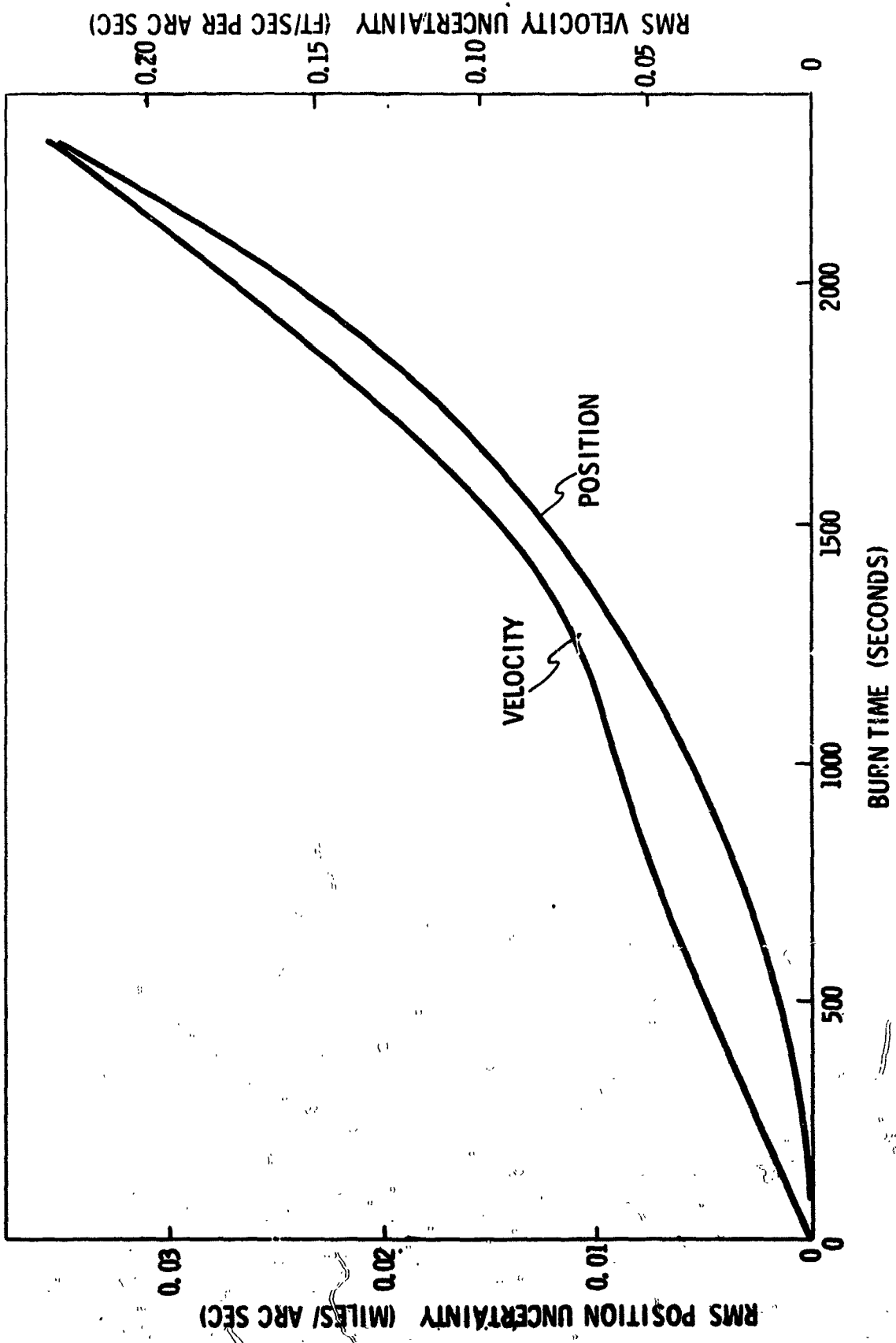
Fig. 1.2-6   Sensitivity to Initial Misalignment.
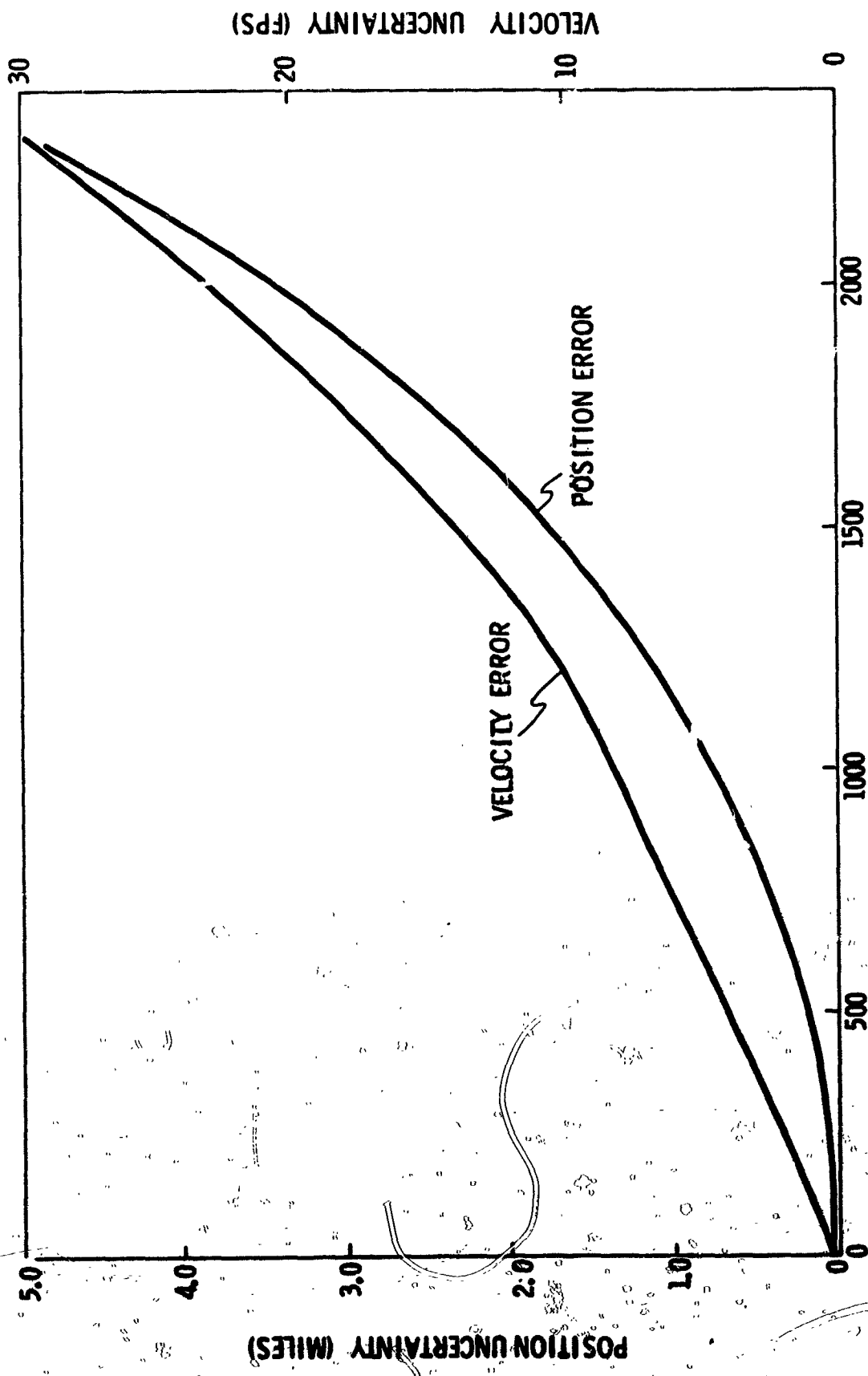
Fig. 1.2-7 Normalized Uncertainty Growth – All Error Sources Active.

Table 1.2-1

Sensitivity Coefficients at 2302 Seconds

SOURCE	POSITION ERROR SENSITIVITY	VELOCITY ERROR SENSITIVITY
Accelerometer Bias	31 miles/cm/sec^2	147 fps/cm/sec^2
Accelerometer Scale Factor Error	0.0089 miles/ppm	0.045 fps/ppn
NBD	0.41 miles/meru	3.8 fps/meru
NBD with 1 hour prealign time	1.94 miles/meru	14.2 fps/meru
ADOA	0.14 miles/meru/g	1.38 fps/meru/g
Initial Misalignment	0.035 miles/arc second	0.22 fps/arc second

Table 1.2-1 gives position and error sensitivity coefficients applicable to the reference transplanetary injection.

1.2.2.2 Midcourse

A statistical error analysis of the midcourse phase of an interplanetary mission was performed in order to assess the accuracy requirements which must be placed upon both the inertial equipment and the on-board optical systems. To accomplish this objective a general computer program was developed which could also perform a similar error analysis for both the flyby and orbital cases. This section includes a detailed description of the algorithms employed in this computer program, together with some typical results for the midcourse leg of an interplanetary trip. Figure 1.2-8 gives a flow chart of the major elements of the error analysis program.

Central to the understanding of the error analysis computation procedure is the fact that the mission under consideration is divided into a number of decision points. The frequency, spacing, and total number of these points is completely flexible and is specified at run time. At each point a decision is made as to whether or not to make a velocity correction and what measurement or measurements to take. If it is decided to implement a measurement or a velocity correction at any point, this is done.

The error analysis procedure begins with an initial state vector[*] and covariance matrix of position and velocity estimation errors. These could be the end result of a transplanetary injection or might be the terminal conditions from a previous error study of part of the same mission, although the program is capable of processing an entire mission at once, including changing gravitational centers. This latter restart capability has proved useful in the analysis of flyby missions.

These initial conditions are then extrapolated to the time of the first decision point under a two-body approximation to the free-fall situation. The state is extrapolated by solving Kepler's problem along the reference trajectory between the initial time and the time of first decision point. Sim-

---

[*]The state normally is six dimensional, consisting of the position and velocity components of the spacecraft in an ecliptic cartesian coordinate system with center either at the sun or one of the planets. An option is included to adjoin any planet diameter to the state, bringing the possible dimension to seven.
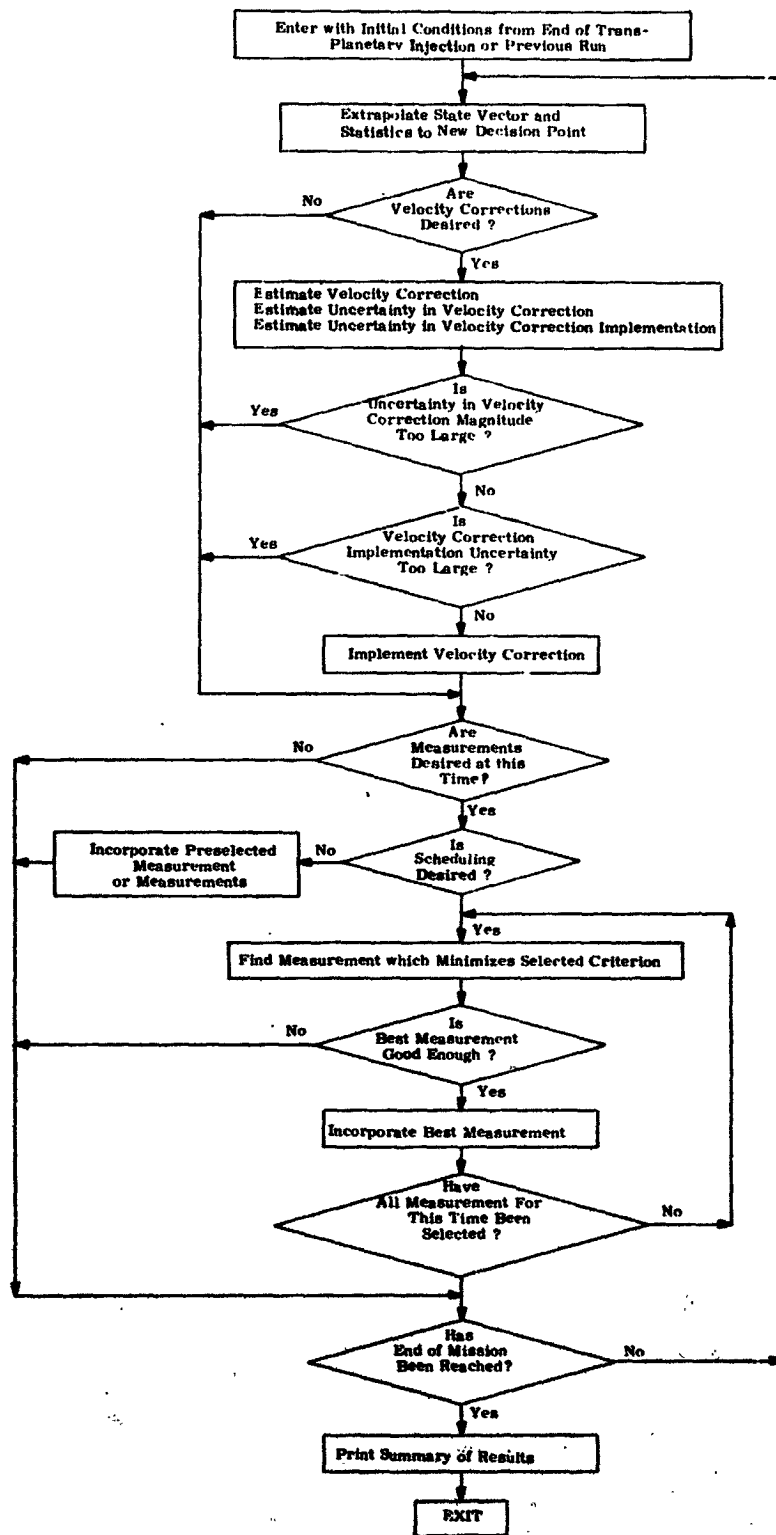
Fig. 1.2-8 Flow Diagram of General Error Analysis Program.

ultaneously, a set of partial derivatives are computed which can be used to generate the state transition matrix associated with the solution to the linear perturbation equations between these two times. All this is done using a solution to Kepler's problem developed by Battin [9]. A similar procedure has been published by Goodyear [10]. The covariance matrix is extrapolated according to the relationship:

$$P(t_1) = \Phi(t_1, t_0) \, P(t_0) \, \Phi^T(t_1, t_0)$$

where t_0 is the initial time, t_1 the time of the first decision point, and $\Phi(t_1, t_0)$ is the state transistion matrix.

Once the state and statistics have been extrapolated to the decision point, the mean squared value of the velocity correction which would be required at this time to cause the spacecraft to intersect the reference trajectory at a preassigned destination point is computed. The mean squared value of the error in the estimation of this velocity correction is also computed. Both computations are performed as outlined in reference 4.

The mean squared value of the error which might be expected in implementing the velocity correction at this time is then computed. This error consists of two parts. One is the tailoff uncertainty involved in shutting down the engine. This can be measured with the accelerometers but cannot be predicted ahead of time. The second is the implementation error caused by inertial component errors. In this statistical error analysis all directional information about the individual velocity corrections is lost because the noise sources and initial errors are assumed to have equal probability of being in any direction. Consequently the only guidance error sources of first order importance to the statistical analysis of those phases of the mission where the assumption of impulsive velocity corrections is reasonable, are those which affect the length of the velocity vector to first order. In terms of the model discussed in Volume IV, Chapter 2 of this report, these are accelerometer bias and accelerometer scale factor errors. The variance of the expected implementation error is thus computed in the following fashion.

$$\sigma^2_{imp} = \overline{\Delta SF^2} \ \overline{\Delta V^2} + \overline{a_b^2} \ \overline{\Delta t^2} + \overline{v_{go}^2}$$

where:

σ_{imp}^2 = variance of velocity correction implementation errors

$\overline{\Delta SF^2}$ = variance of accelerometer scale factor errors

$\overline{\Delta V^2}$ = mean squared value of the velocity correction

$\overline{a_b^2}$ = variance of accelerometer bias errors

Δt = duration of the velocity correction impulse

$\overline{v_{co}^2}$ = mean squared value of the error attributable to thrust tailoff uncertainties

  Two ratios are now formed. The first is the ratio of the mean squared uncertainty in estimation of the velocity correction to the mean squared velocity correction. The second is the ratio of the variance of implementation errors to the mean squared velocity correction. If both these are less than separate input criteria and the velocity correction option is active, the velocity correction is implemented.

  In a statistical sense the velocity correction is implemented by properly adjusting two covariance matrices. The first is the covariance matrix of state estimation errors (P) and the second is the covariance matrix of deviations from the reference trajectory (X). If we define:

$$\sigma_g^2 = \overline{\Delta SF^2}\ \overline{\Delta V^2} + \overline{a_b^2}\ \Delta t^2$$

we have:

$$P = P' + \frac{1}{\sqrt{3}}\begin{bmatrix} 0 & & & & \\ & 0 & & & \\ & & 0 & & \\ & & & \sigma_g^2 & \\ & & & & \sigma_g^2 \\ & & & & & \sigma_g^2 \end{bmatrix}$$

$$X = X' + \frac{1}{\sqrt{3}}\begin{bmatrix} 0 & & & & \\ & 0 & & & \\ & & 0 & & \\ & & & \sigma_{imp}^2 & \\ & & & & \sigma_{imp}^2 \\ & & & & & \sigma_{imp}^2 \end{bmatrix}$$

where the prime denotes the value of the matrix before the velocity correction. Note that the ability to measure the tailoff uncertainty causes less

error to be introduced into the estimation of the deviation from the reference than into the actual deviation. The spherical distribution of the velocity error permits the use of the convenient diagonal form in the additive terms.

Once the velocity correction decision has been made the program continues to the questions of whether to make a measurement at this time and what measurement to take. One of three options may be exercised at this point. The first is to not make a measurement at all. In this case the state and statistics are extrapolated to the next decision point and the entire process repeated. This option has proved useful in simulating the non zero-g environment of the North American-Rockwell spacecraft [1]. For periods of approximately two weeks while the spacecraft is spinning, it may not be possible to make navigation sightings. The second option is to incorporate a predetermined measurement or sequence of measurements. Once this is completed the state and statistics are extrapolated along the reference trajectory to the time of the next decision point. The third option is to enter the measurement selection process. This will now be described.

Of prime importance in the selection of the individual measurements is the criterion function used to select them. Four criteria were implemented in this program; they are all to be minimized:

1. the volume of the error ellipsoid,
2. the trace of the covariance matrix of estimation errors,
3. the length of the longest eigen-vector of the covariance matrix of estimation errors,
4. the mean squared position estimation error at a pre-selected target point (usually the destination point).

Suggestions for more work in this area are included in Chapter 3 of this volume.

The volume of the error ellipsoid of estimation errors was selected because of the ease with which it can be computed, thus effecting a saving in computer time. It can be shown [11] that the ratio of the volume of the covariance matrix after the measurement is incorporated to that before the measurement for an optimal linear filter is:

$$\frac{\text{Volume After}}{\text{Volume Before}} \qquad \frac{\sigma^2_{meas}}{\underline{h}^T P \underline{h} + \sigma^2_{meas}}$$

where:

σ^2_{meas} = variance of noise on the measurement

$\underline{h}$ = geometry vector which couples the measurement to the state vector

P' = covariance matrix of estimation errors before measurement incorporation

To avoid reducing the volume by shrinking an already small error, a check is made in the direction of each coordinate axis to determine if the error in one or more of these directions is much smaller than the others. If this occurs, these dimensions are eliminated from the measurement selection process. A better way to perform this check would be to do it in principle axes. This was not done because the time saving advantage of this criterion would be lost in computation of the rotation matrix.

In principal axes the covariance matrix is diagonal with its eigen-values displayed along this diagonal. Using this fact together with the following compact form of the covariance matrix update equation:

$$P = \left[I - P'\underline{h} \, (\underline{h}^T P' \underline{h} + \sigma^2_{meas})^{-1} \, \underline{h}^T \right] P'$$

one can show that the error in the direction of the largest eigenvector of P' is minimized by maximizing:

$$\frac{\lambda_i \, h_i^2}{\underline{h}^T P' \underline{h} + \sigma^2_{meas}}$$

where:

λ_i = largest eigenvalue of the covariance matrix

h_i = component of $\underline{h}$ in the direction of largest eigenvector

P' = covariance matrix before measurement incorporation

The largest eigenvalue may be found without computing the others by using a Bernoulli iteration to factor the characteristic polynomial of the matrix.

The procedure used to compute the mean squared position error at a preselected target point is to extrapolate the covariance matrix which results after incorporating a trial measurement forward to the time at which the vehicle will arrive at this target point on the reference trajectory. The

best measurement is that which minimizes the trace of the upper left 3x3 matrix of the resulting extrapolated covariance matrix. The procedure for obtaining this 3x3 matrix without computing the full 6x6 state transition matrix is outlined in detail in reference 4.

One of the above criteria is selected in any given computer run to select measurements. The measurements are chosen from one of the following six types:

1. Planet diameter
2. Planet-star (planet center to star)
3. Star occultation
4. Star-elevation (planet limb to star)
5. Sun-star
6. Unknown landmark

The possibility of using sun-planet measurements was eliminated because of the large uncertainty involved in defining the limb of both the sun and the planets. The first eight planets of the solar system and the 37 Apollo navigational stars[12] can be used for planets and stars. Planet position and velocity information is generated using a Fourier-Bessel series expansion of the planetary orbits[4].

A number of constraints are used to eliminate measurements which should be rejected for physical reasons. These include:

1. Two lines of sight farther apart than the optical instrument can permit.
2. Line of sight to a star too close to the line of sight to the sun.
3. Star behind the planet.
4. Line of sight to a star too close to the line of sight to the planet limb.
5. Line of sight to a planet edge too close to the line of sight to the sun. (Not made if the spacecraft is in the planet shadow).
6. Planet or star behind the sun.
7. Lines of sight to dark edges of planets are rejected in those cases where infrared equipment is not assumed.

Additional constraints for the cases of star occultation and unknown landmark are discussed in Volume III of this report.

The error associated with making each type of measurement is modeled as an appropriate combination of the basic instrument pointing error

and the uncertainty involved in defining a planet limb. Different numerical
values are used for each planet and for the dark and light edge sightings.
A thorough discussion of these models and the choice of numerical values
is presented in Volume III of this report.   A summary of the error model
for each measurement type is tabulated below:

Planet Diameter $\qquad \sigma^2_{meas} = \sigma^2_A + \sigma^2_B$

Planet-Star $\qquad \sigma^2_{meas} = \dfrac{\sigma^2_A \, \sigma^2_B}{\sigma^2_A + \sigma^2_B}$

Star Occultation $\qquad \sigma^2_{meas} =$ light edge phenomenon uncertainty

Star Elevation $\qquad \sigma^2_{meas} = \sigma^2_A$

Sun - Star $\qquad \sigma^2_{meas} = \dfrac{\sigma^2_A}{2}$

Unknown Landmark $\qquad \sigma^2_{meas} =$ predetermined fixed value

In these, σ^2_A and σ^2_B are associated with the two different lines of
sight to the near body involved in the measurement. They are the sum of the
instrument error variance and the appropriate (light or dark edge) phenom-
enon uncertainty for that near body:

$$\sigma^2_A, \; \sigma^2_B = \sigma^2_{inst} + \sigma^2_{phen}$$

Once the best measurement is found, it is incorporated if it gives a
sufficient reduction in the selection criterion. Once the required number of
measurements for this decision point have been selected and incorporated,
the state and statistics are extrapolated to the time of the next decision point
and the entire process is repeated.

The error studies which have been conducted   date of this
writing are based upon two missions. These are a   Mars twilight
flyby and a 1977 triple planet flyby. Both are described   references 1 and
3. Many parametric surveys were made. A sample of the results obtained
for the midcourse legs will now be presented here. More results may be
found in Volume III of this report.

Figures 1.2-9 to 1.2-11 deal with the first leg of the 1979 Mars
twilight mission. Figure 1.2-9 displays the sensitivity of RMS position
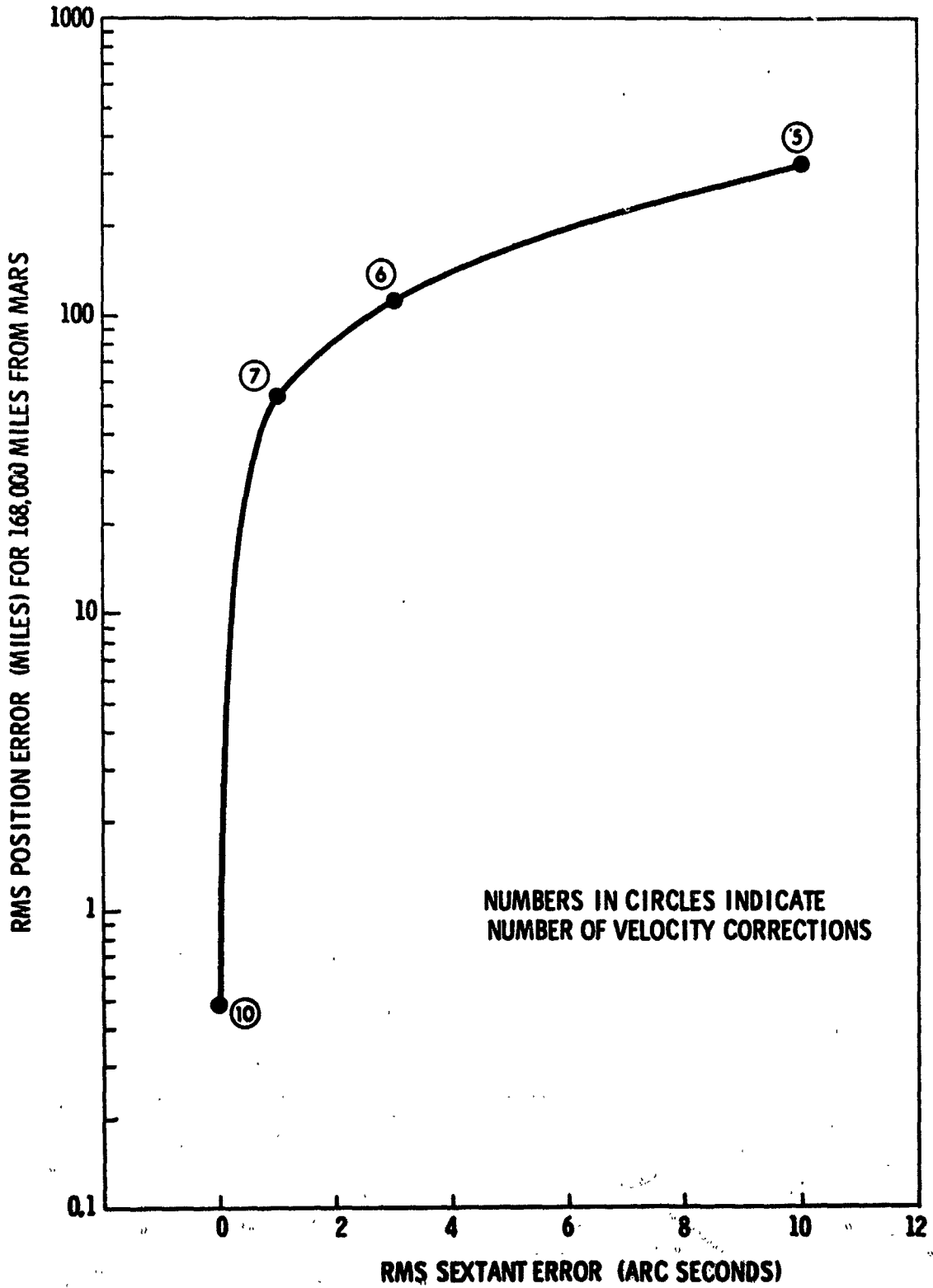
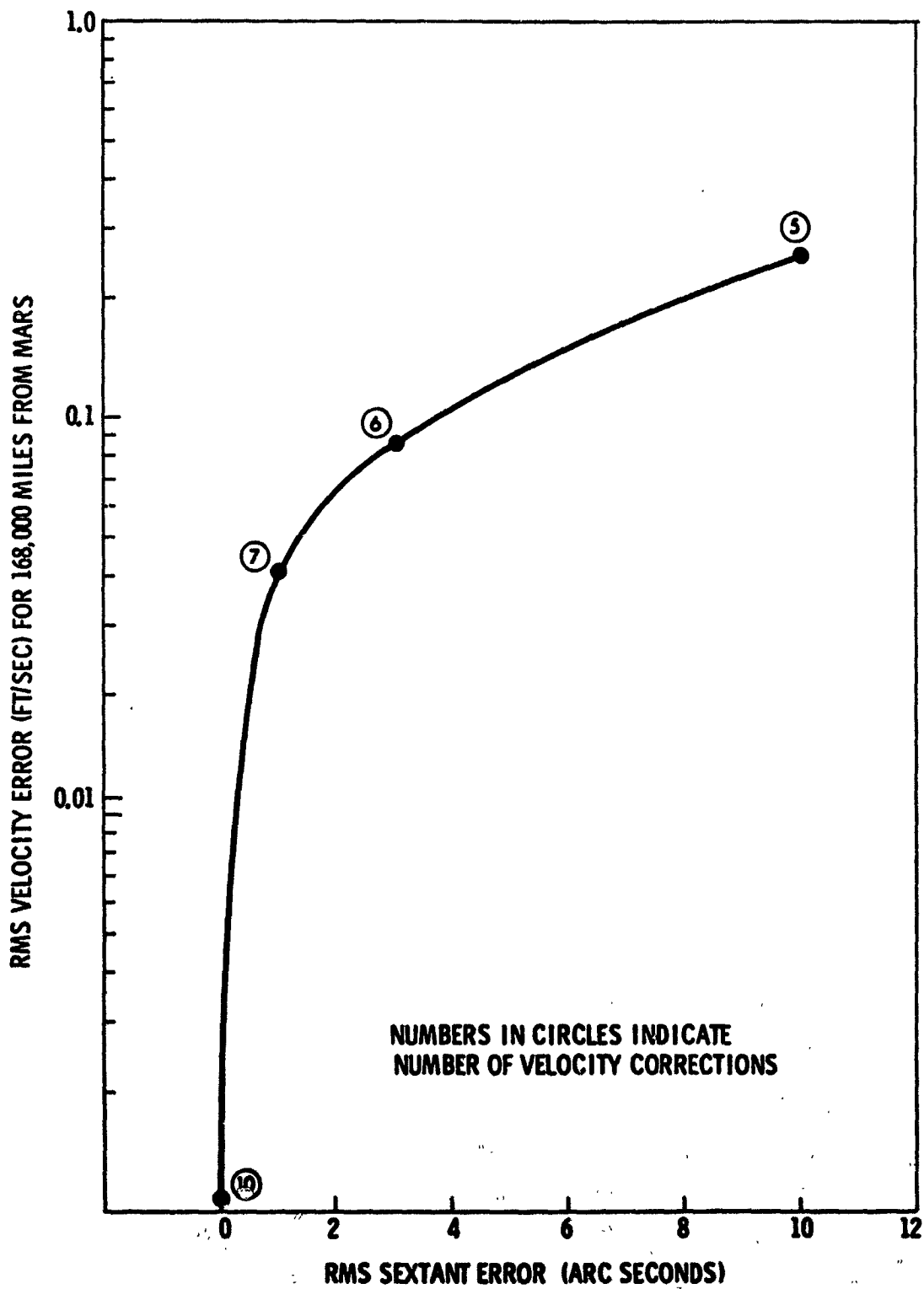Fig. 1.2-9   Sextant Error Effect on Position Errors.

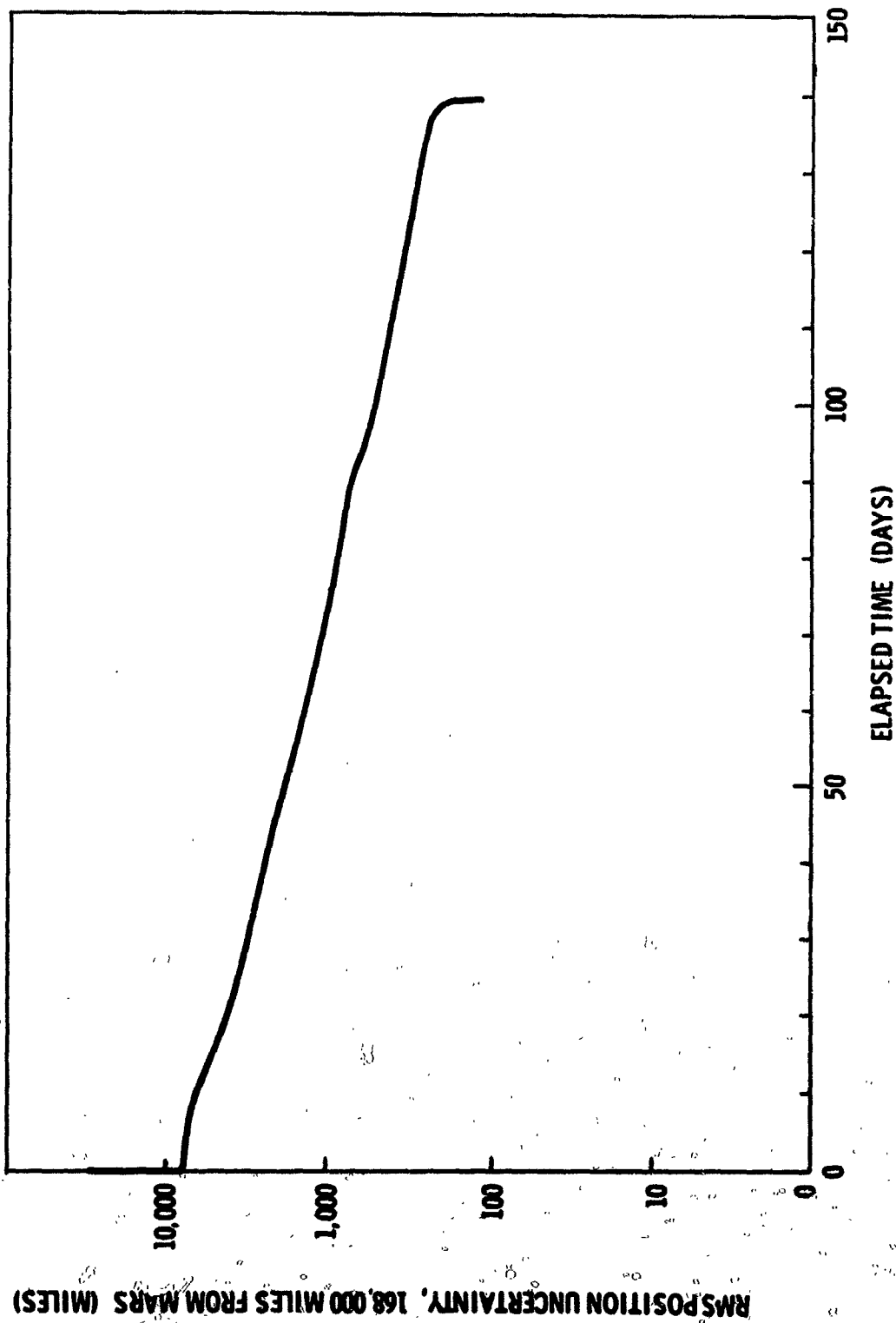Fig. 1.2-10   Sextant Error Effect on Velocity Error.

Fig. 1.2-11 Time History of Terminal RMS Position Error for Arc Second Sextant.

ELAPSED TIME (DAYS)

RMS POSITION UNCERTAINTY, 168,000 MILES FROM MARS (MILES)

errors at a target point 168,000 miles from the center of Mars to sextant pointing errors. These results were computed using the terminal RMS position error as the measurement selection criterion. Figure 1.2-10 is a presentation of the associated RMS velocity estimation error for the same leg. Figure 1.2-11 illustrates the time history of these position estimation errors. This figure displays the RMS terminal position estimation error which would result if all action were ceased at the time of the data point. A 3 arc second sextant was used in this case. Figures 1.2-12 and 1.2-13 are for the first leg of the 1977 triple planet flyby. They correspond to Figures 1.2-9 and 1.2-10.

Together these five figures display two items of general interest. The first is that the errors which result at the end of an interplanetary leg are quite sensitive to sextant accuracy. The second, which is illustrated by Figure 1.2-11, is that the periods near the departure and destination planets are the regions of highest information rate. This is because strong measurements are being taken using the near planets in these regions.

The terminal errors for these interplanetary legs are essentially independent of the various phenomenon errors. The reason for this is that at large ranges the additional angular uncertainty due to inability to clearly define a planet limb is insignificant compared to the sextant pointing error. Sextant inaccuracies dominate the errors during interplanetary legs.

Several runs were made to compare the various criteria for selecting measurements. All but minimizing the error in the direction of the largest eigenvector were run. The IBM 360-75 computation time required for each of the other three for a 173 decision point trip from Earth to Mars was as follows:

Volume Criterion	=	1.745 minutes
Trace Criterion	=	2.637 minutes
Terminal Error Criterion	=	2.916 minutes

which indicates that the volume criterion, as expected, is noticeably faster than the others. Unfortunately, the principal axes of the covariance matrix do not rotate fast enough during this phase to enable the dimension reduction algorithm to prevent reduction of the volume by reducing an already small uncertainty. The trace and terminal position error costs give almost the same terminal position error; the velocity error is smaller, however, when the terminal error cost is used.

Figures 1.2-14 and 1.2-15 deal with the first leg of the 1979 Mars twilight flyby. They demonstrate that the position and velocity estimation
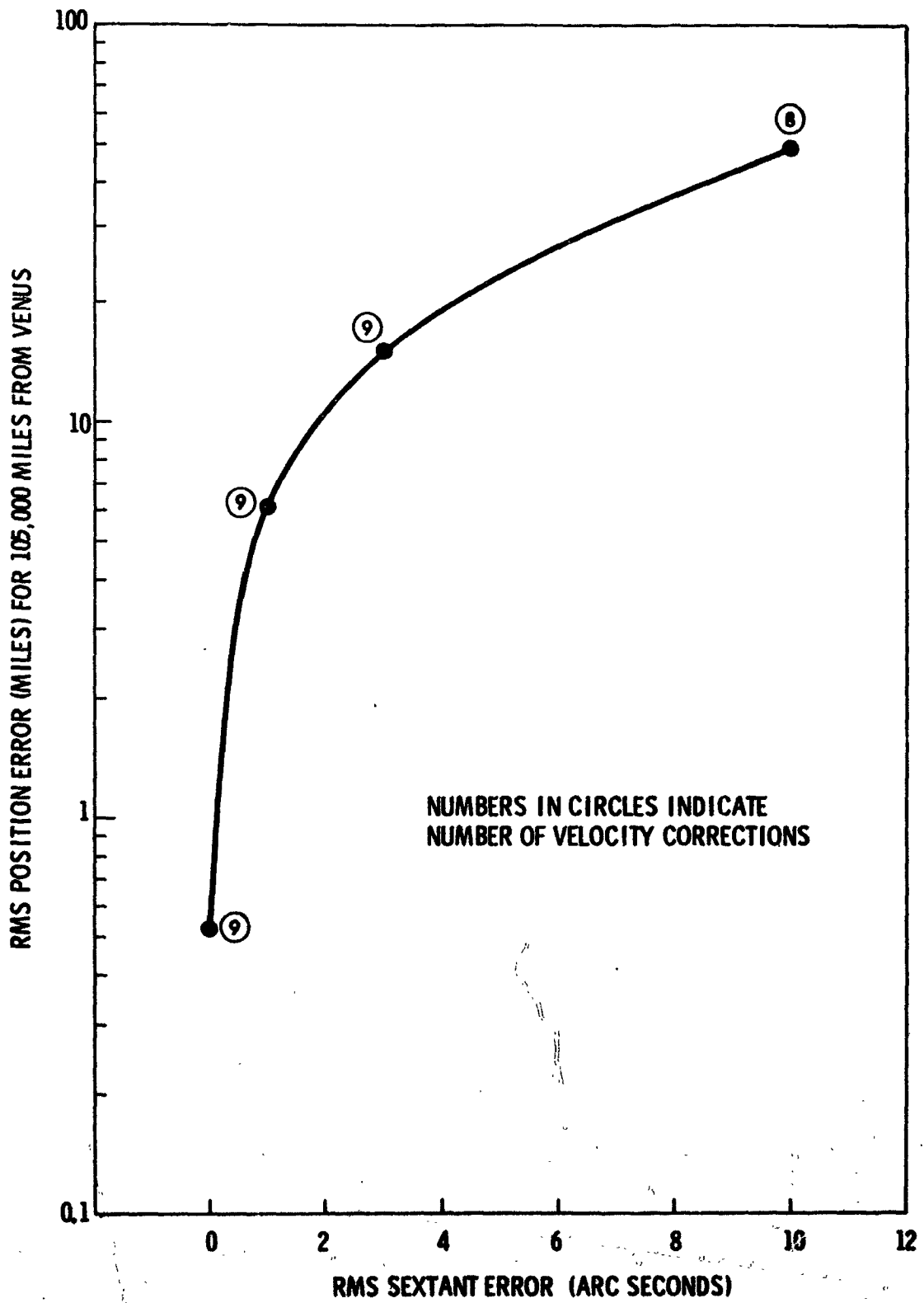
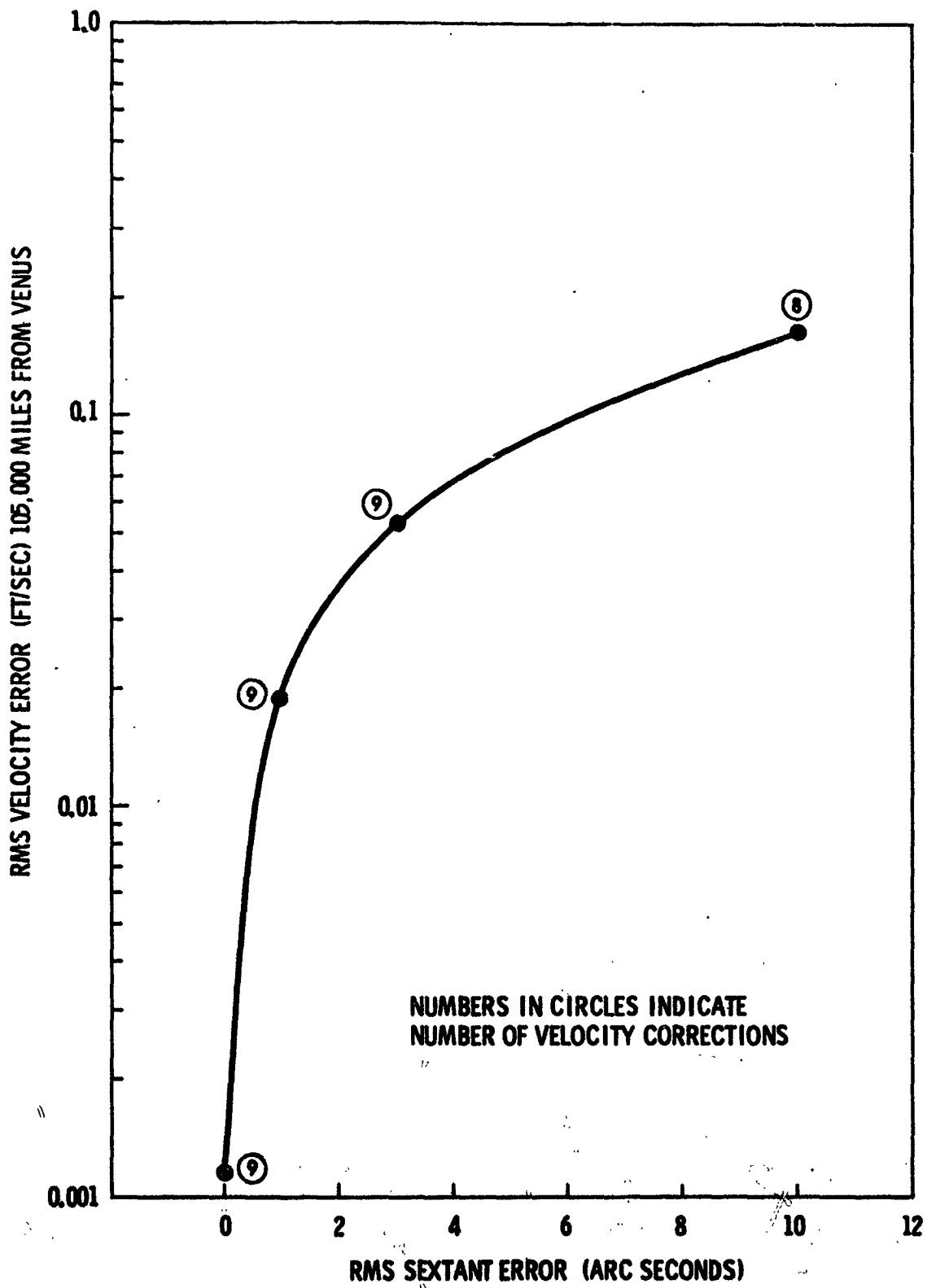Fig. 1.2-12 Sextant Error Effect on Position Errors.

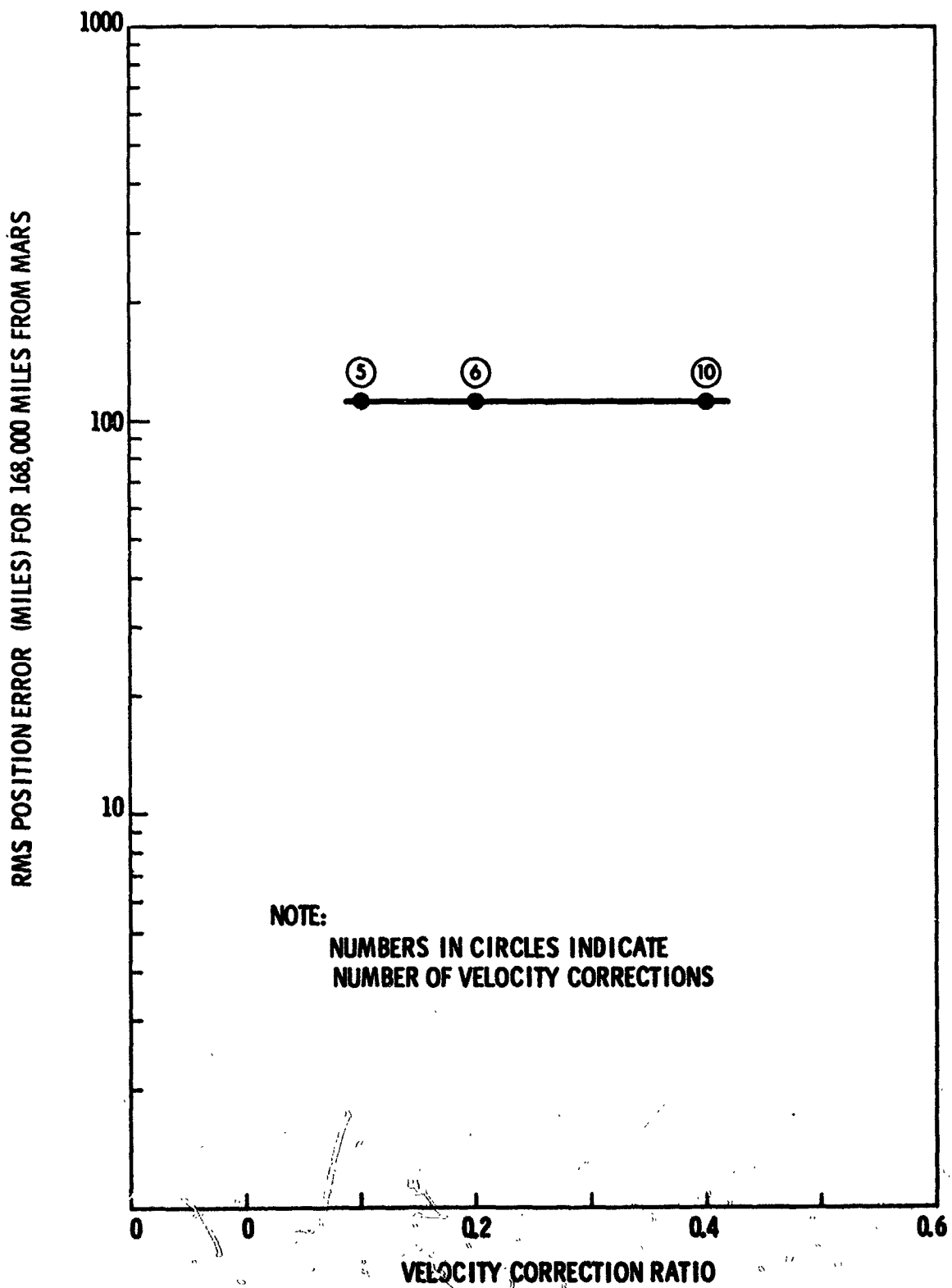Fig. 1.2-13 Sextant Error Effect on Velocity Errors

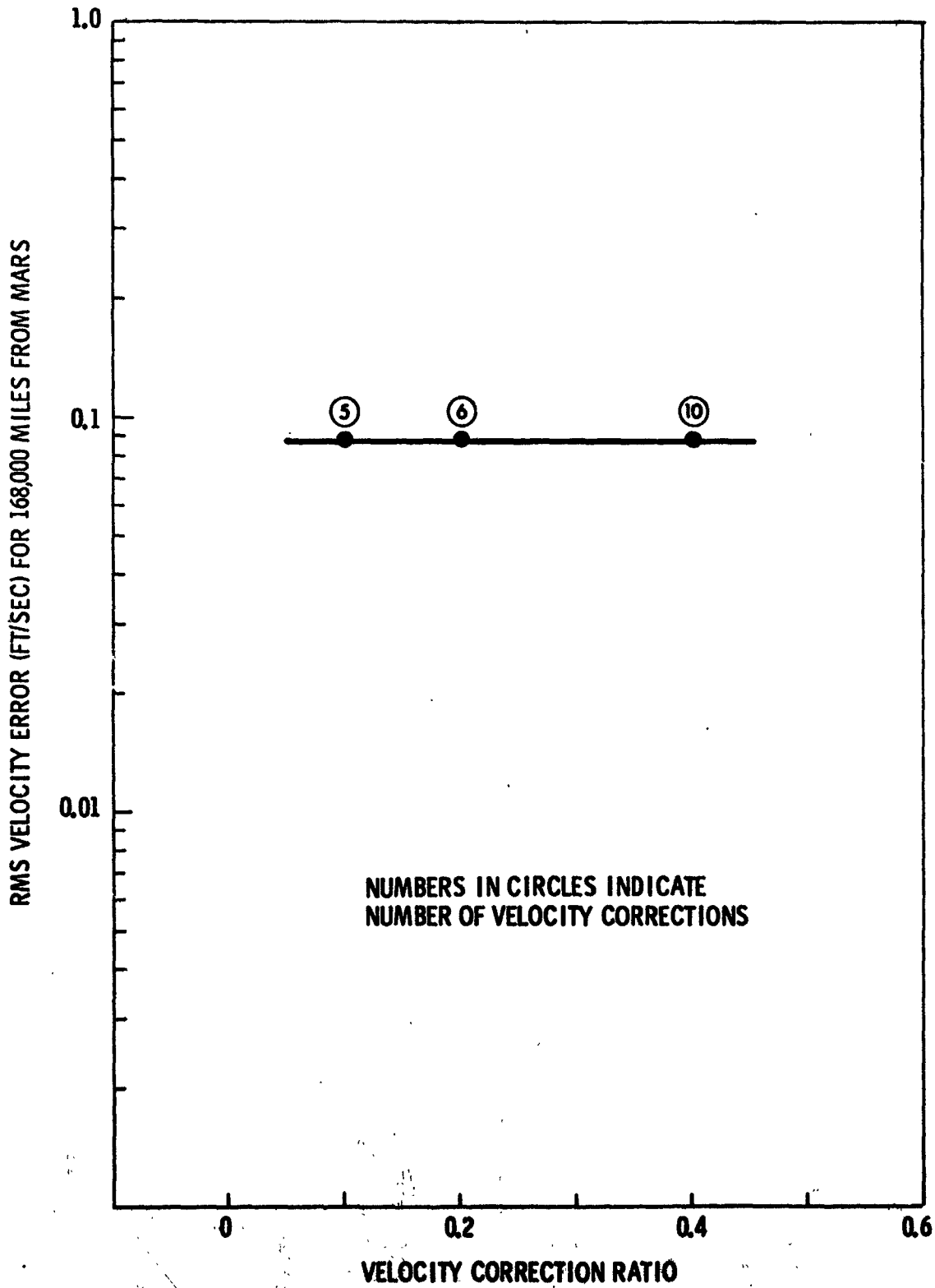Fig. 1.2-14 Variation of Position Error with Velocity Correction Ratio.

1-30

Fig. 1.2-15 Variation of Velocity Error with Velocity
Correction Ratio.

errors are insensitive to choice of the velocity correction decision ratios. The number of velocity corrections, however, do increase as these ratios, increase. The curves are flat because the driving noise is small; the number of velocity corrections increase because the estimation does not have to be of such good quality before the decision is made to implement a velocity correction.

The terminal errors are also insensitive to whether or not infrared equipment is available during the interplanetary legs. The reason for this is again the great ranges to the planets. At these ranges the angular difference between two planet edges (one dark, one light) is so small as to be insignificant.

The only measurements which are ever selected during the mid-course period are planet-star measurements. Planet-star and star-elevation measurements give information in essentially the same direction at great ranges. Since a planet-star measurement basically consists of two star-elevation measurements it has a smaller measurement uncertainty according to the error models described in Volume III of this report. Inasmuch as the information for these two are in the same direction, the routine always chooses the better quality measurement. Sun-star measurements are never chosen due to the large phenomenon error involved in looking at the sun.

A final comment on the midcourse legs is that situations can arise where the onboard navigation equipment cannot use the nearest planet for information. These occur when the sun, planet and spacecraft are almost colinear, with the spacecraft farthest from the sun. If the spacecraft is outside the planet shadow, looking at an edge of this planet also means looking at the sun, thus the near planet cannot be considered available for use. Such a configuration arises on the Mars to Earth leg of the 1979 Mars flyby after leaving Mars, and again with Earth before arrival.

1.2.2.3 Planetary Flyby

The error analysis of the planetary flyby situation was performed using the same computer program that was described in the previous section. Some typical results from the near planet sectors of the 1977 triple planet flyby and the 1979 Mars twilight flyby are presented in this section. Additional results for these phases may be found in Volume III of this report.

Figures 1.2-16 and 1.2-17 summarize some key results for the hyperbolic flyby of Mars in the 1979 Mars twilight mission. Figures 1.2-18
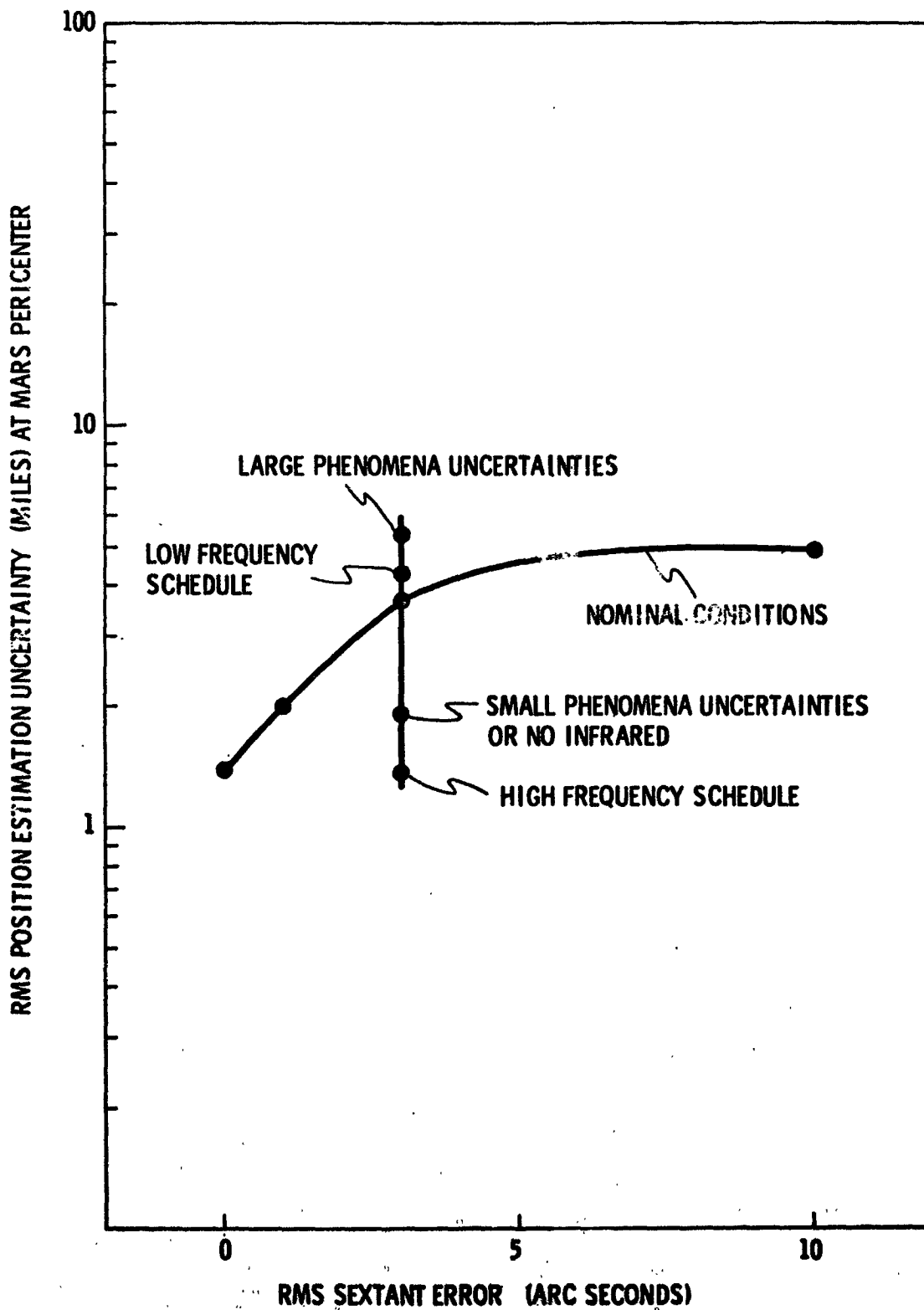
Fig. 1.2-16 Parameter Variation Effects on Position Estimation Uncertainty During Mars Flyby (No Velocity Corrections) - Pericenter.
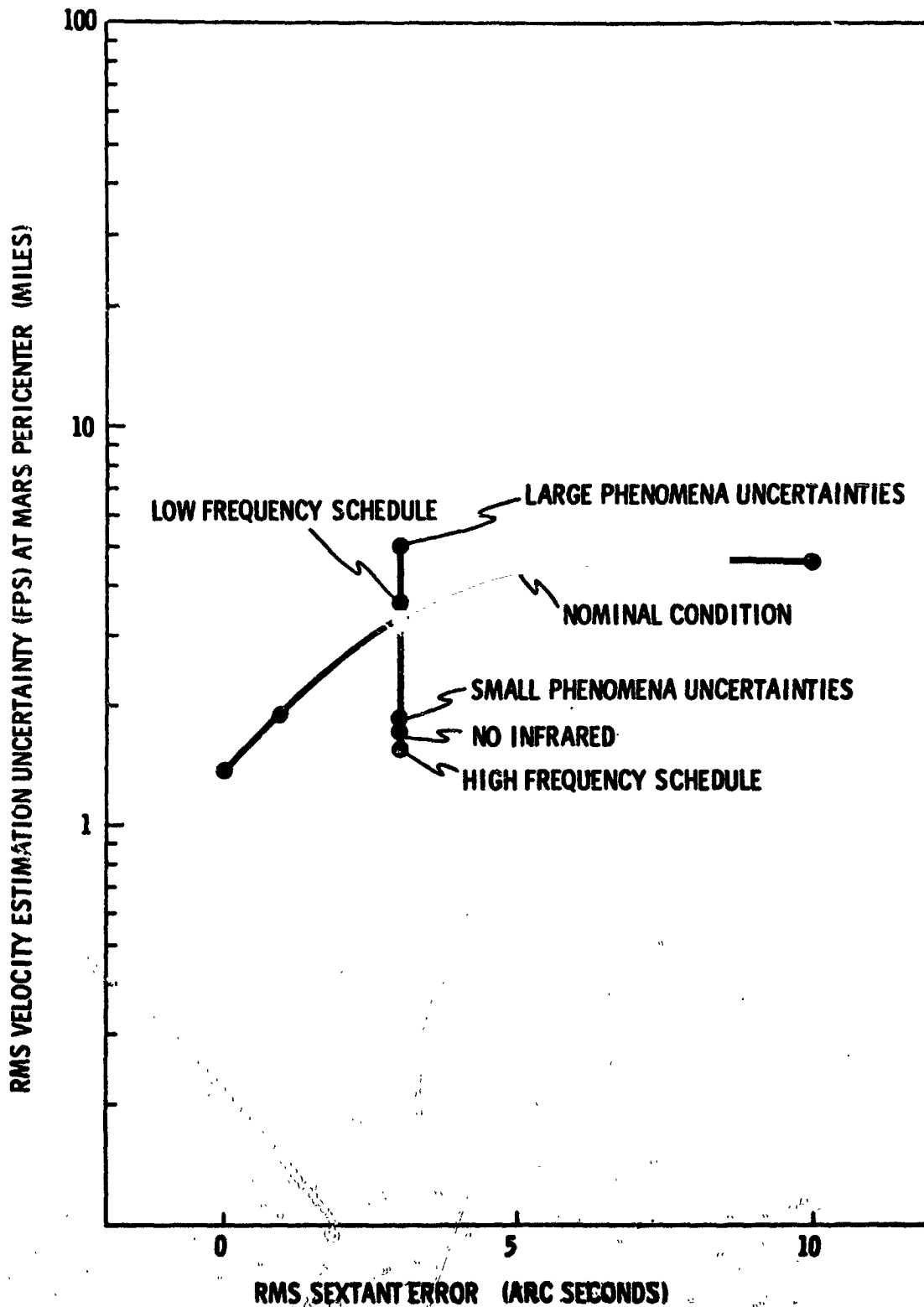
Fig. 1.2-17   Parameter Variation Effects on Velocity Estimation
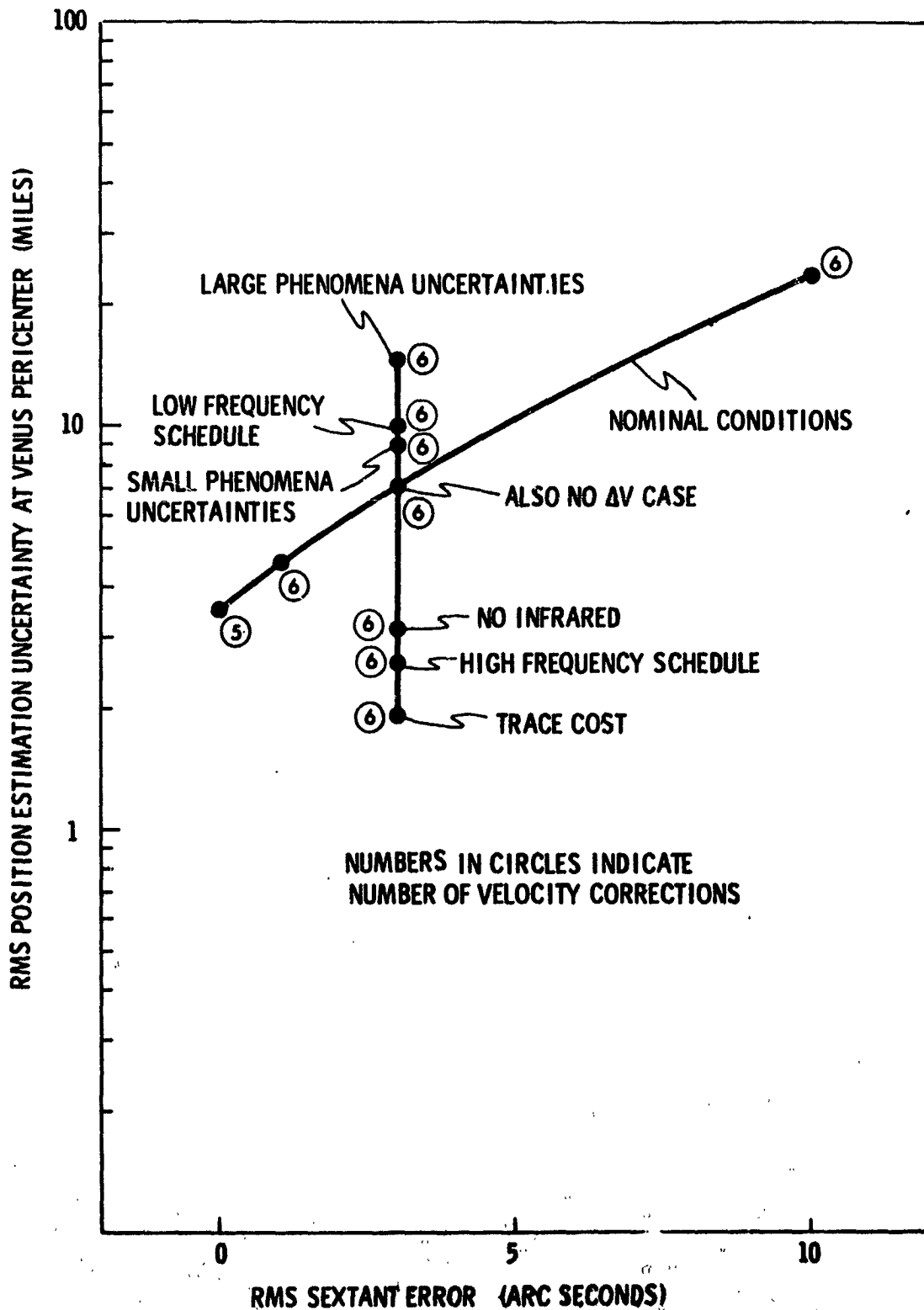Uncertainty During Mars Flyby (No Velocity Corrections)
- Pericenter.

Fig. 1.2-18 Parameter Variation Effects on Position Estimation
Uncertainty During Venus Flyby - Pericenter.

and 1.2-19 present similar results for the first Venus passage on the 1977 triple planet flyby. In both sets of runs the measurement selection criterion was the RMS position error at the outbound intersection with the sphere of influence. Smaller position errors at pericenter passage could have been obtained if the target point were chosen as the perihelion point.

One key result illustrated by these figures is the fact that the slope of the error versus sextant accuracy curves is not as large as in the midcourse phase. Coupling this with a marked increase in the sensitivity of the errors to phenomenon uncertainty, one can conclude that inability to clearly define a planet limb become relatively more important as the spacecraft gets closer to the planet. This is because the angular uncertainty introduced by the phenomenon error increases as range decreases while the sextant pointing error remains fixed.

Another characteristic illustrated by these figures is the fact that changing the measurement frequency can effect as much or more reduction in error as a better sextant or better knowledge of phenomena uncertainty. In these runs the nominal schedule was three measurements per hour everywhere except one hour each side of pericenter passage where the frequency was increased to ten per hour. The high frequency schedule used 30 measurements per hour in the center two hours and the low frequency schedule used three measurements per hour throughout. * It is felt that the high frequency schedule is at, or even slightly beyond, what can be obtained without violating the assumption that the measurements are independent. If this should prove to be a serious problem it can be dealt with analytically by using an optimal linear filter designed to work with additive colored noise on the measurements[13, 14].

Another interesting result revealed by those graphs is the interpretation of the no infrared points on all the plots and the small phenomena uncertainty points in the Venus flyby case. One would intuitively expect that smaller phenomena uncertainties would lead to smaller errors and that inability to use a particular instrument (infrared) would lead to larger errors. The reverse occurred for the data points mentioned. This is primarily a consequence of the fact that the selection criterion is minimizing RMS position errors at the sphere of influence - not the point of pericenter passage.

_____

*Note that even with the low frequency schedule an automatic system would be useful. With the high frequency schedules it is probably a necessity.
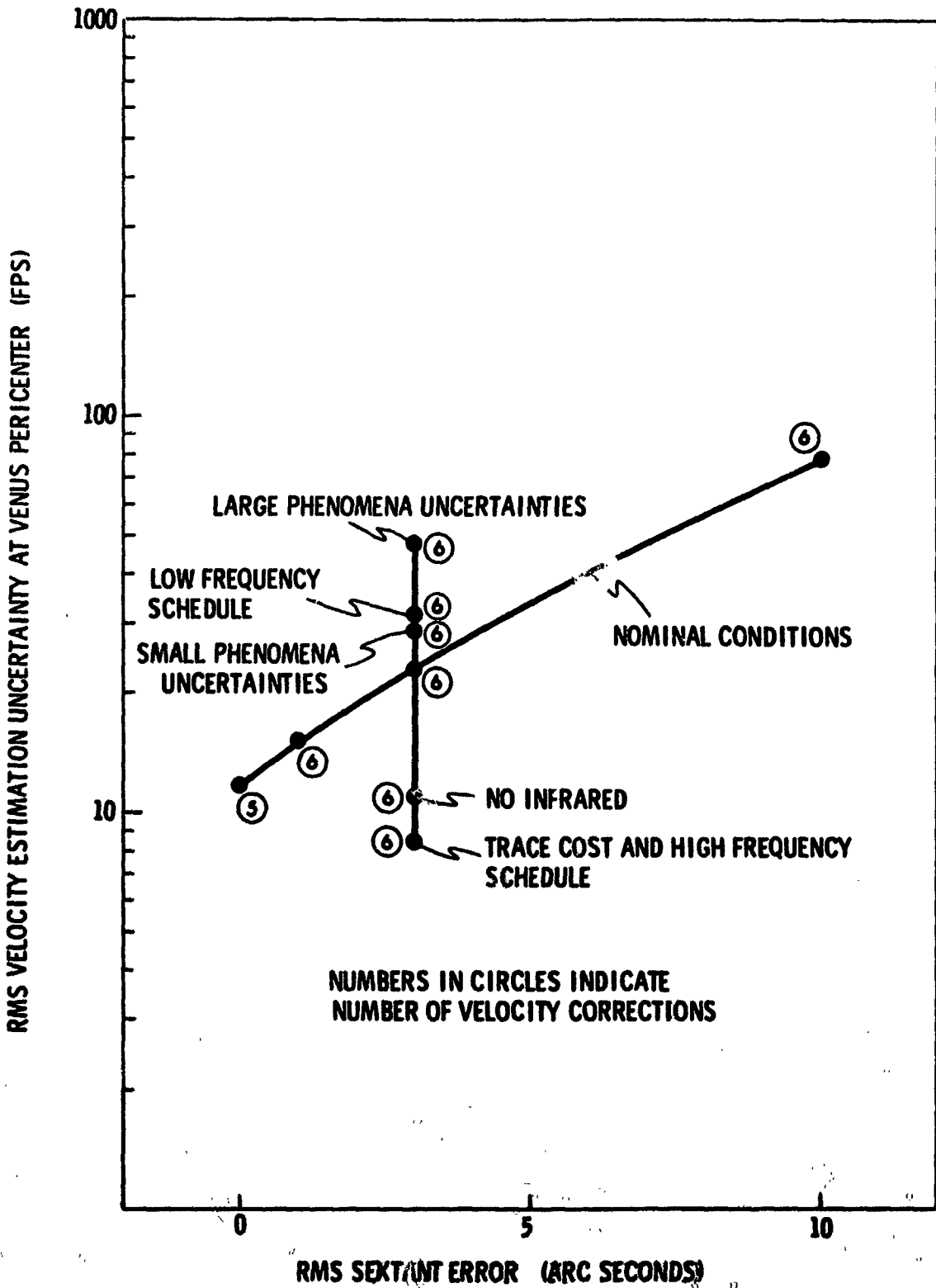
Fig. 1.2-19 Parameter Variation Effects on Velocity Estimation Uncertainty During Venus Flyby - Pericenter.

The change to smaller phenomenon uncertainty and/or to no infrared caused this objective to be achieved with a different sequence of measurements. The point of pericenter passage, which is an intermediate point, can have different RMS position errors in different cases partly because of the different paths to the final objective.

Two more results support this hypothesis. The first is presented in Figures 1.2-20 to 1.2-23. These figures correspond to Figures 1.2-16 to 1.2-19 except that they present the errors at the intersection with the sphere of influence. Note that all data points fall in the locations one would intuitively expect them to. The second additional result is illustrated in Figure 1.2-24. This graph is a plot of the following quantity versus the decision po: number for the Mars flyby:

$$\frac{\text{Total cost reduction without infrared}}{\text{Total cost reduction with infrared}}$$

Note that the difference in measurement schedule at first favors the infrared case but by the time of pericenter passage (the last data point) the reverse is true. Although this was caused primarily because the selection criterion minimized the error at a time much later than at perihelion, it does infer that a noticeable reduction in error might be achieved by optimizing the overall measurement schedule instead of individual measurements as has been done here.

Several runs were made to explore the relative merits of the various measurement selection criteria. The relative terminal error behavior between the trace and terminal error costs was the same as in the interplanetary case - they both yield approximately the same results. The volume cost in this case also gave approximately the same errors. Figure 1.2-25 illustrates the time history of the reduction of terminal errors with the volume cost and high frequency schedule. On the inbound leg of the hyperbola (the initial flat section of the curve) it does not take measurements in directions which reduce the terminal position errors. Near pericenter passage (the steep sloped section at the center) when the error ellipsoid rotates most rapidly it quickly reduces the terminal error. This reduction rate then begins to level off again as the spacecraft flys out toward the sphere of influence.

As a final observation for this set of data, note the data point for no infrared in Figures 1.2-20 and 1.2-21. This large error at intersection with the sphere of influence is a consequence of the fact that shortly after leaving pericenter on this Mars Flyby the spacecraft enters a position where only the dark side of the planet may be detected. Without infrared equipment no observations on Mars can be made during this period.
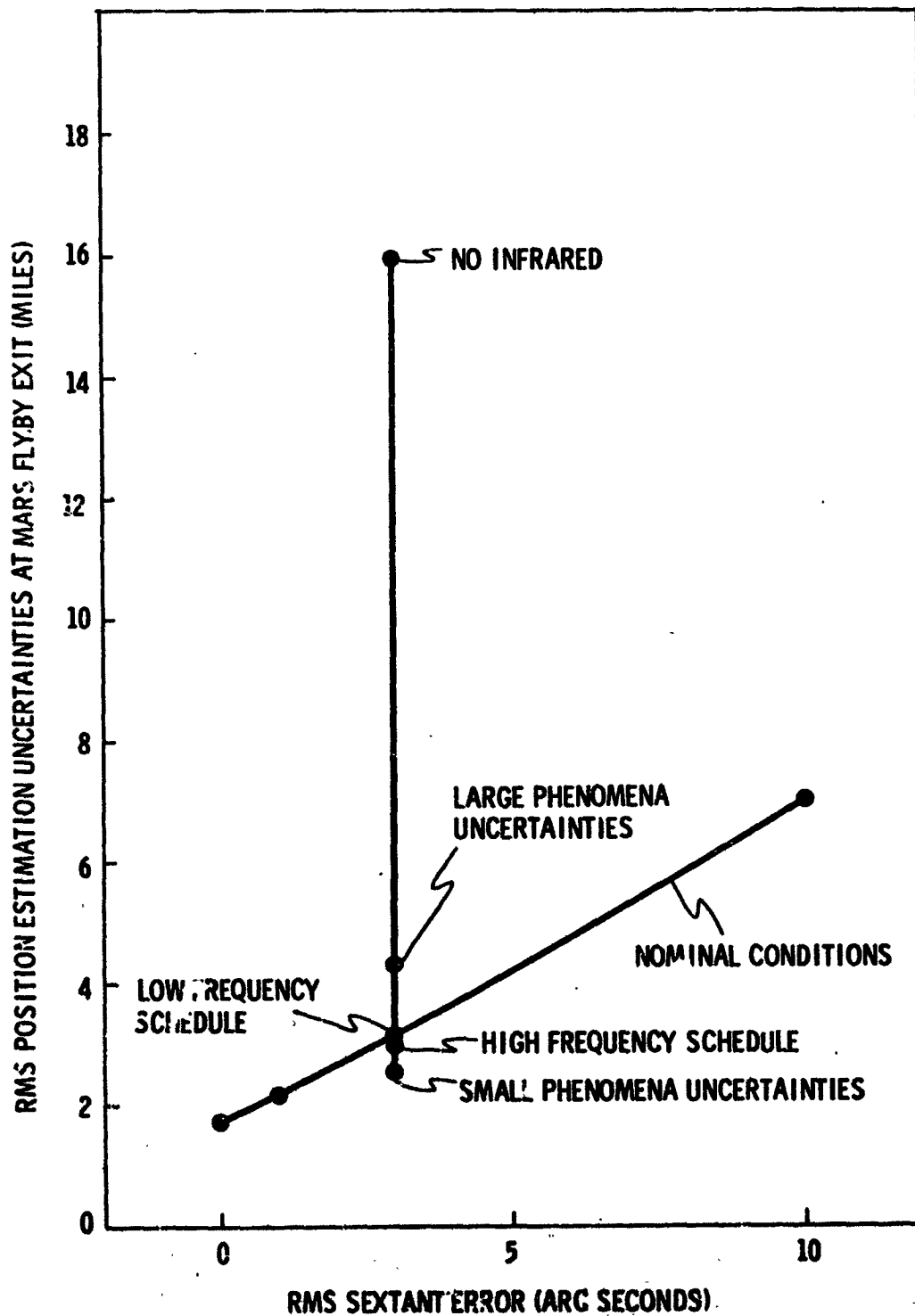
Fig. 1.2-20   Parameter Variation Effects on Position Estimation
Uncertainty During Mars Flyby   Exit - No Velocity
Corrections.
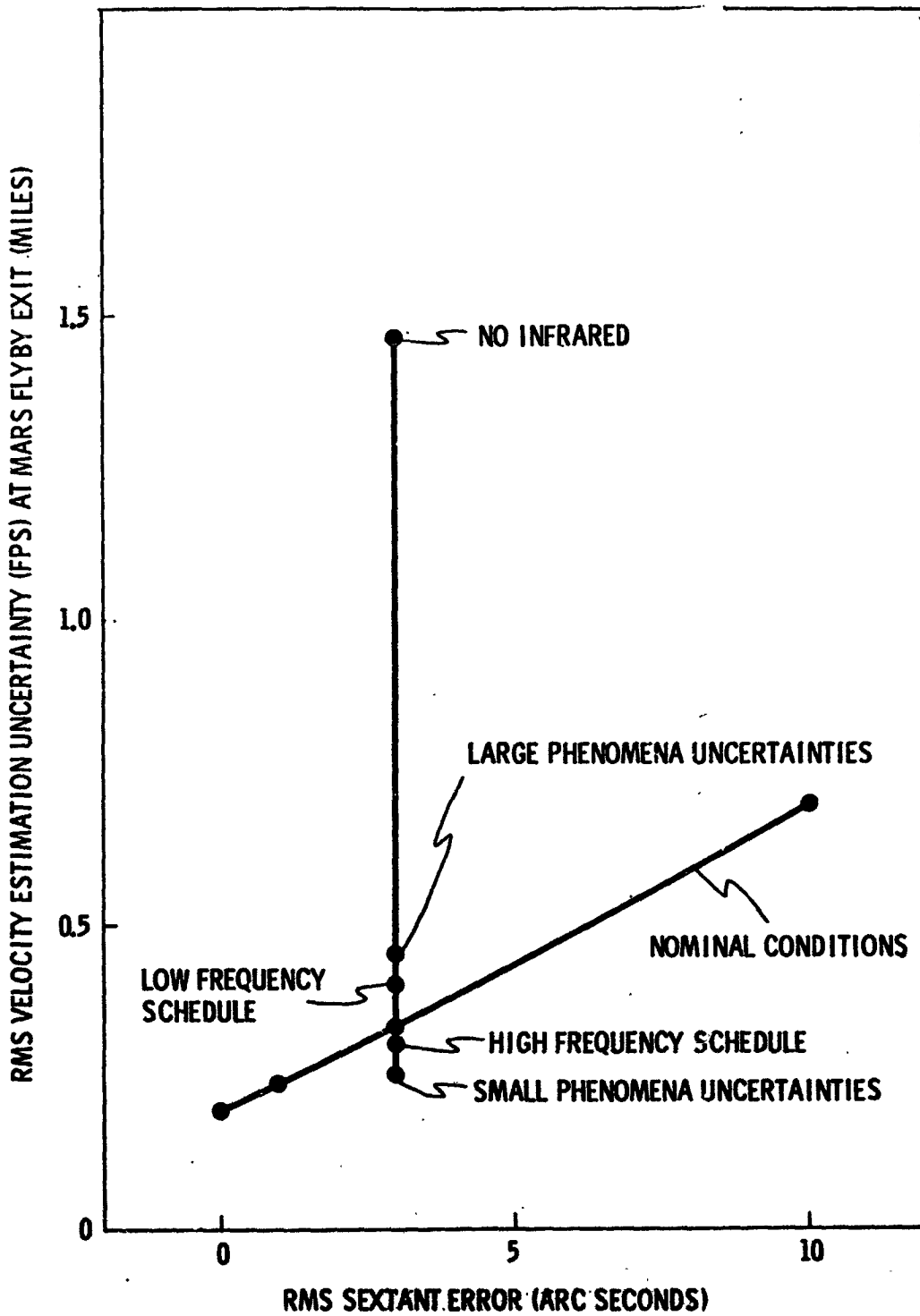
Fig. 1.2-21   Parameter Variation Effects on Velocity Estimation
Uncertainty During Mars Flyby   Exit - No Velocity
Correction.
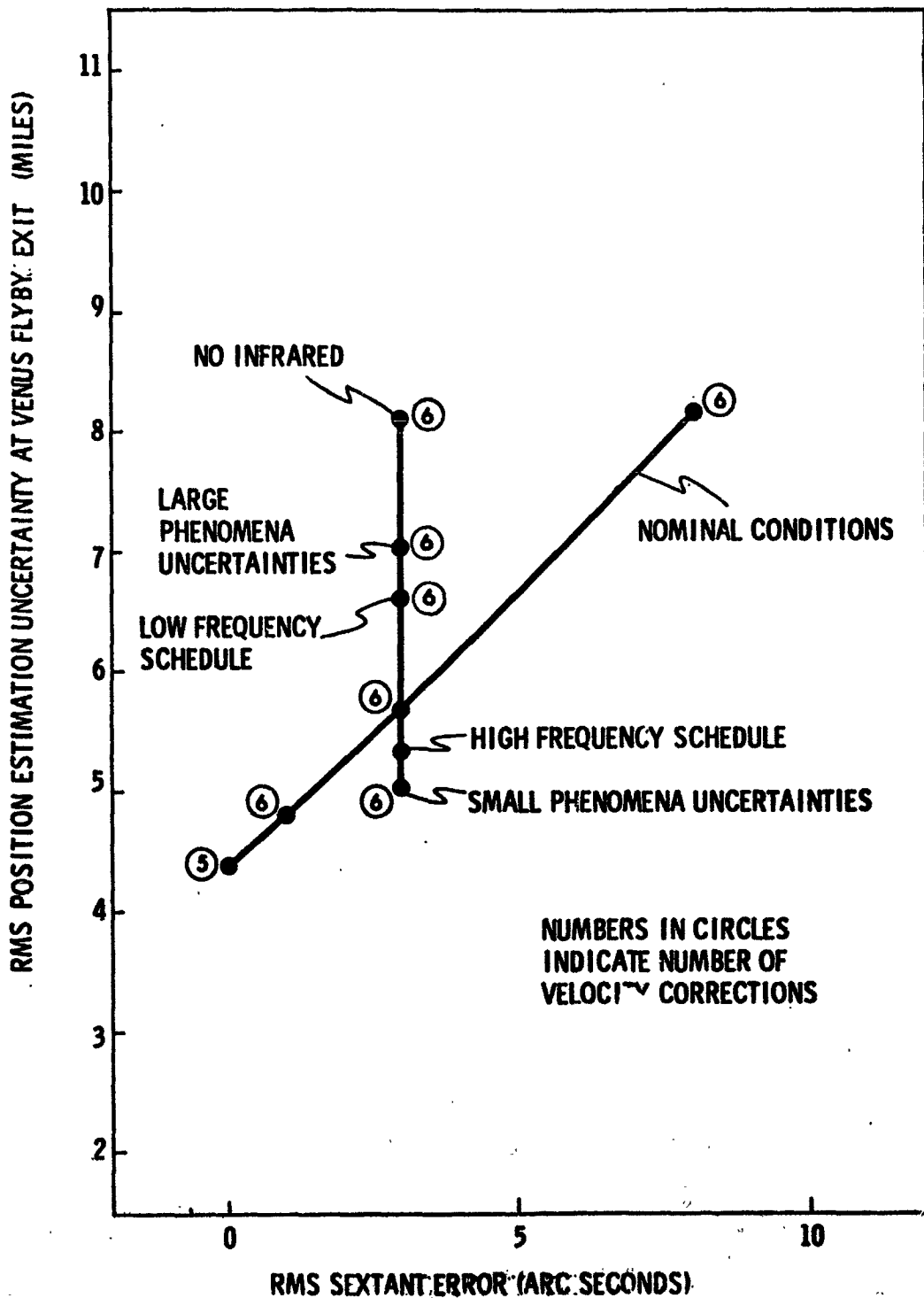
Fig. 1.2-22   Parameter Variation Effects on Position Estimation
Uncertainty During Venus Flyby   Exit.
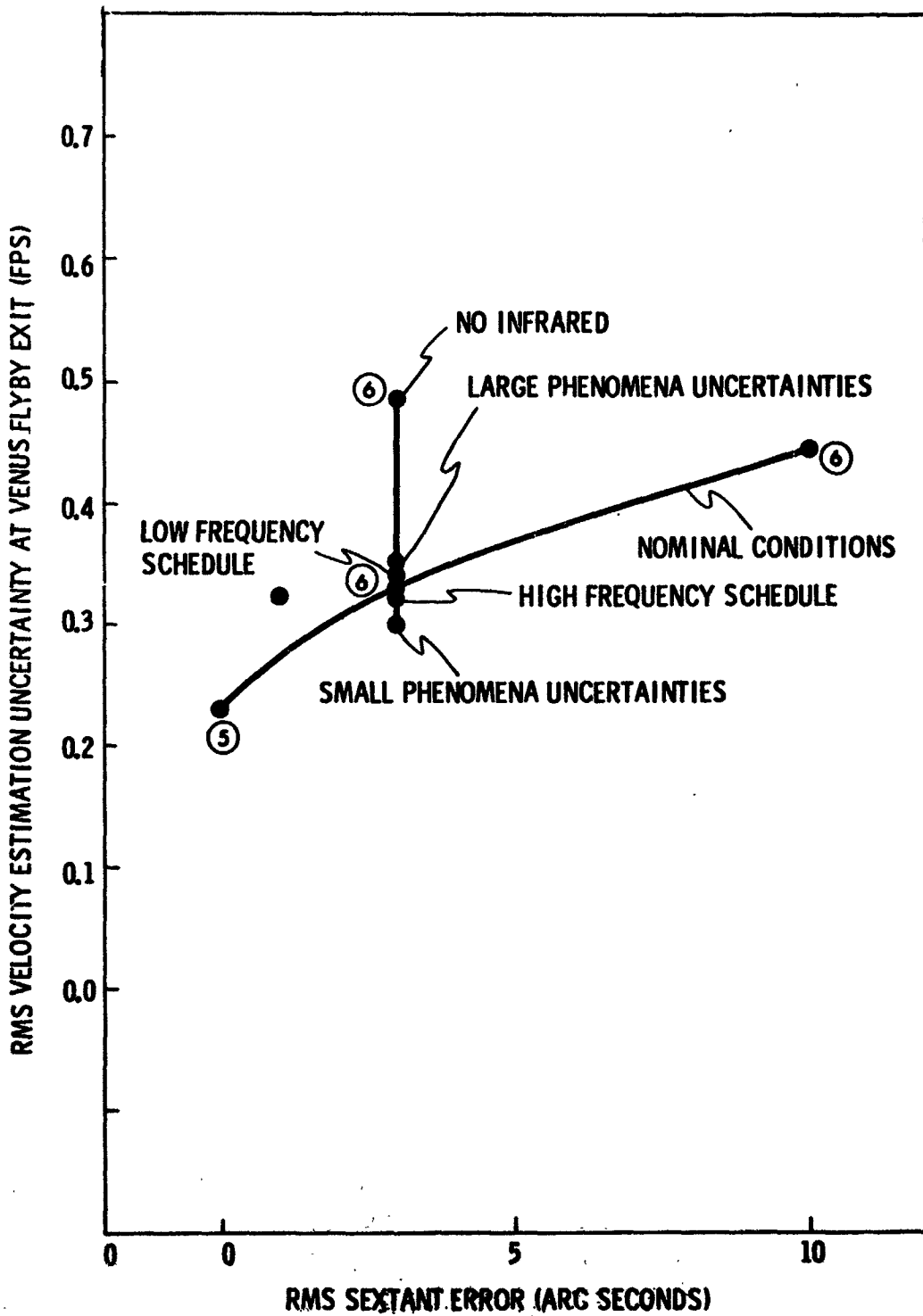
Fig. 1.2-23   Parameter Variation Effects on Velocity Estimation
Uncertainty During Venus Flyby   Exit.

TOTAL COST REDUCTION WITHOUT INFRARED
_____
TOTAL COST REDUCTION WITH INFRARED

DECISION POINT NUMBER
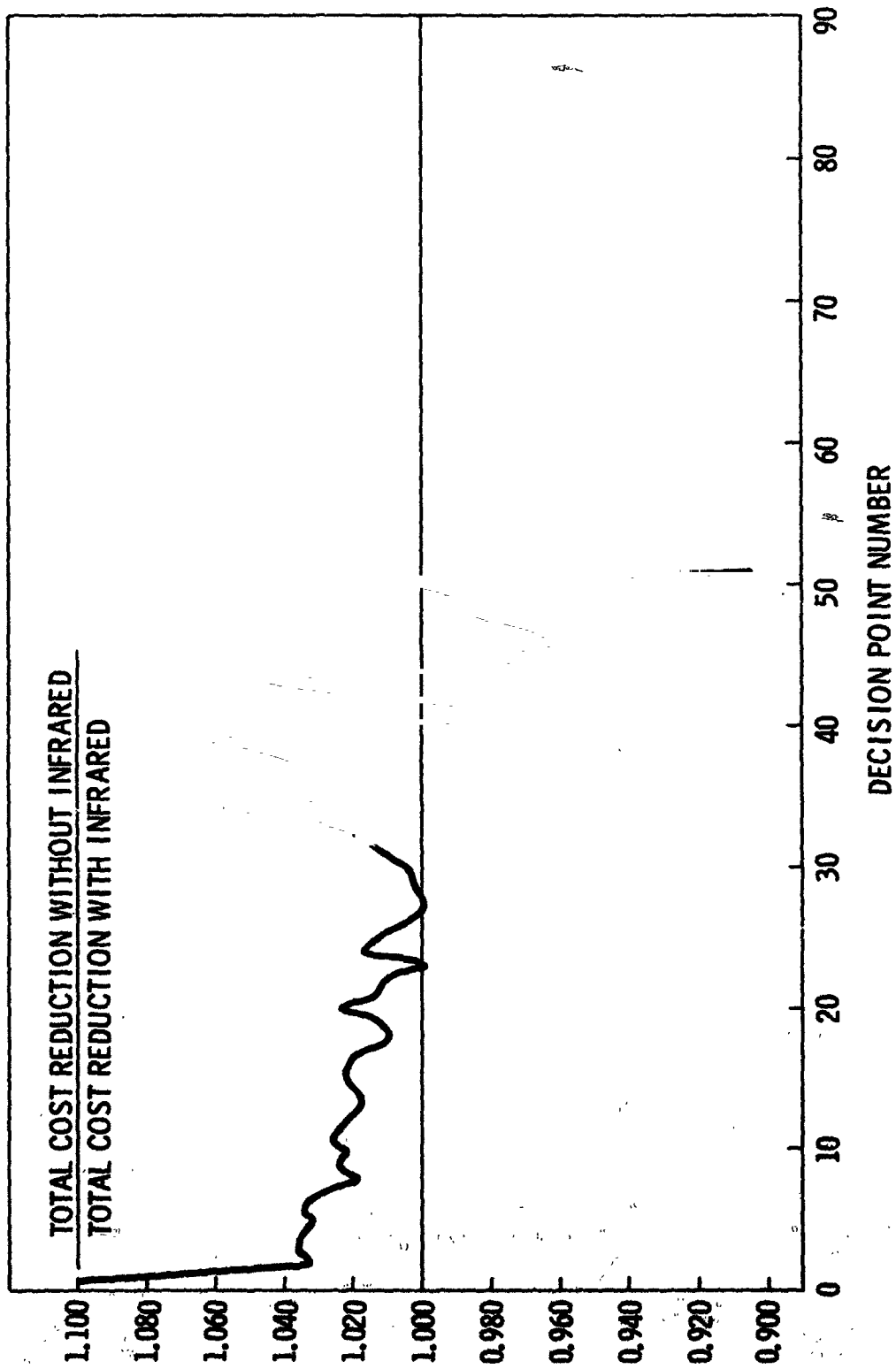
Fig. 1.2-24   Relative Cost Reduction Time History.
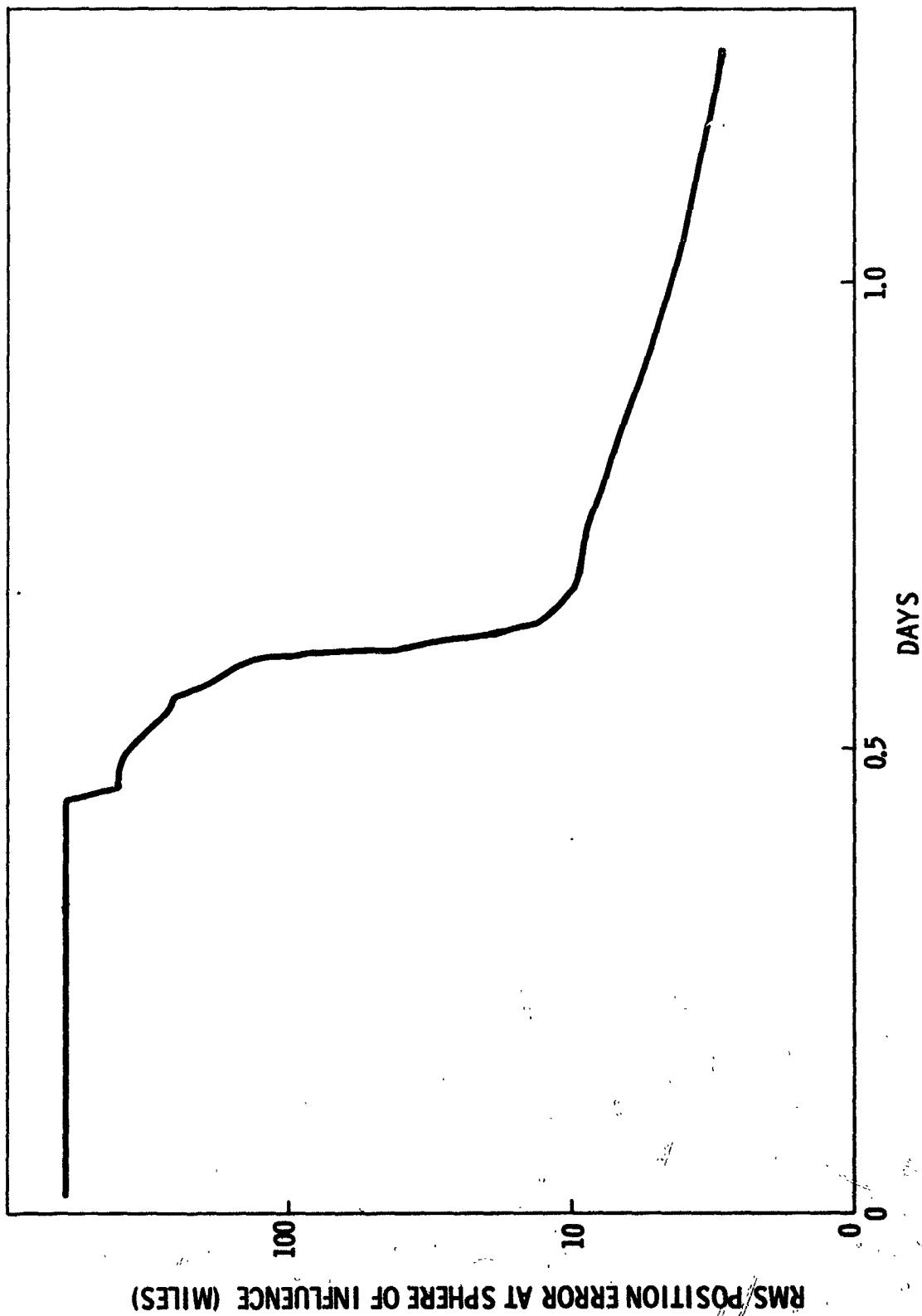
Fig. 1.2-25   Time History of Terminal Position Reduction for Volume Cost.

1.2.2.4   Earth Atmospheric Entry

An analysis was performed to determine the contribution of individual inertial subsystem errors and initial condition deviations to entry guidance system position and velocity errors. This analysis was performed in two phases: 1) the generation of an entry reference trajectory and, 2) the propagation of errors along this reference trajectory. The reference trajectory was generated using an entry steering scheme which is essentially the same as that used for Apollo Earth atmospheric entry.[15] The only modification to this scheme is that the constant drag phase was modified to decrease the g-load on the crew by decreasing the reference drag with velocity. The position, velocity, acceleration, and spacecraft orientation time histories which characterize this reference trajectory were then used as input to a computer program which employed them in the differential equations which describe the position and velocity errors. These differential equations were numerically integrated to give the desired sensitivities.

The data to be presented in this section was generated using a reference trajectory and vehicle with the following characteristics:

Initial Velocity	=	50,000 feet per second
Entry Angle (γ)	=	-7 degrees
Lift to Drag Ratio (L/D)	=	0.5
Deceleration Parameter ($W/C_d A$)	=	.75
Range	=	2,500 nautical miles

See Figure 1.2-26 for an illustration of this trajectory

The entry solution at planetary return velocities was based upon the assumption that an Apollo-type earth entry module and heat shield could cope with return velocities up to 55,000 ft/sec.[1,2] This type of entry body has typical L/D ratios of 0.5 or less, thus immediately presenting a guidance problem. Reference to Figure 1.2-27 shows that the equilibrium load factors experienced by this type of body at a return velocity of 50,000 ft/sec can reach as much as 9 g's for L/D = 0.30. Human exposure to this g level is allowable only for a few minutes. In Figure 1.2-28 there is graphically displayed the narrowing tolerance allowable on the entry angle as entry velocities increase. This tolerance is bounded on the lower side by entries so shallow that maximum downlift fails to result in capture and on the upper side by entries so steep that permissable g loads are exceeded. The
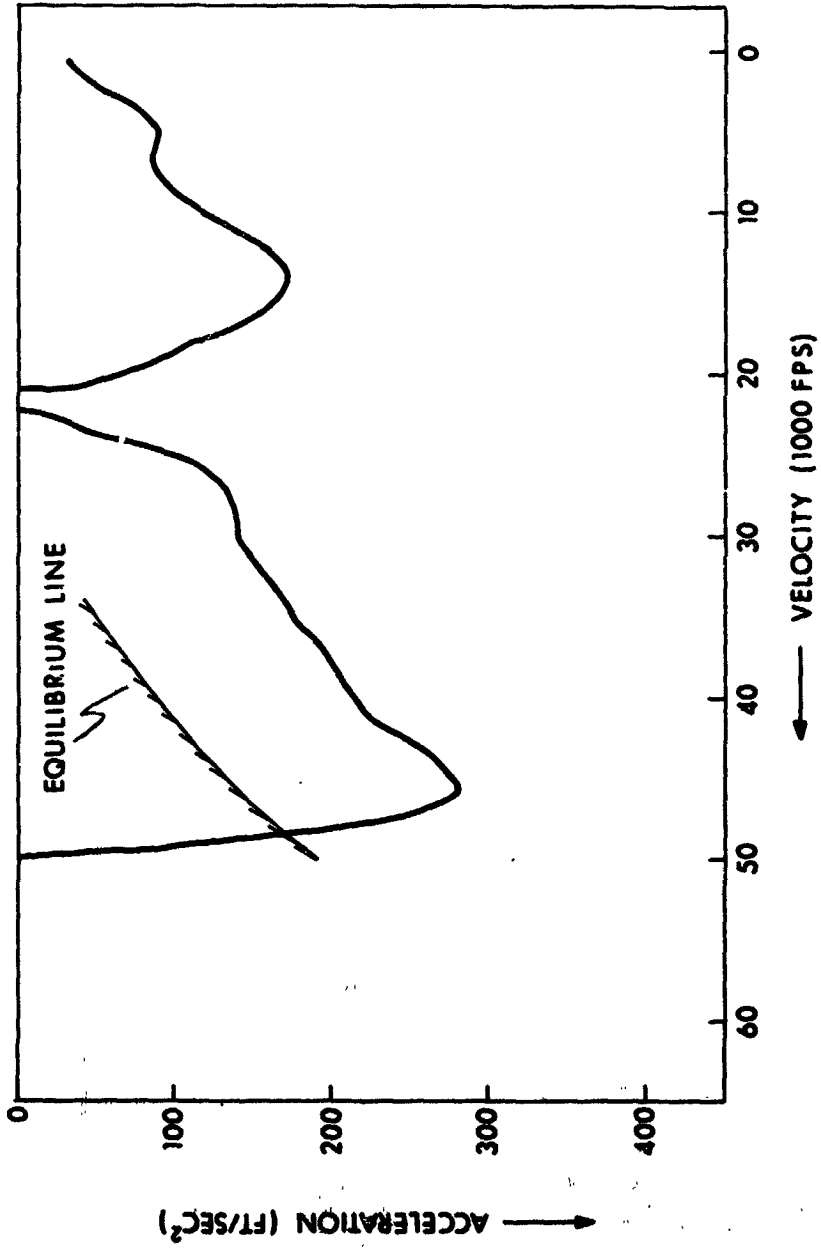
Fig. 1.2-26   Reference Entry Trajectory.

VELOCITY (1000 FPS)

ACCELERATION (FT/SEC²)
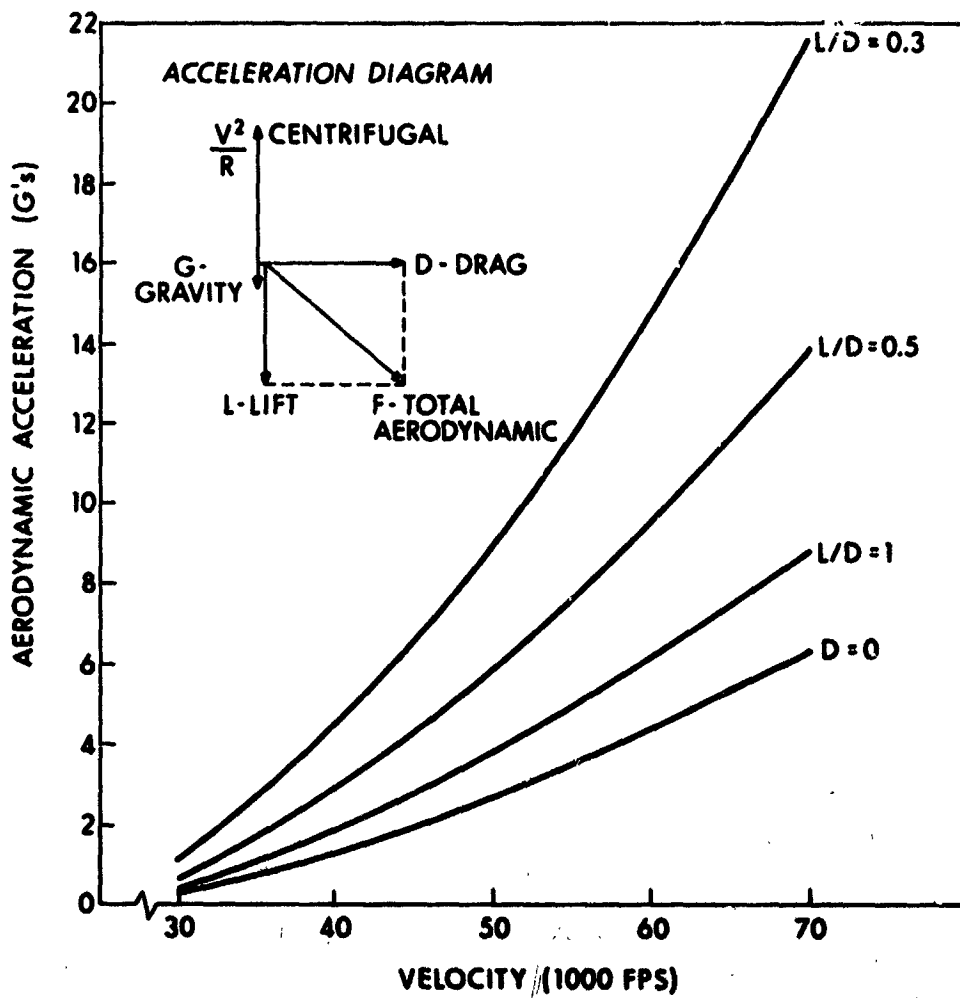
EQUILIBRIUM LINE

Fig. 1.2-27 Aerodynamic Acceleration Required for Equilibrium.
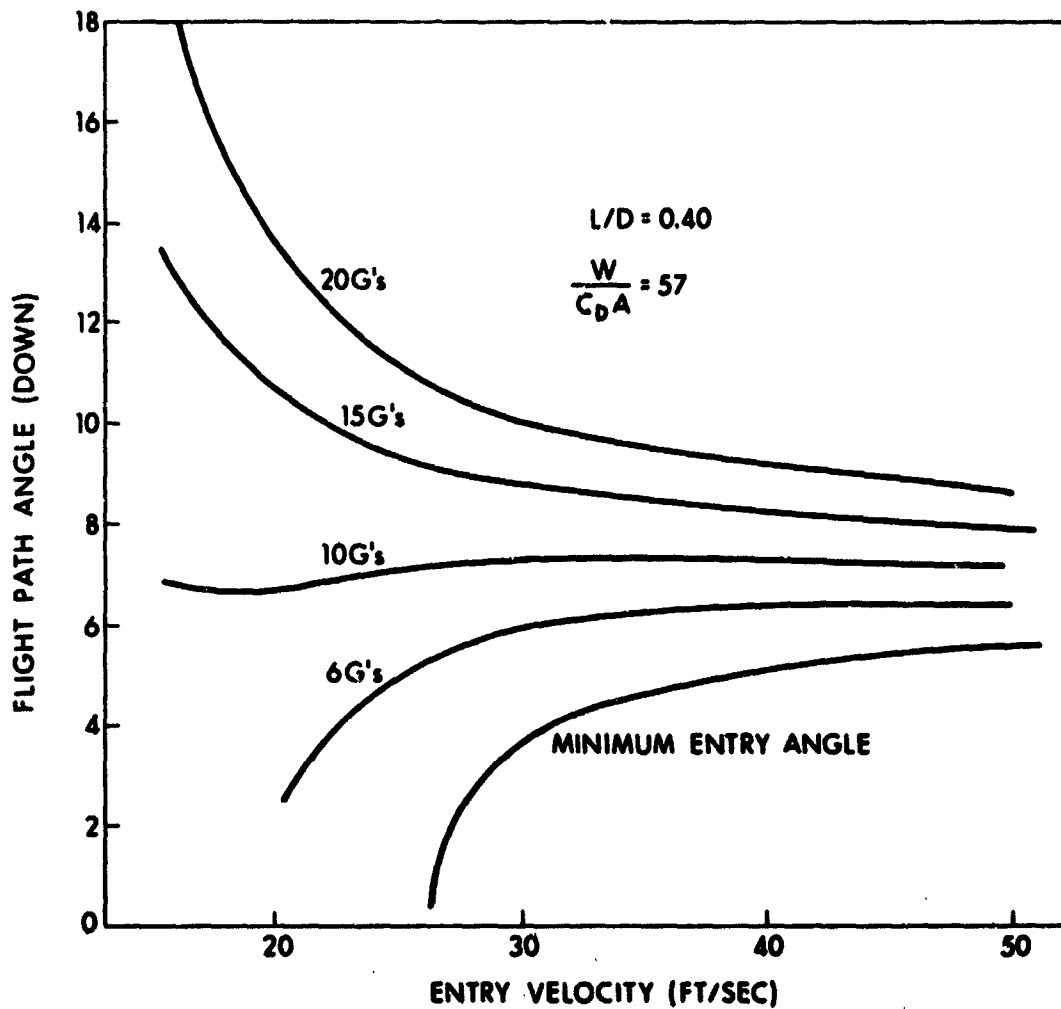
Fig. 1.2-28   Limit Earth Atmospheric Entry Angles as a Function of
Allowable Load Factor (Approximate).

1-48

reference trajectory employed here used the entry maneuver depicted in Figure 1.2-26 together with selected initial conditions and inertial component errors. The end result of the propagation of these quantities through the entry maneuver consists of position and velocity uncertainties at final parachute deployment (24,000 feet).

RMS Position Uncertainty: 1,000 ft
RMS Entry Velocity = 1 ft/sec
RMS Entry Angle Uncertainty = .01°

The state vector uncertainties at the beginning of entry at 400,000 feet are basic to guidance requirements for entry. This contract effort has not generated final answers in this area (see Discussion of Further Work in Section 3.2.1).

The results of the Entry Study are presented in the form of error sensitivity coefficients for those error sources which had a dominant effect on position error at the end of the maneuver. The end of the maneuver was defined as chute deployment at approximately 25,000 feet of altitude.

The accelerometer errors did not have a strong impact on terminal errors:

5.0 Feet Range or Track Error per Micro-g of accelerometer bias.
8 Feet of track error and 2 feet of range error for each part per million of scale factor error.

Errors in initial misalignment of the inertial subsystem produced the following effects in coefficient form:

30 Feet of Range and 50 to 80 Feet of Track Error for every second of arc misalignment.

A dominant effect on final errors was found to come from gyro drift between the alignment process and the beginning of the entry maneuver. This pre-alignment time (t_p) was evaluated at zero and 1 hour:

	$t_p = 0$	$t_p = 1$ Hour
Track Error in feet per unit meru of gyro drift rate:	150	4510
Range Error in feet per unit meru of gyro drift rate:	300	2000

Acceleration sensitive drift terms in the gyros also have a significant effect on the Uncertainty in final position:

Range	300 feet per meru/g
Track	80 feet per meru/g

1.2.3 Summary of Requirements

The following requirements represent a) conclusions reached from the brief studies described in Section 1.2.2 and, b) qualitative reactions to the two mission studies set forth in References 1 and 2. These requirements are necessarily of a tentative nature only, both due to the short term of the study contract and to the lack of mission definition.

1.2.3.1 Navigation Requirements

On-board navigation is required to supplement state vector information supplied by the Deep Space Network. This is especially true as target planets are approached, where the data is needed in a reference frame centered on the target planet. Navigation is recommended using a sextant-type instrument and recursive filtering techniques in conjunction with an on-board digital computer. Flexibility in measurement types is recommended from among the following:

> Planet Diameter
> Sun-Planet Angle
> Planet-Star Angle
> Star Occultation
> Star Elevation Angle
> Sun-Star Angle
> Unknown Landmark

Several of these measurements can be accomplished by the same instrument design. An IR sensor enables measurements to continue while passing close to the dark side of a planet.

Accuracy requirement studies indicate that an instrument improvement in accuracy from 10 arc seconds to 1 arc second for mid-course navigation (See Section 1.2.2.2) yields equivalent position and velocity uncertainty improvements from 6:1 to 8:1. During actual planet encounters of flybys (see Section 1.2.2.3) the benefits obtained in going from a 10 arc second instrument to a 1 arc second instrument can be exceeded by a higher frequency sighting schedule if the instrument is automated or by substantial improvements in navigation phenomena uncertainty resulting from unmanned probe flights.

1.2.3.2 Guidance Requirements

A guidance study of a representative transplanetary injection (See Section 1.2.2.1) demonstrated that an array of inertial subsystem uncertainties now considered as reasonable development goals would provide terminal uncertainties of no larger than 5 miles and 30 feet per second at the end of the burn. The case studied had an exceptionally long burn time. Shorter burn times will yield smaller errors than these. During the midcourse phase velocity corrections are small, and the guidance function is non-critical assuming that the velocity correction is implemented at a g-level resulting in engine firing times in the order of seconds.

The terminal phase of a return-to-earth orbit and the atmospheric entry maneuver were not given the thorough study they deserve. The same nominal inertial error coefficients operating on a reference entry trajectory did not generate unacceptable errors in the entry footprint. However, this phase is critically influenced by uncertainty in entry angle. Studies of flight path angle, γ, uncertainty have not been made, and the ability to make a late velocity correction to bring γ uncertainties within narrow bounds is a must.

Guidance system performance is degraded by inertial drift of the inertial reference frame alignment during the 1 hour before engine turn-on. With an automatic tracking head on the sextant instrument, inertial reference alignment could be updated continuously during transplanetary injection and the build-up of error to the start of atmospheric entry could be eliminated. Therefore an automatic capability in the radiation sensor system is recommended.

1.2.3.3 Critical Control Problems

During the course of this study contract, little effort was spent on control problems because these are defined by constraints which were not available. Certain problems were anticipated as being worthy of future study, however.

The multi-million pound interplanetary vehicles proposed for earth orbit assembly will be difficult to control during transplanetary injection. This is due to the combined influence of fuel slosh of a million pounds of fuel and the elastic flexure of long and slender vehicle assemblies. During this injection period a large fraction of the vehicle mass will be expended. To a control system analyst this vehicle will appear as a significantly time-

varying, high-order plant. To make matters even more difficult it is quite likely that the key parameters of bending and slosh will be poorly specified, adding additional uncertainty to an already comples system model. Careful design of autopilots and guidance steering laws will be a necessity here.

There will be a specification on vehicle attitude control both for thermal balance and communications antenna dish orientation. Possible accuracy requirements here will have to be weighed against minimization of maneuver fuel consumption.

It is anticipated that re-entry control for future manned missions will involve the same rolling modulation of the lift vector as was designed for the Apollo mission. This is not presently a control problem.

1.2.3.4   Reliability Problems

An evaluation of some mission timelines in early studies indicates that for the inertial subsystem, "ON" time could well be limited to one-hundred (100) hours with 16,000 hours in "Standby" or "OFF". If the "standby" mode is defined with gyro wheel power off, then the "ON" time for wheels is not greater than for Apollo. However, it is highly improbable that final mission timelines will limit inertial subsystem operating time to 100 hours. Experience has shown that the tests, operational checkouts, and mission tasks will cause this figure to increase drastically.

The standby power situation is drastically different from Apollo, however, in that the estimate of 16,000 hours in standby puts the spo'ight on standby power supplies and temperature controls as highly susceptible to failure. Design effort must be expended on these elements or else a reliable "cold wheel turn-on" must be developed. Doing away with "Standby" in this manner would have a real minimizing effect on long-duration power consumption and on the inertial subsystem reliability figure.

Even this step, however, does not eliminate a serious reliability problem which characterizes advanced manned missions. This problem is the question of shelf-life. The shelf-life performance of the inertial subsystem hardware will be the subject of acute interest. A related question is the influence on shelf-life of periodic turn-ons and turn-offs for checkout or operational purposes.

The ultimate objective is to attain a very high probability that when the inertial subsystem is needed during the mission that it will work with the design specification requirements. With this in mind, a design concept evolves using multiple inertial sensors for redundance, a strapdown con-

figuration for maintainability, and a long-duration "standby" concept which doesn't act so as to reduce reliability.

The Computer Subsystem is central and basic not only to the control, gui'ance, and navigation system but to related spacecraft and mission systems as well. Accordingly, this on-board computer subsystem will have longer on-times when it is performing mission support functions than other parts of the CG&N system. The concept of "Graceful Degradation" following partial failures in the computer is the basis behind the multiprocessor structure [15] explained in Volume II whereby the computer subsystem is able to recognize a partial failure and continue to perform its operational functions though at a reduced rate and capacity. Only through such a fundamental concept as this, combined with quality assurance and maintainability design of a high order, can the computer subsystem approach the required values of MTBF for Advanced Manned Missions.

The design of radiation sensor subsys' ms (See Volume III) involves some serious compromises in the area of reliability and maintainability versus performance, flexibility, and versatility. A simple, one-power telescope with a fixed orientation through the walls of the mission modules could be shown to have a very high MTBF.

Measurement of navigational angles would then involve spacecraft rotations and astronaut timing. Such a device would not be accurate, would place great demands on attitude maneuvering capability and fuel supply, and would require the full, undivided attention of the astronaut. At the other end of the spectrum, one can adopt the concept of a multiple-degree-of freedom instrument with electro-optical sensors, automatic capability, and astronaut monitoring participation. With the mounting of more than one instrument outside the vehicle, the advantages of multiple sightings, no spacecraft maneuvering, and redundancy can be cited. However, this high degree of sophisticated equipment can be predicted to have a much lower reliability. In addition, this type of instrument does not easily lend itself to maintenance and repair in space because of its external mounting and because of its accurate assembly. For Radiation Subsystems, the reliability problem is a very serious challenge indeed. Further work in this area will have to devote primary attention to achieving a good balance between desirable instrument capabilities and acceptable reliability.

In summary, the reliability problems which are raised by long-duration advanced manned missions are very serious. The present contract has only begun to come to grips with these problems.

2. DESIGN STUDIES AND DEVELOPMENTAL HARDWARE

2.1 General Considerations

The objective of the design studies has been to explore the design of the guidance and control system embracing the widest range of the requirements established in Section I. It should be appreciated that this wide coverage of requirements may be at variance with the desire for the ultimate in simplicity. A priori, simplicity can be considered to favorably influence reliability. However, it has been the history of the space program that very complex spacecraft have conducted sophisticated missions with a high degree of success.

In designing the radiation sensor and inertial subsystems, great attention has been paid to obtaining the required performance over a wide range of spacecraft orientation and rates. Similarly for the computer and displays, greatest consideration has been given to ease of programming and operation. Versatility of the system is required for automatic operation plus the ability for control both locally and remotely. Remote operation either by GSE or by the uplink/downlink telemetry system will be required in the checkout phases. Where the spacecraft is assembled in Earth orbit, remote control during assembly may be required, and checkout in orbit will be a requirement.

Some developmental hardware has been built (within the schedule and budgetary limitations of this contract) where the design studies have demonstrated the need to advance the state-of-the-art in a particular area. When such requirements have appeared, the need for developmental hardware has been judged against three criteria before proceeding or continuing the work. Firstly, the novelty of the design was considered where work was needed on materials and techniques. Secondly, the lead time of the item was considered because long lead items require earlier completion of firm designs. Thirdly, the impact of the design on the overall system configuration was a criterion, where failure to adopt the technique would prevent system interfacing.

2.2 Systems Integration

The design model for the Control, Guidance, and Navigation System is based on the on-board guidance and navigation philosophy incorporated into the MIT Apollo GNCS design. Changes are made to improve performance and reliability, and to reduce interaction with external disturbances. Moreover, changes are also made to enable ease of operation in planning, testing, and flight phases of missions. In particular, changes have been made in the computer subsystem to increase the speed and logical power. These computer changes give the design margins required

to allow the use of automated software generation techniques. This trend towards increased automation extends to the operation of the other subsystems also.

In the following paragraphs the operation of the various parts of a representative system and the system consideration affecting their design will be described in brief.

2.2.1 Design Model

The component subsystems of the design model are illustrated diagramatically in figure 2.2-1. In the control function of the system, information on vehicle attitude and acceleration are fed from the inertial system to the computer. The computer compares these inertial inputs with the control requirements and makes appropriate commands to the vehicle's propulsion, attitude control thruster, and angular momentum control systems. Control requirements may be internally generated under autonomous program (either in unmanned mission or in automatically sequenced mission phases) or may be directly fed into the computer by the operator through the display and controls. The requirement for control and the means of control vary for different mission events. Orbital velocity corrections are made by controlling propulsive thrust direction and magnitude by feedback from the inertial accelerometers, stability enhancement will probably be made by use of vehicle attitude, and possibly thrust direction with respect to the vehicle. Vehicle attitude changes are made by computing the optimum angular mome· ...m changes to apply to the vehicle to bring about a timely maneuver with the minimum use of resources. Precision attitude hold may be a requirement for scientific experiments and communications, where the inertial attitude information may be enhanced by inputs from the radiation sensors. Initial alignment of the inertial attitude is an important use of the radiation sensors. Alignment is made by identifying bright sources and establishing their direction. Planets and stars will be used, but the use of the sun may require the use of a special sensor, which in certain vehicle designs requires siting on the opposite side from the main radiation sensing subsystem.

The navigation function of the system consist of maintaining within the computer a knowledge of the vehicle state vector (position and velocity), and estimates of the state errors and their correlation. Updates of this state vector may be made from both external and on-board navigation. On-board navigation is carried out by the precision measurement of subtended angles by the use of the sextant in the radiation sensor package. The primary mode of mid-course navigation is star-planet measurements, although other modes may be used at times when the orbit lies close to a planet or satellite.

The guidance function of the system lies entirely within the computer, insofar as guidance consists of interpreting the navigation state and controlling the vehicle
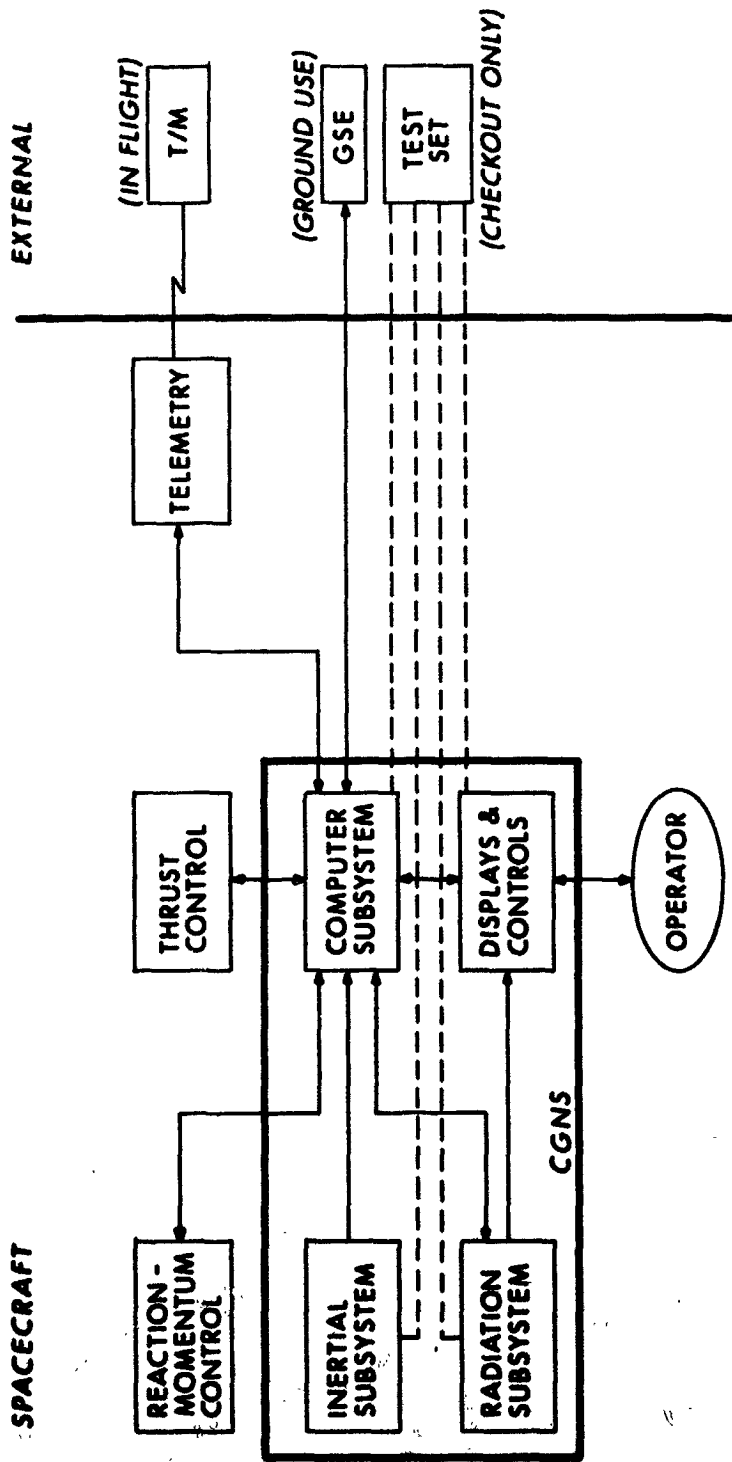
Fig. 2.2-1   Design Model Subsystems.

to produce a new desired navigation state. In the broader sense, guidance can cover the use of the complete system to enable the vehicle to conduct the required mission. In future missions, the limited resources of consumables on-board the vehicle make the reliability of the guidance equipment critical to mission success.

Communications with the system are essential at all phases of system design and testing, vehicle checkout and missions. For long missions, easily assimilable displays and easily operable controls are required for the astronaut. External connection for control, monitoring and testing is required. External navigation information is processed via this channel, but the bulk of information is probably on the system condition itself. The reduction of this data to reasonable bandwidth itself represents a significant new task for the computer.

2.2.2 System Parameters

Control, Guidance, and Navigation System physical parameters have been obtained by extrapolation of Apollo experience, data from developmental hardware, and judgement of the impact of new techniques. The design model itself has certain variable parameters in terms of size. On some missions a degree of sensor redundancy might be required and the size of the computer varies with the requirements for processors and memories. Because of these considerations, the estimates for power, weight, and volume are based on the concept of a simplex system, which will perform the required functions in principle.

The weight estimates for various parts of the system are shown in figure 2.2-2. It is significant that with the trend to integrated circuits and compact interconnection techniques, the principal heavy items are those continuing mechanical devices. These estimates do not include figures for heat exchanges or interconnection. Electrical interconnection weight penalty should be light due to the increased use of time division multiplex, particularly in the monitoring of analog signals.

Reliability figures are merely attempts at intelligent guesses based on Apollo figures modified by changes in types of component and complexity. At this stage it would seem that ultra-high reliability might best be obtained by a combination of in-flight repair and redundancy. In order to guess at the degree of repairability or redundancy reliability figures need only be known to an order of magnitude. Illustrations of this will be given below.

One of the requirements originally envisaged for control, guidance, and navigation of advanced manned missions is a probability of subsystem success for a two hour critical mission period of 0.999,999, this corresponds to a failure rate of 0.5 failures per million hours. With current techniques the achievement of such a low failure rate is not anticipated for complex electronic equipment. The table

	WEIGHT (#'s)	POWER (W)	SIZE (FT³)	FAILURE (10⁻⁶/HR)
RADIATION SUBSYSTEM				
SEXTANT	40	30	0.6	200
TELESCOPE	20	10	0.4	50
SUN SENSOR *	4	5	0.1	20
INERTIAL SUBSYSTEM				
SENSOR PACKAGE (NO REDUNDANCY)	40	60	0.6	250
DDA*	8	10	0.1	150
COMPUTER SUBSYSTEM				
PROCESSOR	10	20	0.2	50
ERASABLE MEMORY (16K)	10	20	0.1	80
FIXED MEMORY (64K)	10	10	0.2	40
TAPE	20	30**	0.35	1000**
DISPLAY / CONTROL	15	20	0.3	100

*OPTIONAL   **DYNAMIC OPERATION

Fig. 2.2-2 System Parameters.

shows how this requirement is reduced by the employment of redundancy and in-flight repair. Experience with Apollo has demonstrated that fault identification of macroscopic guidance equipment can be based on reasonableness checks, thus the use of level-two redundancy is feasible. Figure 2.2-3 demonstrates that, with the use of redundancy and in-flight repair, practical failure rates can be tolerated. The failure rate estimates of the previous table lie within these levels, hence, their order of magnitude is tolerable.

Fig. 2.2-3   Required Unit Reliability Using Redundancy

LEVEL OF REDUNDANCY	1	2	3
FAILURES/HOUR Without Repair For 2 Hours	$< 5 \times 10^{-7}$	$< 7 \times 10^{-4}$	$< 8 \times 10^{-3}$
Without Repair For 100 Hours	$< 10^{-8}$	$< 10^{-4}$	$< 2 \times 10^{-3}$
Without Repair For 20,000 Hours	$< 5 \times 10^{-11}$	$< 7 \times 10^{-6}$	$< 4 \times 10^{-4}$

In practice redundancy may be obtained by techniques other than simple duplication. Sensors may be arranged so that algebraically speaking there are more equations (sensor outputs) than unknowns (independant sensed parameters). Logical operations can be split among several separate logical centers with one or more spares. Integrity of digital memory can be preserved by the use of error checking and correction codes. In these ways the overhead of redundancy may be reduced, however, the matrix of alternatives becomes both difficult to analyze and hard to present.

2.2.3 Software Systems

The design model for software systems is aimed at easing the producibility of mission computer programs. To this end a much greater investment in support software is required than has been traditional. The primary requirement on software is to preserve the error detecting and correcting features of the multiprocessor computer. In order that the task of segmenting programs into jobs that can be re-run under error conditions, the software system incorporates a compiler structure so that the programmer will not be aware of this job segmentation.

Another consideration in the producibility of programs is in assuring that they reflect the intent of the programmer. In the past much reliance has been placed in complex simulation as a tool for checkout. However, the limitation of simulation is the inability to reproduce all the myriad permutations of inputs and timing necessary to give complete assurance of correct program operation. While simulation is important to observe the realtime performance of control systems, a more direct system of program analysis is desirable. Thus, in addition to simulation, a soft-

ware system to perform analysis of programs is used. Program analysis will provide a "microscope" to supplement the usual "eyeball" technique of checking program branching.

A further, but secondary advantage of the use of a compiler to prepare programs is the ability to use a variety of user-oriented syntax. For example, it is convenient to code algebraic expressions in the format of the MIT/IL MAC language. A new or modified language is appropriate for the logical parts of program structure. While good syntax is important in easing program difficulties, experience has shown that the major task has always been in program checkout.

2.2.4 Computer Subsystem

The computer subsystem of the Advanced Control, Guidance and Navigation System must exceed the Apollo Guidance Computer in performance, reliability, and flexibility. The structure best suited to meet these goals is a modular one, where processing power and memory capacity are determined respectively by the number of processor modules and memory modules incorporated and active in the subsystem. Performance and reliability are traded off by an organization capable of graceful degradation, which means that the failure of a processor, memory module, or other sub-unit would result in reduced performance rather than breakdown of the system.

A modular system of this type is called a multiprocessor, and its principal disadvantage is the relative paucity of experience with this sort of computer. In order to realize the reliability goal, the multiprocessor must be able to reassign processors and memories without letting a wrong command be issued and with no loss of data. This requires overhead expenditures of equipment and time which aggravate the reliability problem and reduce performance respectively. A major part of the effort reported here is to design a multiprocessor with a minimum overhead cost. Difficult as it is to design, the multiprocessor structure represents by far the most promising way to realize the advanced system goals.

The design model of the computing subsystem is a multiprocessor with up to about ten processors and about as many data memory modules. A smaller number of instruction memory modules, a few input-output buffers, and possibly some specialized executive control sub-units would be included. Communication among these sub-units is effected by two serial, time-multiplexed bus systems. Each of the sub-units would be comparable in electronic complexity to about one half of the Apollo Guidance Computer. However, because of several years technological advances, they would be substantially smaller and less demanding of power. Processors would execute instructions at about ten-fold the rate of the AGC, using local high speed semiconductor scratchpad memories, integrated circuit logic, and read-only memories for microprograms.
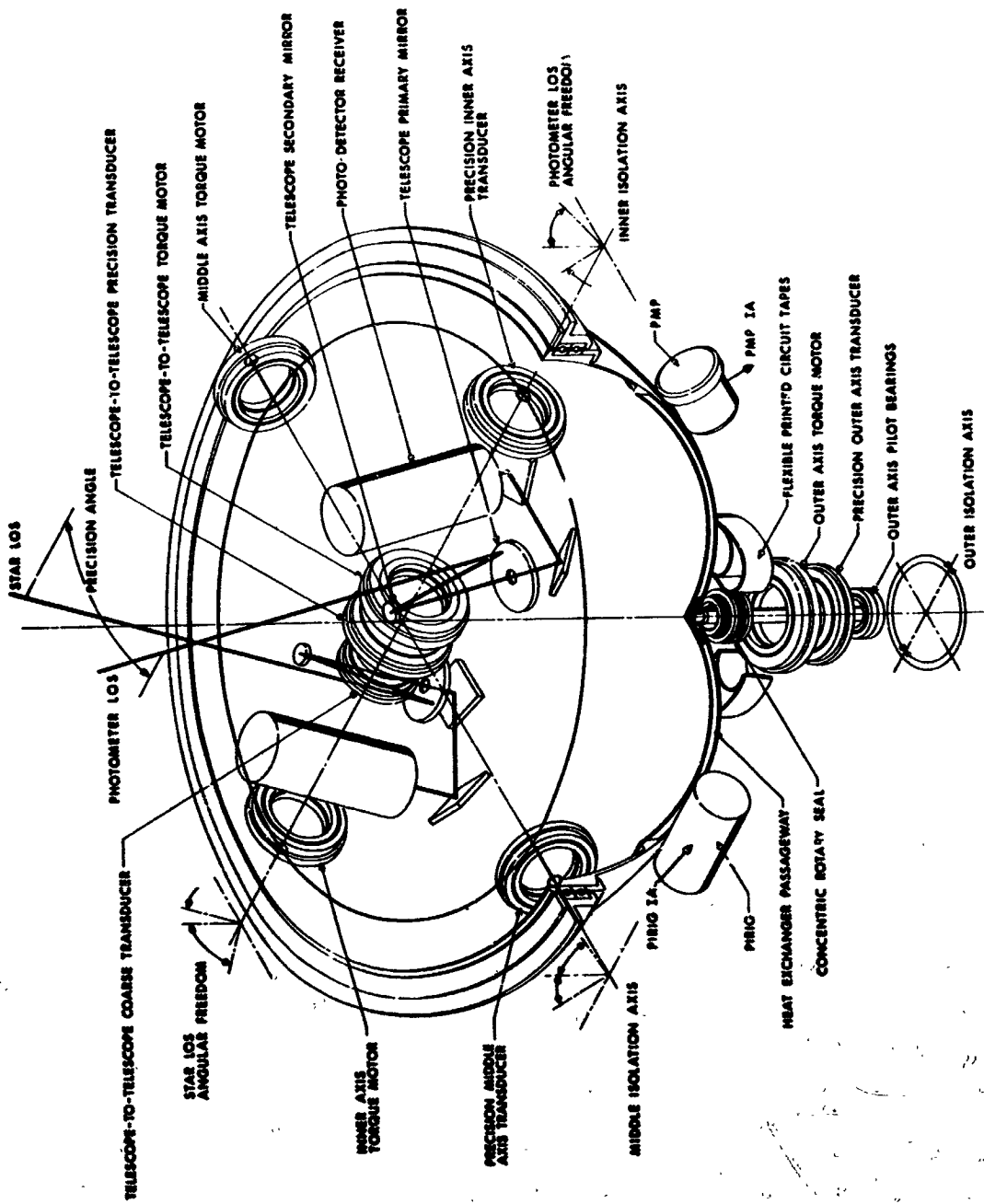
Fig. 2.2-4 Automatic Sextant.

2-8

Data memory units would use ferrite core or plated wire magnetic memories plus many of the techniques used in the processors.

Instruction memories would combine read-only or non-destructive read-out sections with an erasable (NDRO or not) section loaded from bulk storage such as a magnetic tape.

The input-output buffers and executive control units would be small processors using microprograms, local storage and logic.

The transmission of data between the computer and its environment in the spacecraft and in ground communication stations would rely heavily on serial time multiplex techniques. The various signals emanating from and directed to the various subsystems and systems would be buffered, conditioned, and converted between Analog and Digital, if necessary, either at the remote system or in a station local to a group of remote systems. The purpose is the elimination of the many costs of cabling plus the enhancement of design flexibility. Incorporation of a new data terminal requires a small number of cable changes rather than a massive redesign.

2.2.5 Radiation Subsystem

The objective of the radiation subsystem in this design model is to perform the inertial alignment and navigation functions described in section 2.2.1. In the design model here, we have considered a highly automatic design in order to reduce the astronaut load of guidance and control operations, however, provision has been made for the astronaut to monitor all operations. Alternative designs with greater astronaut participation are possible and these are discussed in Volume II, section 4. In general, such direct visual instruments increase the work load and are not as accurate.

The design model RSS (see Figure 2.2-4) consists of a fully automatic photometric sextant with vidicon executive monitoring, in conjunction with a coarse viewing instrument such a a scanning telescope to provide initial alignment by star identification (as an alternative, where a fully automatic capability is required a sun-sensor may be used). We will concentrate further discussion on the automatic sextant, as coarse alignment devices are within the state-of-the-art.

The automatic sextant consists of two separate optical systems mounted on a common trunnion axis, one to track stars and the other to locate a navigation planet limb. The precision navigation angle is directly measured between the two lines-of-sight, the trunnion axis defining the plane of measurement. The trunnion axis is separated from vehicle motion by two degrees of freedom, the first being perpendicular to the spacecraft wall (shaft) and the second along the wall (elevation).

A further degree of freedom about the trunnion axis isolates the common motion of both lines-of-sight. A differential drive between the two lines-of-sight sets up the precision angle. In all, three motions isolate base motion, and a fourth sets the precision angle.

The star LOS uses a sensitive vidicon tracker whereas the planet LOS uses a photometric scanner. Both devices relay images to a CRT display for astronaut monitoring of the function of the instrument.

In the alignment mode the star LOS is used to sequence between two known stars to initialize the inertial reference maintained by the inertial subsystem.

A problem exists in the area of pre-launch testing of the inertial subsystem where it is desirable to have a single axis of rotational freedom to re-orientate the components with respect to gravity and the earth's polar axis. As no in-flight justification for this axis exists it may be desirable to incorporate the ISS on the inner axis (shaft) of the RSS as shown in the figure.

2.2.6 Inertial Subsystem

The inertial subsystem performs spacecraft guidance measurements as its primary function, in addition to its role in attitude control. An inertial orientation reference is maintained by gyroscopes, and accelerometers measure increments of the integral of specific force. Historically it has been the practice to have an actual physical inertial reference (stable member) stabilized by the gyroscopes and carrying the accelerometers. However, in the design model here we employ gyroscopes and accelerometers in the body mounted mode. This enables us to eliminate the complexity of the gimbal system needed to mechanically isolate a stable platform. The reliability and accesibility possible with the body-mounted system is desirable, and the performance is adequate for all currently envisaged propulsion systems (chemical or nuclear).

The main accuracy problems of the body mounted system lie in the pulse restraint of the gyroscopes and the computer algorithm used to maintain the attitude parameters connecting body axes with the desired inertial frame of reference. Measurements on gyros, and analogous work on pulse torquing of the accelerometers, indicate that the required accuracies will be achieved. Table I contains overall performance figures based on current knowledge of instrument and control loop parameters. The figures are well within the mission requirements established in the previous section. General purpose computer algorithms have been written that will accurately maintain attitude providing that body oscillation (angular vibration) amplitudes are not too great at high frequencies. In the presence of large high frequence angular oscillations, the use of a special purpose algorithm computer

TABLE 2.2-1

<u>Gyro Performance</u>

Bias Drift	NBD	1.5 meru
Acceleration Sensitive Drift	ADIA	2 meru/g
	ADSRA	2 meru/g
	ADOA	0.5 meru/g
Torquer Scale Factor	Linearity	50 ppm (<0.3 rad/sec)
	Stability	20 pp. (@0.03 rad/sec)
	Range	±1 rad sec

<u>Accelerometer Performance</u>

Bias	0.1 cm/sec/sec
Scale Factor Linearity	50 ppm (<1g)
Stability	10 ppm
Acceleration Squared	10 ug/g/g

<u>Alignment of Instruments</u>

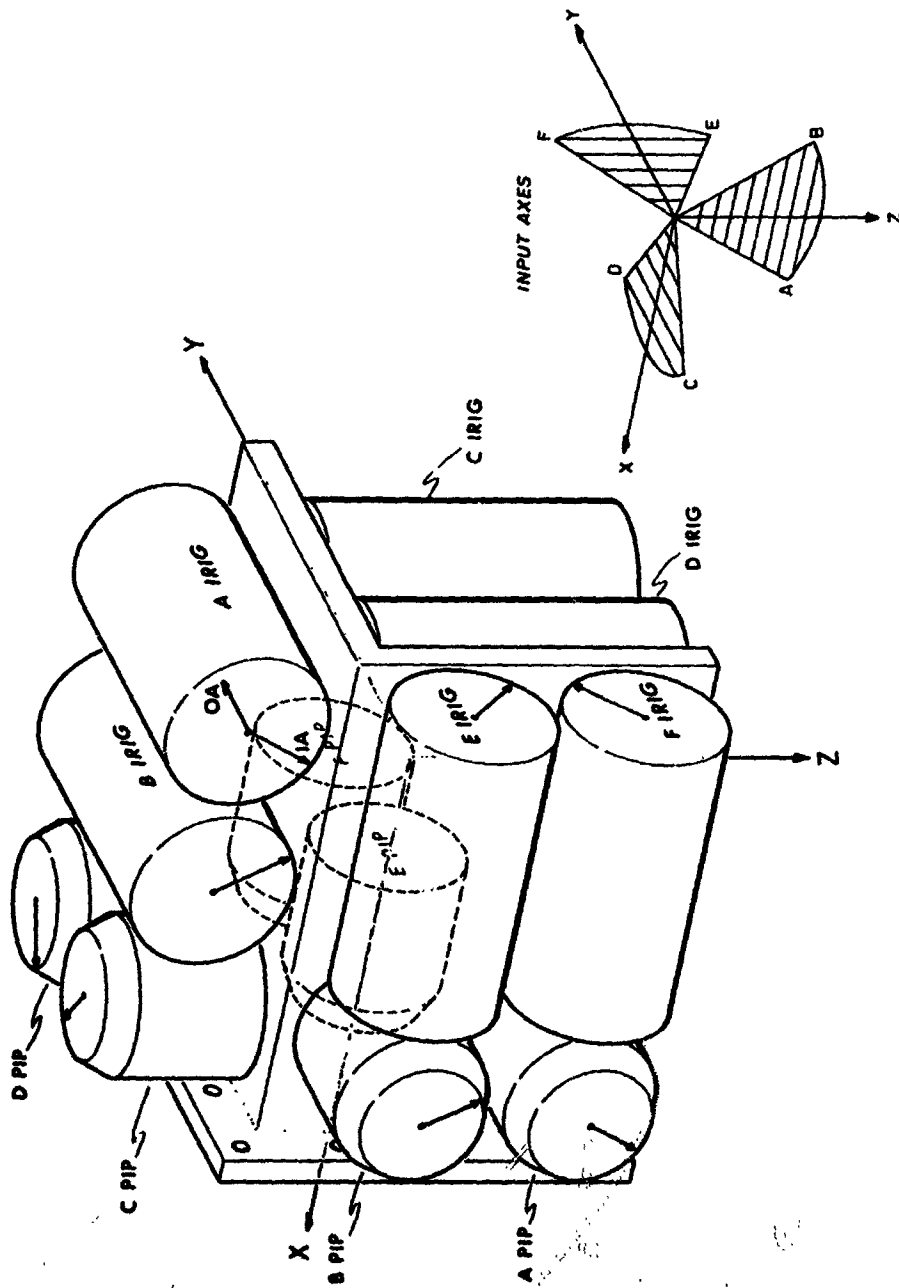|	
Non-orthogonality of Instrument	20 arc sec
Optical Alignment	60 arc sec

Fig. 2.2-5 Hexad-Array Strap-Down Configuration Package.

becomes desirable. Suitable algorithms are available for use in a digital differential analyzer (DDA) mechanization of such a computer.

Economies in achieving the desired reliability of the inertial subsystem can be obtained by the use of redundant inertial components. In the design model six gyroscopes and six accelerometers are used in a symmetrical non-orthogonal configuration. Figure 2.2-5 shows in diagramatic form the mechanical arrangement. The sensor input axes are arranged in a unique symmetrical pattern that corresponds one to one with the array of normals to the faces of a regular dodecahedron. This configuration allows a measure of self-contained failure isolation and detection by comparing instrument outputs. Up to three of either instrumentscan fail before complete system failure occurs. Overall system viability is further enhanced by the use of modular plug-in instrument packages.

Anticipated algorithm requirement consistent with one meru performance with coning input of 1/2 degree amplitude in the range 4-10 cps and as much as 1 rad/sec slew rate are shown below. Coning represents the most severe disturbance in all cases.

	General Purpose 3rd Order	DDA 1st Order
Update rate	100-250 /sec	1500-4000 /sec
Quantization	2-6 arc sec	2-6 arc sec
Word length	30 bits	30 bits

The use of redundancy leads to certain logistical problems of how to resolve conflicting information. In flight, knowledge of expected vehicle behavior gives a good guide to resolving these problems, however, when the vehicle is being assembled on the ground, no such criteria exist. For this reason it may be desirable to introduce an axis of rotation for testing as mentioned in section 2.2.5. Such an axis could be established by combining the space sextant with the inertial package. Rotation of the axis (and Earth) would provide test inputs to the gyroscopes, and the motion of the Earth's gravitational vector with respect to the package would allow for accelerometer checking.

2.2.7   Temperature Control System

Certain parts of the CG&N System require accurate control of temperature, while the majority of components only require cooling to maintain temperature within a broad band. General temperature control of a spacecraft system by the use of a coolant loop suffices to maintain general temperature control requirements. Specifically, in the manned spacecraft the electronic systems are more tolerant than the operators, and, thus, the environmental control system based on the

THERMOELECTRIC MODULE (2)

SPACER/INSULATOR (2)

HEATSINK

ALIGNMENT SCREW (1 of 2)

18 IRIG

THERMOELECTRIC MODULE (1)
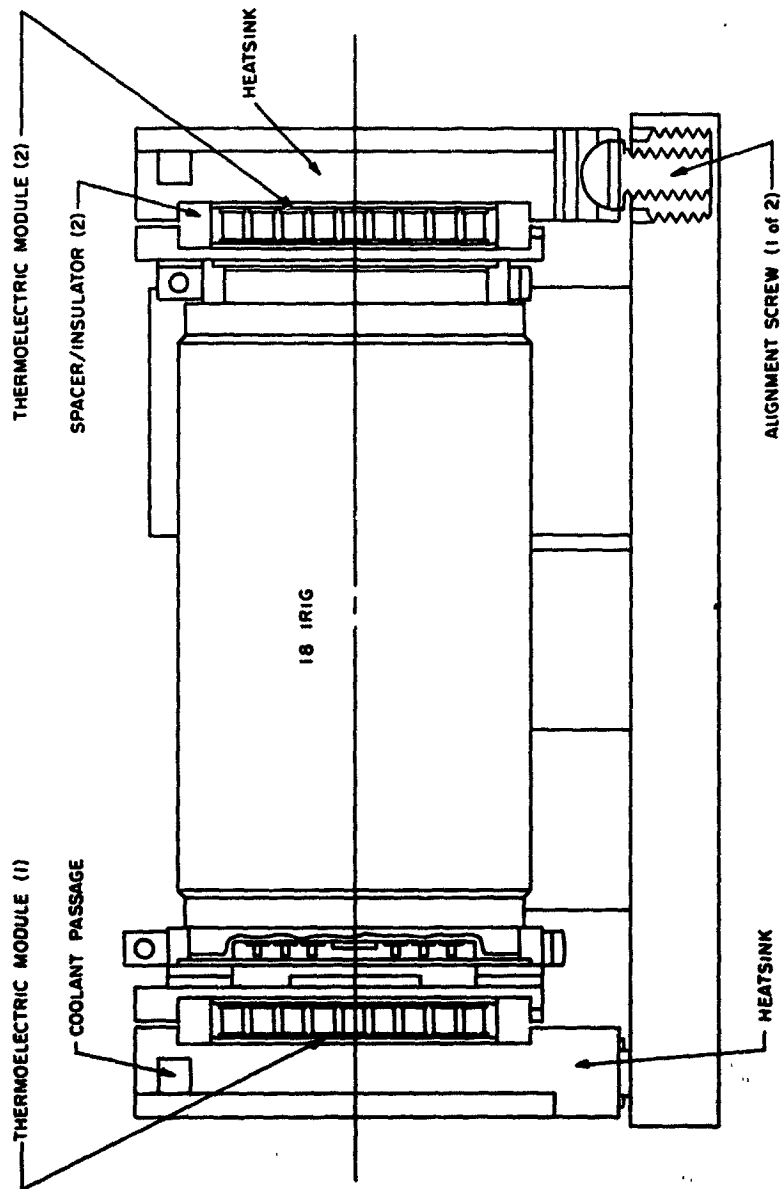
COOLANT PASSAGE

HEATSINK

Fig. 2.2-6   Final Design Gyro Mount.

requirements of the latter will suit the former. However, critical components (usually mechanical in nature) such as oscillators, gyroscopes and accelerometers require special treatment. We will concentrate our attention here on the control of the inertial sensors, as these are the most bulky and heat-dissipating.

In the past, inertial components have been temperature controlled by applying heat to the instrument and allowing it to dissipate through a thermal resistance down to a heat sink. Heater power had to be sufficient to allow for all changes in heat dissipation within the instrument, changes in thermal resistance and variation in heat sink temperature. In the CG&N design model the employment of this continuous control heat has been avoided to reduce heat dissipation and power consumption. Two techniques have been used. First, the employment of simple by-pass techniques enable the heat sink to be controlled somewhere in the neighborhood of the required control temperatures. Second, the use of the reversible heat pump obtained by the employment of strongly thermo-electric materials enables bi-directional control of the instrument temperature.

Modern thermoelectric devices show a high coefficient of performance when compared to conventional heaters, in addition, they can cool as well. In the Appendix (A) we show results using an experimental gyro mount where coefficient of performance in excess of 3 is obtained when the heat sink is within 10 degrees of the control temperature. i.e., the thermo-electric device only uses one third of the power of an equivalent heater. Since performance of these experiments, the design of the gyro mount has changed.

The design model gyro mount is shown in figure 2.2-6. It contains an important new concept in mechanically separating the alignment function from the thermal control function. Alignment is performed by rotating the complete gyro cradle on the kinematic mounting formed by the three screw feet. Thermal control is by the use of individual thermo-electric cooling units and heat sinks at either end of the instrument. Conduction of heat from the sinks to the unit base may be enhanced by the use of two-phase heat pipe techniques. The use of separate temperature controllers on each end of the instrument corrects for assymetric heat dissipation in the instrument (e. g., when torquing) and gives a useful degree of redundancy allowing degraded performance where one controller fails.

2.2.8 Two Dimensional Display

The objective of the two dimensional display project has been to examine ways of instrumenting some general purpose display to replace the host of individual instruments currently used in spacecraft. In order to remain within the current state-of-the-art, no three dimensional techniques were considered, and of two dimensional techniques, the Cathode Ray Tube was chosen. In the realm of man-to-machine communication, the CRT display has already demonstrated its value. The application of this type of display to the spacecraft environment will take advantage of its flexibility in communicating a variety of different information media under the control of a computer or central processor. Specifically we have studied here the elimination of unnecessary interaction between computer and display. Comparable techniques can be employed for other two dimensional display devices.

2.2.8.1 Types of Display

Spacecraft and aircraft cockpits are presently filled with a mass of meters and instruments. Much of this displayed information is needed only occasionally, and for short periods. The general purpose CRT display shows only the information needed, without confusion and in the most easily assimilated form.

The spacecraft computer, scanning all information sensors, shows, any undesirable emergency or alarm condition on the CRT display in needle, bar, dial, or digital form. Flashing pictures may be used to attract the pilots attention, and corrective action advice can be displayed concurrently.

A variety of so-called "contact analog" displays can be generated. These artificial pictures of highways in the sky or underwater are beginning to be used in aircraft and submarines. The pilot is presented with an apparent 3-dimensional picture of his position in the environment and the proper path he should follow. The "8-ball" Flight Attitude Indicator used in Apollo belongs to this class of displays. Due to the complexity and varied data content the FDAI "8-ball" was chosen for a detailed study of instrumentation techniques. Appendix B describes the techniques and trade-off to conserve computer time and memory. Map or starfield pictures for landing and telescope positioning are related uses of the contact analog display.

The problem of real-time man-computer communication on the spacecraft can be handled by the CRT display. A direct replacement of the present DSKY readouts is obvious, with symbols other than numbers possible for dir-

ections, warnings, mode requests, etc. A progressive conversational inquiry
tree would permit decisions. Pushing the corresponding button would tell
the computer which decision was chosen, and a new set of choices would be
presented. This technique reduces human errors in button-pushing codes,
restricts answers to those which are germane, and speeds up the commun-
ication and command process. The pilot can be guided thru the procedure
he is to perform without any additional check list.

2.2.9 Interconnections

All the requirements put on a highly reliable long-life CG & N system
tend to increase the complexity of system interconnection. Even in the Ap-
pollo PGNS (and spacecraft), system harness contributes a significant pro-
portion of the weight. At a time when the size of active electronic modules
is reducing rapidly, wiring technology remains fairly static. For advanced
manned missions it is essential that techniques be employed to reduce the
weight of interconnect harness.

Review of current techniques show that interconnections are not used
efficiently. For example, a single wire may be assigned to conduct an
alarm signal with little likelihood of occurrence in operation at all. This
example shows how the power handling capacity and information band width
of the channel (wire) is hardly utilized at all. The technique proposed to over-
come this problem is the use of time-division multiplex in the form of pulse
code modulation. Such techniques are frequently employed where there is
a more formal limitation on channels such as radio communications. The
cost of such a system is the additional electronics required for signal con-
ditioning wherever a signal is to be transmitted in code. However, elect-
ronics sizes are becoming so small as to be not critical, and in any case
the signals may have had to be processed anyway. (e.g. for telemetry) The
reliability of these devices is not critical providing it will not react back
into the main body of the equipment.

Provided that the concept of time division multiplex is adopted where
applicable, a number of additional benefits result ("fall out"). Firstly, with
the reduction of the number of system interconnect channels, redundancy tech-
niques are more easily instrumented to maintain the integrity of communica-
tion of essential signals. Secondly, as all signals are transmitted in digital
form, it is much easier for the system to perform a degree of "introspection"
in that the computer can examine the state of many internal signals. Thirdly,
pre-processing of telemetry signals is possible in the computer whereby the
required data rate can be reduced easing the load on radio communications.

For example, D. C. levels within the normal range expected do not need to be transmitted at all.

For pulse code modulation of signals, standardization of circuitry and message format is highly desirable. The relative inflexibility of large scale integrated circuits is the prime consideration for standardization plus the need for common processing ability at the computer interface. For convenience, message lengths equal to half the computer word-length would enable packaging two to a word in memory. Assuming a computer word length of 20 bits, the half word would give sufficient combinations to serve both as address and data (0.1%). Full word messages with both address and data may be desirable under some circumstances.

3. CONCLUSIONS AND RECOMMENDATIONS

3.1 Summary of Study Accomplishments

As reported on in the four volumes of R-600, tne study and development funded by NASA Contract NAS-9-6823, Task II, covered a wide range of problems involved in Control, Guidance and Navigation for Advanced Manned Missions. In retrospect it is clear that an effort of just ten months duration could only initiate a program in the related areas of systems, computer subsystems, radiation sensor subsystems, and inertial subsystems. Nevertheless, the following results were achieved and form the basis for further work in the future.

In the Systems area (Vol I) a study was carried out of the guidance and navigation system requirements for advanced manned missions. Evaluation of inertial subsystem performance and its effect on a transplanetary injection of a large vehicle showed that acceptable injection errors can be obtained from inertial subsystems having performance that is attainable today with reasonable effort. Guidance requirements for midcourse corrections were found to be non-critical. Guidance performance in the final hours of a return-to-earth transfer orbit and during atmospheric entry were studied and found to be very critical. In fact, the design of this final mission phase was identified as requiring the greatest advances from the standpoint of reliability as well as performance.

A navigation requirements study was organized and constructed on a flexible, comprehensive basis so that, for a variety of missions in the Solar System, it is possible to determine the types of measurements, the optimum choice of navigational target bodies, and the resulting velocity correction schedule and navigational uncertainties in position and velocity. This study program was applied to a Mars flyby and a triple-planet flyby involving Mars and Venus. Evidence accumulated that flexibility and automaticity were just as important as basic accuracy in radiation sensor subsystems under development.

Utilizing inputs from systems studies and from development in the area of computer, radiation, and inertial subsystems, a Design Model was created showing a representative Control, Guidance, and Navigation System for Advanced Manned Missions. Inherent in the thinking going into the Design Model were the goals of reliability, flexibility, and performance. Related development and some hardware tests were carried out in the areas of two-dimensional displays on cathode ray tubes and the use of thermo-electric devices for the precise temperature control of inertial components.

In the computer subsystem area (Vol II), the studies and development began by recognition of the Apollo experience with the computer's role in the Apollo system which has been the object of demands on performance, speed, and capacity far beyond what was originally envisioned. Requirements for advanced computers were described having in mind order of magnitude improvements in requirements and a flexibility in use that will provide a firm basis for meeting unknown future demands.

A multiprocessor concept was developed and is explained in Volume II. Related concepts of time multiplexing, data and instruction memory, processor operation, executive control, and input/output function were all developed. The necessary electrical design of the required logic was investigated. In the areas of hardware research and development to make possible the multiprocessor computer, substantial progress was reported in the area of braid memory and an I/O multiplexed bus. The all-important areas of integrated circuits and interconnections and packaging received only limited attention due to the scope of this particular contract.

The multiprocessor concept was brought to the point where it is believed to be ready for and worthy of the next, more heavily funded stage of development.

In the area of radiation sensor subsystems (Volume III), the geophysics and planetary studies brought together the latest and best information of possible navigation phenomena for use in the solar system. This effort was then used to create mathematical error models of navigational sighting phenomena for use in navigation error sensitivity analysis and in the requirement studies developed for Volume I. These requirements studies, in turn, fed back design specifications to the radiation sensor subsystem effort. Basically, accuracy requirements appeared to be not an order of magnitude greater than those for Apollo. Other subsystem features such as flexibility and automation were found to be significant. In parallel with this effort, but using its emerging conclusions, there was carried out a hardware design effort. Space sextant design studies resulted in a four-degree of freedom instrument for visual use by astronauts and a different design, also having four degrees-of-freedom, but based on electro-optical sensors. Angle transducers such as resolvers, theodosyns, and ring lasers were evaluated. Reports were provided on design details such as bearing heat transfer, design of folded optical paths, design for minimum scattered light, and the human eye as a sensor particularly where flashing light beacons are involved. In summary, a wide spectrum of possibilities was investigated following the general requirements determined in the systems study.

Inertial subsystem technology (Volume IV) involved an effort that focussed both on performance and reliability. Against the background of emerging requirements, a program was undertaken to develop and evaluate a concept using strapdown inertial techniques.

The objective was to obtain an understanding of the reliability and performance potential of the strapdown system in comparison with the better known and developed gimballed inertial subsytem. By going in this direction, the foundation has been laid for making a wise choice at some point in the future.

Analytical studies were made of the strapdown concept algorithm and its associated errors. The Pulsed Integrating Pendulum (PIP) in a strapdown environment was analyzed for its error sources. The single-degree-of-freedom Inertial Rate Integrating Gyro (IRIG) in association with its pulse-torque to balance electronics was studied and reported on.

At the same time, development effort was put into obtaining developmental PIPs and gas-bearing IRIGs for actual test evaluation. A gyro test package development tool and strapdown test facility was designed and constructed. Test concepts were evolved and mechanized in the test facility.

The inertial subsystem analytical and hardware effort has brought the concept of strapdown inertial subsystems to a point where developmental testing can be used to obtain an accurate evaluation of the potentialities of such systems.

In summary, the study accomplishments reported in these four volumes have generally pointed the way for soundly based further work. The national space program will eventually arrive at an appropriate stage where there must be a development program for a specific control, guidance, and navigation system for Advanced Manned Missions. it is timely now to consider the continuing work which can bridge the gap between the accomplishments reported on in these four volumes and the technological base that must be created before an advanced system program can be launched on a large scale. The following section addresses itself to recommendations for further work to bridge this gap.

3.2   Recommendations for Further Work

This section is devoted to emphasizing those aspects of continuing development work on advanced systems which seem most crucial in a time span where the long range goals of the national space program are being evolved against a background of other heavy demands on our national resources. Consequently, the recommendations emphasize steady but moderate levels of attack on the technical problems until the time when the nation is in a position to commit itself to the next major goal for a manned mission. This type of work should result in progress in knowledge, techniques and requirements.

3.2.1   Analytical Tasks

Surely the recommendation for further effort in this area which would bring the largest amount of return for the least amount of effort is to use the tools which were developed in this effort to continue the mission requirements study. The results presented in this report represent only a small sample of what could be obtained with more time and effort. Much more interpretation of the data and detailed study of individual problem areas can still be done within the framework of the analytical tools which have already been established as part of this contract effort. In short, we have made the investment in development time but have not yet fully realized   potential returns on this investment.

Much interesting and important work must yet be done in the area of transplanetary injection from earth orbit. To inject some of the extremely large vehicles under consideration can require very long burn times - up to 40 minutes. On some of these injection trajectories the vehicle travels almost half way around the earth. The experience gained in generating the trajectories for the error studies have indicated that a fresh look at the guidance scheme used is in order. Ideally it shouod be formulated as a minimum fuel optimization problem with three types of constraints: 1) the time of arrival at the sphere of influence   after a free coast period should be fixed, 2) the velocity vector at this arrival time is fixed, 2) a state variable constraint to prevent altitude from dropping below a specified value must be imposed. This last state variable constraint was not considered in the scheme used here. This led to some dangerously low altitude on some paths.

The control problem associated with the transplanetary injection also deserves attention. Controlling these massive flexible vehicles while they expend a large fraction of their mass is a challenging task. The fact that bending and slosh modes will be significant but poorly specified hardly makes matters easier. This job will amount to designing a controller for a poorly specified time-varying plant.

Much additional work can also be done in the navigation area. This study revealed some inference that optimizing the overall measurement schedule instead of individual measurements might yield good results - particularly in the near planet cases. The techniques for doing this are established, it is just a matter of applying them.

More work on criteria for measurement selection is also in
order. One potentially useful one is to minimize the velocity uncertainty
at a specified target point. It it would yield smaller velocity deviations
at the outbound intersection with it the sphere of influence, a saving in mid-
course fuel   required for the next interplanetary leg might be achieved.
Experimenting with combinations of criteria on a given trip should also
yield good results.

One of the options which was built into this error analysis proce-
dure but never used is the ability to estimate planet diameter. This area
should be pursued to determine its effect on error reduction. An interest-
ing modelling problem arises here — how much of the reduction in planet
diameter uncertainty can be subtracted from the part of the measurement
noise due to phenomena error?

In any continuing effort the moons of at least Earth and Mars should
be included for celestial navigation purposes. A detailed trade off study be-
tween the various unknown landmark schemes should be performed.

Finally, a key area where much more detailed study is required is
that of Earth entry. As indicated in Section 1.2.3.2, the critical guidance
problem of atmospheric entry should be given further study to come up with
definitive requirements on performance and reliability. This study should
begin with a mission model which includes a terminal portion of the return
interplanetary leg as well as the atmospheric entry itself. The mission mod-
el should be joined by a representative crew timeline covering such activities
as activation and checkout of the earth entry module, final velocity corrections,
etc. With this material as a foundation, the entire mission phase should be
studied. Initial conditions in the guidance system should be defined, using
optimum on-board sighting schedules and prolonged Deep Space Network
tracking. The actual study would then deal with the requirements placed on
steering laws, inertial performance, reliability indexes, etc. by entry cor-
ridor goals, human tolerance to prolonged g loads, heat load capability of the
entry shield, etc. The results of the study will probably represent the most
stringent specifications on the guidance system reliability and performance.

Contributions coming to the above analytical tasks from the Radiation
Sensor area would include the following:

An updating of the analysis error models based on the final
material in Vol. III.

An analysis of limb phenomena "locators", as contrasted with
general limb phenomena models.

Analysis of sensor designs based upon the "locator" phenomena
selected in order to obtain a best estimate of anticipated uncertainties.

In the Inertial Subsystem area an analytical task of particular interest in an investigation of weighting and trade-off criteria for optimization of strapdown inertial subsystem algorithms and sensor compensation techniques. Development of failure prediction techniques for gas bearing gyros is part of the broader analytical area represented by the reliability demands for advanced manned space missions.

3.2.2 Design Study Tasks

The navigation instrument concept described in Chapter 2 of this volume and defined in more detail in Vol. III is very promising. It seems appropriate now to proceed with the design of an engineering model to be used as a developmental tool. Similarly, design studies should proceed on the scanner photometer package associated with the navigation instrument.

Several design activities can be recommended for the inertial subsystems area. Design improvements of the 18 IRIG, Mod B, as described in Vol. IV, should be carried on as a continuing effort particularly because of the long lead times involved. Development of the inertial sensor module kinematic mount concept should be accelerated because of its key role in a maintainable, high-performance inertial subsystem. Finally, in the electronic design area, work should proceed on the optimal torque-to-balance instrument control loop as described in Vol. IV.

3.2.3 Hardware Development Tasks

In the Radiation Sensor area, the engineering model of the navigation instrument mentioned in Sec. 3.2.2 should be constructed. Only by taking this step can the fundamental soundness of the concept be demonstrated. Similarly, another worthwhile hardware effort would be the construction of a video tracker.

In the Inertial Subsystem task, the effort completed under the present contact has produced a strapdown inertial test package, test station, and algorithm facility. Continuing effort will logically build upon this accomplishment a test and evaluation of the integrated test package - real test algorithm.

In the Computer area, the simulation effort begun in 1967 should be continued and expanded to include preparation and execution of programs. Prototype construction of sub-units should start as soon as feasible, and a multicomputer hybrid simulation should be designed and executed in due course. These tasks are essential to the expeditious development of the high unconventional structure which is deemed necessary for extended space missions.

3.3 Recommendations on a Development Plan for an Advanced Control, Guidance, and Navigation System.

3.3.1 General

The following paragraphs attempt to offer some program guidelines for consideration when the national space program establishes an advanced

mission as a major goal. Emphasis is placed on areas of interaction between the CG&N, as a subsystem, and the rest of the mission.

Any advanced manned mission established in the future as a national goal will be able to draw on a wide spectrum of preliminary studies already in hand. Technical aspects of advanced missions have been researched over the past decade not only by the National Aeronautics and Space Agency but by other public and private agencies as well. The technical material already at hand will form the starting point for overall system definition.

At this early stage, the CG&N subsystem effort should be brought into the program. The multiple areas of interaction between the CG&N Subsystem and the total System make this early, integral participation essential. Furthermore, it is probable that a space station program will precede any manned interplanetary missions. Participation in early space station mission planning by CG&N-oriented agencies would permit identification and development of experiments and qualification hardware related to ultimate CGN goals.

In the following sections, CG&N Program Tasks are identified in the following areas and discussed individually:

> Systems Integration
> Space Guidance Analysis
> Computer Subsystems
> Radiation Subsystems
> Inertial Subsystems

3.3.2   **Development Plan Task**

3.3.2.1   Systems Integration Task Objective

To firm up CG&N subsystem specifications for advanced manned missions. In the systems integration task this involves accomplishing the following sub tasks:

> 1.   Develop, expand, and maintain an Advanced Control, Guidance, & Navigation "strawman" or design model based on inputs from other task groups:
>
> a.   Space Guidance Analysis
> b.   Computer subsystem
> c.   Optical Subsystem
> d.   Inertial Subsystem

2. Conduct continuous liaison with appropriate spacecraft and mission groups to factor into mission, spacecraft, and ACGN design models the following specification

    a. ACGN configuration power, weight, volume, reliability, and performance.

    b. Communication interfaces

    c. Astronaut interfaces

    d. GSE interfaces

3. Conduct development which leads to unified system packaging and electronic techniques.

4. Develop a Display and Control (D&C) philosophy, evaluate individual components and assemblies, and create an ACGN D&C specification.

5. Conduct a reliability evaluation program which looks at materials, processes, and techniques in relationship to long, long term missions. Maintain a system reliability status report. In addition to ACGN hardware, surveillance shall be maintained over interconnect elements such as coaxial cables, feedthroughs, mountings, etc.

3.3.2.2 Space Guidance Analysis Task Objectives

1. **Analytical.** To provide a continuing evaluation of navigational accuracy requirements for advanced manned missions. This involves a general capability to simulate certain missions with computer programs, to conduct error analyses of selected trajectories, and to arrive at recommended measurement schedules, measurement accuracies, and guidance implementation accuracies. Such studies are basic to a rational approach to an ACGN system. In addition, there will be requirements for vehicle control and guidance studies. Ultimately such control studies must be based upon expanding knowledge of the proposed vehicle characteristics. But prior to that phase, work can be done on control techniques which minimize sensitivity to vehicle static gain, bending modes, fuel slosh, etc.

2. **Software.** The development of a new computer subsystem for new manned missions requires support in the areas of computer software. Initial software tasks which are to be undertaken in cooperation with computer subsystem development are the design of:

a. Programming concepts

b. Programming language

c. Program verification methods

Following this phase, a compiler must be designed, written, and debugged for the computer. Similar effort must be applied to the program verification method.

As the nature of the ACGN system and its interfaces with the spacecraft and with the external world are developed, the system level programs can be developed. Finally, as the participation of the ACGN in manned orbital flight becomes defined, then a library of mission modular programs can be built up.

3.3.2.3 Computer Subsystem Task Objective

To design and develop an advanced computer subsystem which will meet general long range objectives for advanced manned missions as established by NASA. Substantial advances are required in the areas of computational speed, memory volume, reliability, and logical design for non-catastrophic degradation.

Initial design tasks involve decisions on multiprocessor logic, error detection and correction, serial multiplex data transmission, etc. It is necessary to evaluate the design, and its logical implementation by a breadboard feasibility machine using commercial or state-of-the-art hardware. Concurrently, circuit joining and packaging work will be under way. Large scale integrated circuits will be evaluated, if not developed.

As second generation hardware reaches evaluation readiness, portions of it will be substituted in the breadboard feasibility machine as a method of evaluating the new design. This should lead the way to an evaluation of elements of hardware design as part of the complete machine.

Meanwhile, to meet a possible need to support orbital flight evaluation of ACG&N hardware an orbital computer prototype should be planned. This machine will be oriented to the multiprocessor concept but will not meet the ultimate specifications either in speed or in capacity. Its purpose will be to support the development of the computer subsystem for the orbital or space station mission.

A set of computer subsystem drawings represents the end product of this early phase of an advanced computer effort.

3.3.2.4 Radiation Subsystem Task Objective

To undertake to reach the following objectives relating to radiation subsystems for advanced manned missions.

1. Conduct a study program to update knowledge of the potential navigational reference features in the solar system and their ability to meet the mission and system requirements. Such phenomena as planet terrestial or atmospheric limbs, planet radiation distribution centers, target image rates, microwave and laser radar ranging, are involved.

2. Use these studies to develop sensors and related electronic and mechanical hardware to utilize the phenomena which have been identified above in addition to star phenomena to be used for celestial attitude reference.

3. Evaluate these sensors to the extent possible in laboratory or atmospheric test programs and also design and develop the necessary experiments which can be used to qualify these sensors on early manned and unmanned missions.

4. Design and develop radiation subsystems for advanced manned missions, based on the results of the above tasks.

This technical area is characterized by the need for geophysical research and associated analysis to determine optimal phenomena - locator - sensor combinations, systems analysis, and engineering development experiments in the laboratory and in space environments.

Sufficient fundamental scientific information on solar system reference features is available, to ensure the feasibility of accurate interplanetary on-board navigation. But this knowledge is limited and any new data from unmanned probes will permit the development of a more optimal system. Thus, one objective will be to maintain a close communication with groups associated with unmanned planetary probe missions so as to be cognizant of all pertinent data. Another need is to have developmental data needs reflected in the instrumentation of future unmanned probes. Future data would be desirable to confirm present estimates thus increasing confidence in existing planetary data. For some as yet unspecified mission it may also be desirable to reduce the uncertainties further which could be accomplished during future unmanned or manned missions. It is anticipated that the uncertainties indicated in Volume III can be considerably reduced

over the next few years using anticipated future probes, which could then be reflected in the software of the first manned planetary missions without significantly impacting hardware design.

Early effort would involve maintaining a design model of the radiation sensor subsystem based upon best available scientific and engineering information. Concurrently, systems analysis and component system development would be accomplished. Several experiments would be identified and designed involving materials, components, and sensors. These experiments would be suggested for inclusion on certain AAP missions.

In parallel and prior to receiving all of this information, a radiation subsystem will be developed for use and evaluation on extended orbital flights such as a space station. This interim subsystem would involve design and construction of an engineering model and a prototype for use in a test and qualification program. In the sequence suggested here, a set of subsystem drawings would be available for use in bringing an industrial contractor into the program.

3.3.2.5 Inertial Subsystem Task Objective

To design and develop a strapdown inertial subsystem which will meet requirements for advanced manned spaceflight missions. Particular emphasis has to be placed on a new concept and order of magnitude in the area of subsystem reliability. Inertial performance requirements established as part of the space guidance analysis task must be met. The subsystem must provide attitude information to the computer of the necessary quality to meet the control needs of the space vehicle. Operational modes must be defined and the power consumption of the subsystem reduced to an absolute minimum. The following subtasks are identified as essential to this subsystem:

1. Continue development of higher performance and reliability inertial components.

2. Develop electronic designs which will make possible the attainment of subsystem specifications.

3. Develop specific packaging techniques for electronics.

4. Develop inertial subsystem test techniques and demonstrate them in a prototype test facility.

5. Develop inertial component alignment techniques and hardware.

6. Develop and evaluate associated computer attitude and velocity algorithms.

7. Analyze inertial component errors and evaluate possible software compensation programs for the computer algorithms.

8. As the result of the above efforts, issue a set of inertial subsystem drawings for use in introducing an industrial contractor into the program.

The objectives of the inertial subsystem task should be met by a continuing program of analysis, design, test, and evaluation. Inertial components should be tested in conjunction with their electronics for required design improvements. which will be fed back to the inertial component designers. Development results in the areas of inertial components, alignment hardware, electronic design and packaging, and thermal control should be brought together in an engineering model or models and later in an inertial subsystem prototype.

Concurrently in inertial subsystem test facility should be under development. This would consist of the necessary electronic GSE, and inertial test table, and a small computer for evaluating algorithms and inertial compensation schemes.

Part way through this sequence, inertial component specifications will be available and vendor competition can be initiated. At the end of this test and evaluation phase, a set of inertial subsystem drawings would be available for use in bringing an industrial contractor into the program.

3.3.3 Program Schedules

There follows a set of figures (Figs. 3.3-1 through 3.3-5) which attempt to recommend an interrelationship between the progress of the five individual tasks described in Section 3.2.3. Necessarily, dates are left off. The deployment of a manned space station is keyed into the development time schedule of the program because of its essential role for ACG&N qualification, even though this qualification role is only a subordinate part of a space station mission.

3.3.4 Conclusion

This final section has been devoted to highlighting from a program point of view those critical tasks which will initiate and carry forward the design and development of a control Guidance & Navigation System for Advanced Manned Missions.

System Integration Schedule

Years	1	2	3	4	5	6

SPACE STATION
Hardware specs
Mission Launch

ACG&N PROGRAM
Orbital Milestones

SPACECRAFT DESIGN LIAISON

ACG&N DESIGN MODEL

D&C INTERCONNECT SPECS

PACKAGING STUDIES

COMPONENT RELIABILITY

SYSTEM RELIABILITY

MECHANIZATION DRAWINGS

TEST DOCUMENTATION

SYSTEM DRAWINGS

Subsystem Prototype
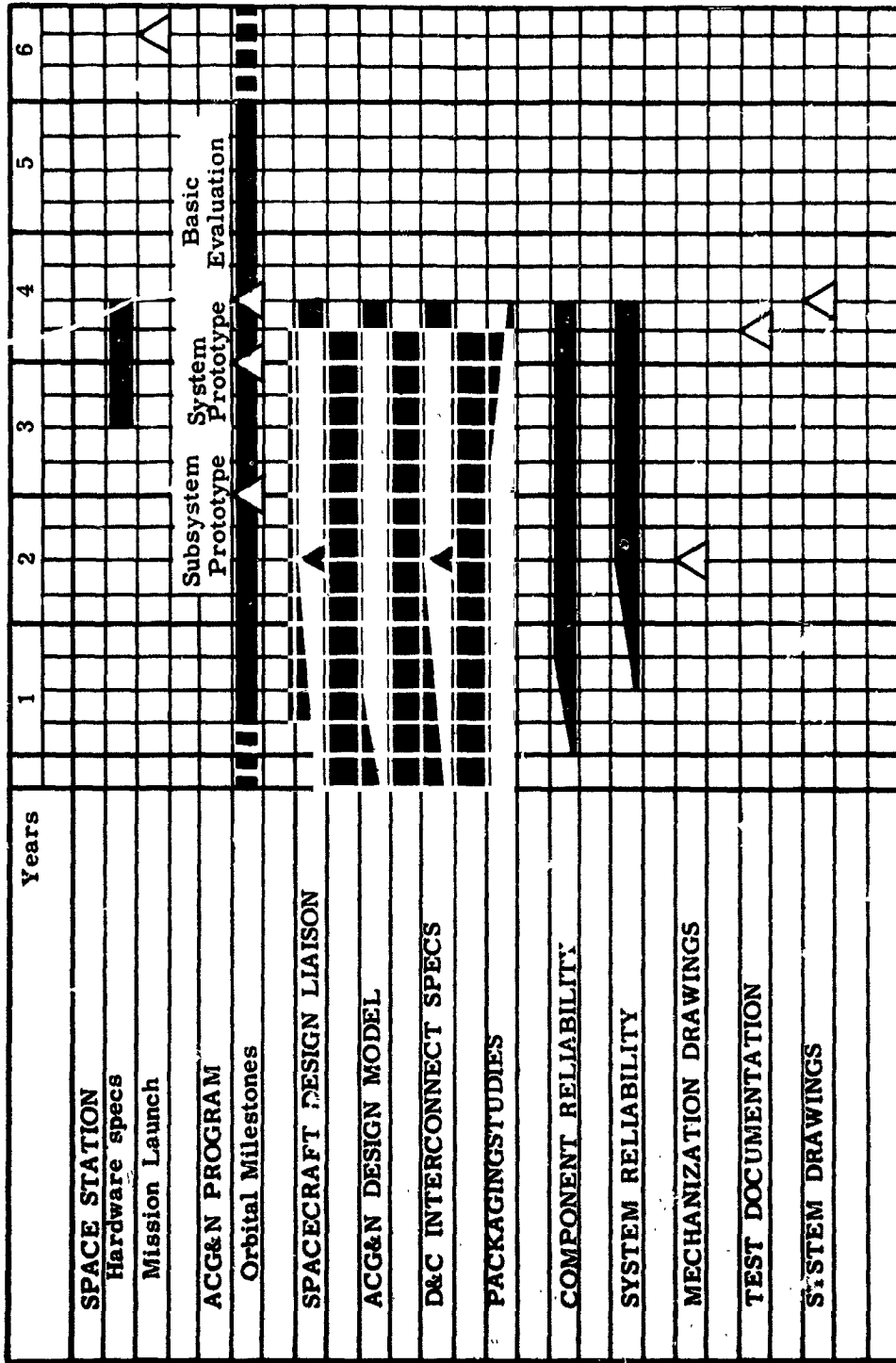System Prototype
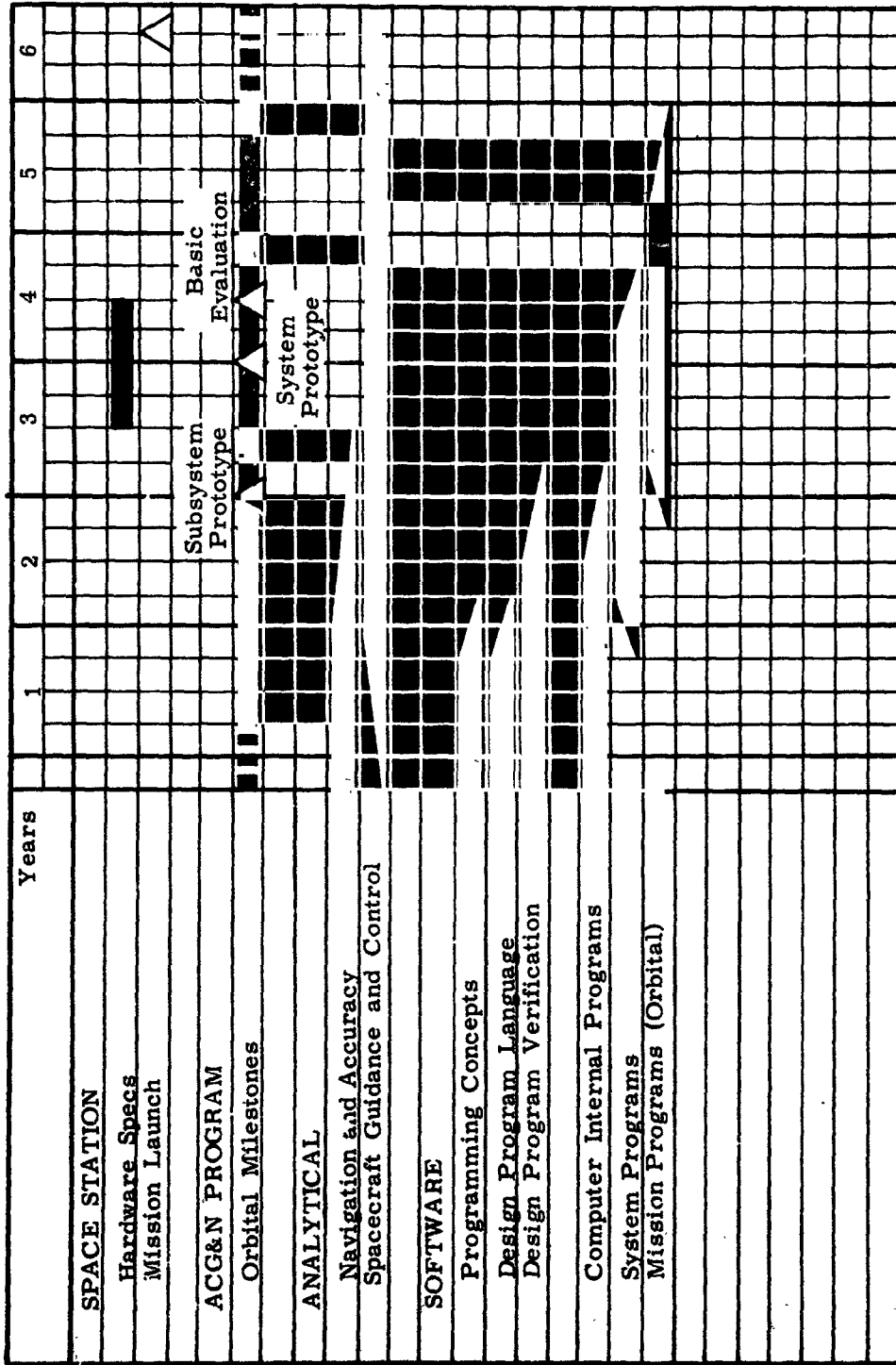Basic Evaluation

Figure 3-1   System Integration

Figure 3-2 Space Guidance Analysis
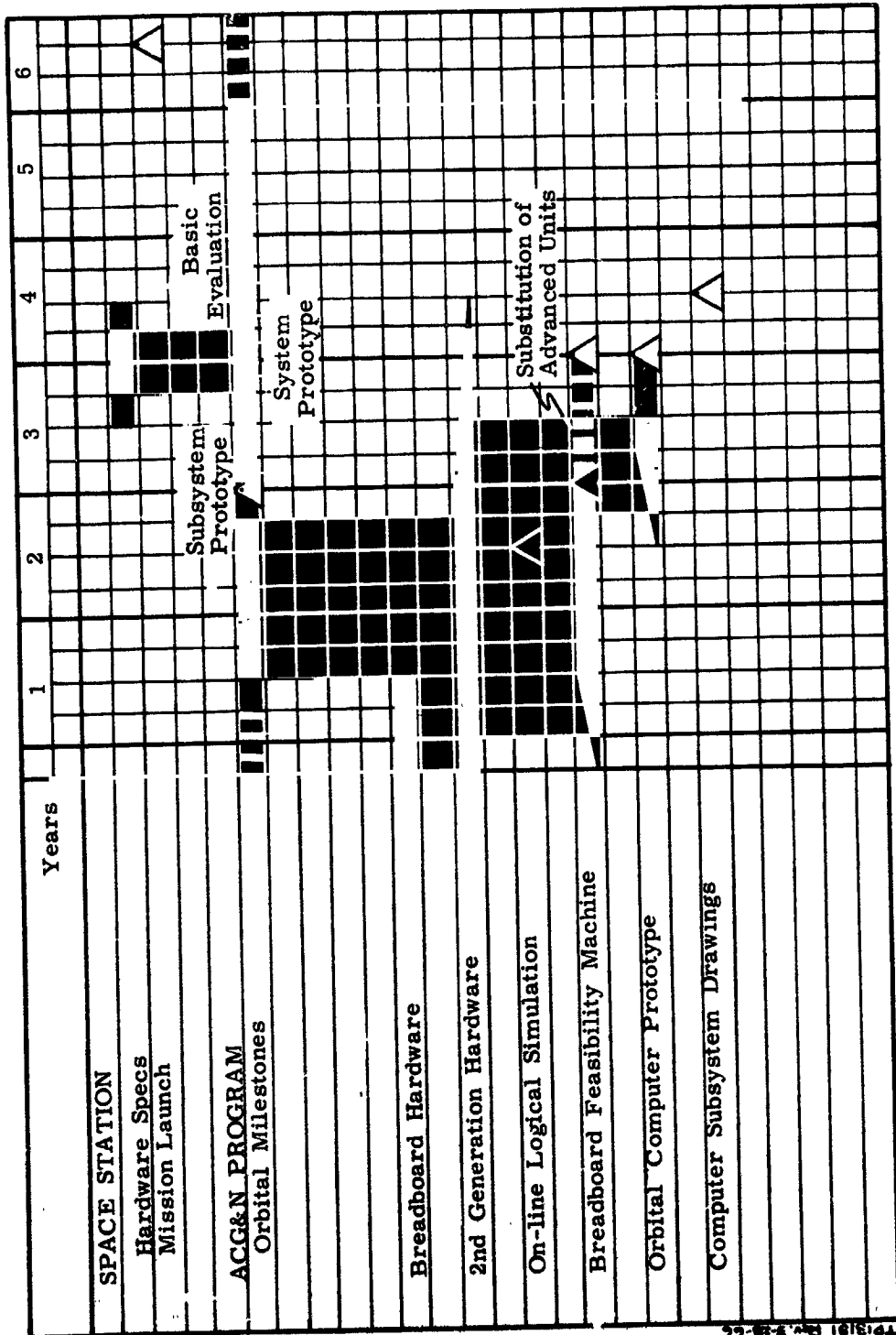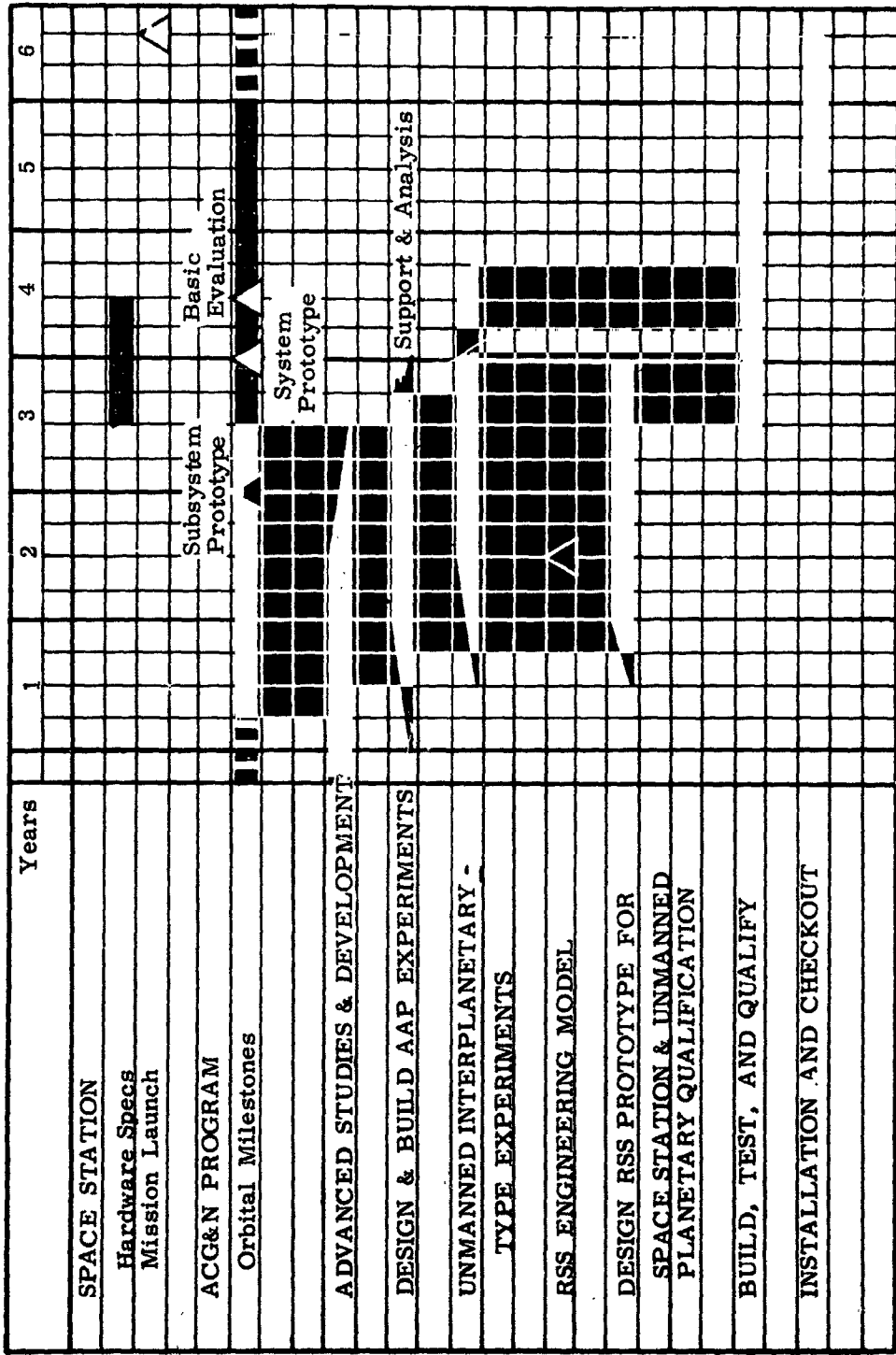
Figure 3-3   Computer Subsystem
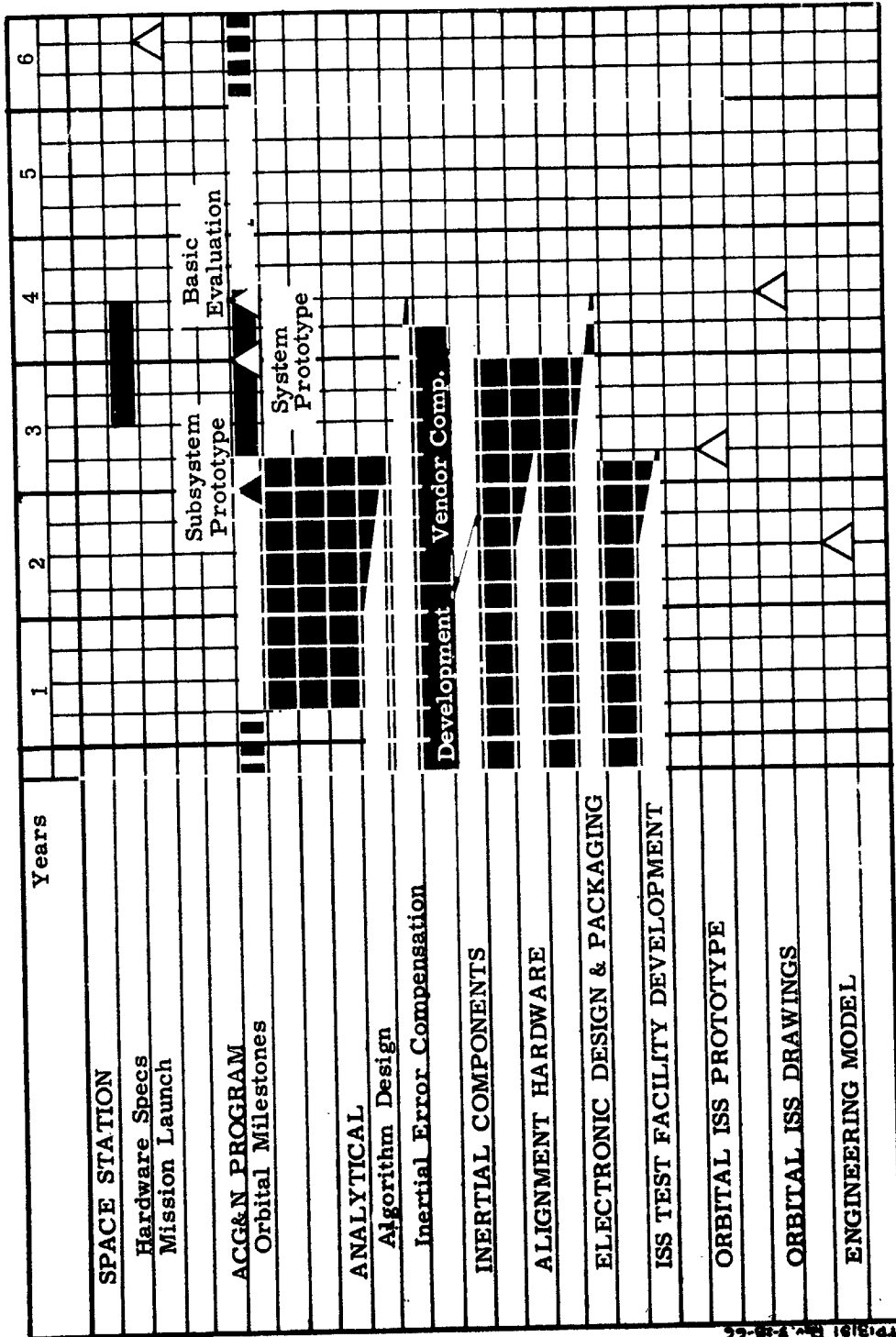
Figure 3-4   Radiation sensor subsystem

Figure 3-5   Inertial Subsystem

A. EXPERIMENTS WITH THERMOELECTRIC DEVICES FOR GYRO TEMPERATURE CONTROL.

A.1 Test Vehicle and Fixturing

The gyro mounting system used as a test vehicle is shown in Fig. A-1. The gyro mount uses spherical seats at either end in an attempt to avoid bending moments on the gyro during alignment, while providing low thermal resistance. In practice the bending moment requirement conflicts with the need for mechanical rigidity. This factor led to the selection of the kinematic mount in the design model.

Each gyro end mount consists of an inner and outer aluminum ring rigidly bound as one member by a threaded, spoked center section of titanium. All three sections are epoxy bonded at the inner and outer thread interfaces. The inner aluminum ring extends in fingers to pick up the gyro and is held secure to the gyro by a clamping strap. The outer aluminum ring has a peripheral spherical contour which mates with a complimentary spherical surface in the mounting cradle.

The entire end mount assembly is plated with a thin film of nickel prior to final machining. This is required for later solder bonding of the thermoelectric modules.

The center titanium piece serves as a housing for the thermoelectric modules, minimizes thermal shunting and provides alignment rigidity. It is formed by milling six (6) symmetrical slots in an annular ring of titanium and threading the inner and outer circular surfaces. Each slot is formed of dihedral surfaces to accomodate two thermoelectric modules per slot.

The torquer generator end mount is twice the thickness of the signal generator end mount. This is required since 4 × 8 array thermoelectric modules are used on one end and 4 × 4 array modules on the other. A total of twelve (12) modules are used in each end mount.

The thermoelectrics, being bi-polar, can pump heat in both directions, therefore, lending themselves to an idealized heatsink temperature requiring no control power to the thermoelectrics. Another advantage in using thermoelectrics is that both the heatsink and ambient temperatures can rise well above gyro control temperature, and yet, proper gyro temperature can be maintained.

Both spherical seats used to hold the gyro end mounts are of split finger construction. This permits the spherical surfaces to yield during alignment and provides for an optimum surface-to-surface interface in the "strap tight" configuration. The mounting cradle is made of aluminum. Two surface pads with two tie-down points per pad are contained on the lower surface of the cradle for mounting to the inertial sensor base.

Following completion of end mount and cradle machining and assembly, and of end mount nickel plating, the two end mounts were sent to Melcor for installation of the thermoelectric modules. These were sandwiched between two copper "L" brackets and soldered into a thermal circuit consisting of the plated aluminum inner and outer assemblies. This method was used for expediency rather than desirability.

Prior to installing a gyro in the end mount and cradle assembly, two simulated gyro end caps were fabricated and installed to ascertain overall system balance and symmetry. Button heaters were installed in these end caps and each interface was instrumented with thermocouples. By varying simulated wheel power and T.E. input power, with the cradle mounted to a controlled temperature liquid cooled heatsink, the following facts were noted:

1. The configuration was reasonably balanced mechanically with a static thermal resistance of approximately 3°F/watt. However, when an equal number of T.E. junctions (96 per mount) was used on each end mount, a fairly large gradient existed during variation of T.E. power. This gradient amounted to 13°F, worse case. To resolve this, it was necessary to series all of the T.E. junctions (192 on the T.G. end and 96 on the S.G. end). In this configuration, the gradient was reduced to less than a degree for all test conditions.

2. The change of temperature at the simulated end mounts for variation of T.E. power was maximum at near zero T.E. power and diminished with increasing power level. This was expected.

Following this series of tests, an actual 18 PIRIG gyro was installed and control temperature maintained with a dc proportional controller. The experimental set up is shown in Fig. A-2. This controller consisted of a Fairchild 726 - 709 IC linear amplifier with a push-pull output stage. Two gyro wire sensors were used for control and two sensors were series connected for monitoring. The amplifier was set for $\pm 0.1^\circ$F/W maximum control variation with a restroration time to steady control temperature of approximately five (5) minutes. Figure A-3 shows a graph which demonstrates control T.E. power, versus coldplate pad temperature. The equivalent heater power is also shown and the ratio;

Equivalent Heat Power/Thermoelectric Power = Coefficient of Performance (C.O.P.)

A.2 Critique of Tests

The first comment on the mechanical configuration used for this investigation is that it is somewhat large. There are certainly ways to reduce the overall size without degrading alignment or temperature control functions. One method which shows considerable promise is to perform all alignment functions at the bed or mounting point for the assembly. The gyro would be thermally isolated from the platform and coolant heatsinks attached to each gyro end. A circular or annular thermoelectric module would provide for control. Such a system would have exceptionally fast response since it would be thermally divorced from the large mass of a platform.

To allow flexibility in interface area and symmetry requirements in the mechanical design, two separate controllers would be used to control each gyro end independent of the other. This would eliminate any concern over torquer power levels or lack of thermal symmetry in the gyro. Sensors should be located in each gyro end with a thermal shroud about the gyro.

Finally, the gyro controllers should be of a low rate pulsewidth modulation type; possibly a clocked, digitally operated device. The losses noted during this test using a dc proportional amplifier were considerable, and a problem of deadband exists at the zero crossover point.

Fig. A-1 Experimental T. E. Setup

ALUMINUM INNER ASSEMBLY

TITANIUM RING

ALUMINUM SPHERICALLY GROUND RING

SPHERICAL SEAT & CRADLE MOUNT

2.000 DIA

1.562 DIA

.343

S.G. END

T.G. END

.687

CRADLE

TYPICAL PLACEMENT
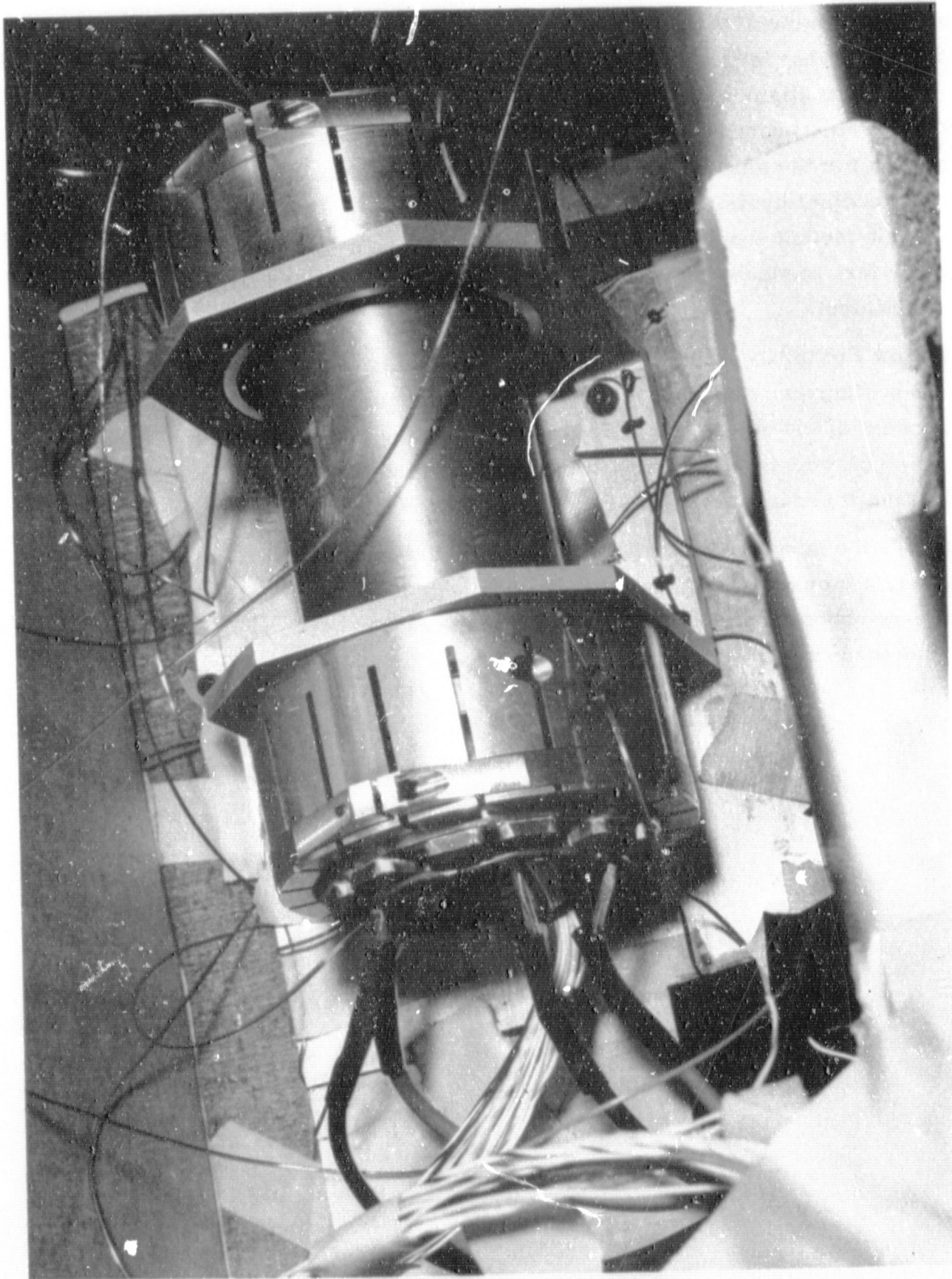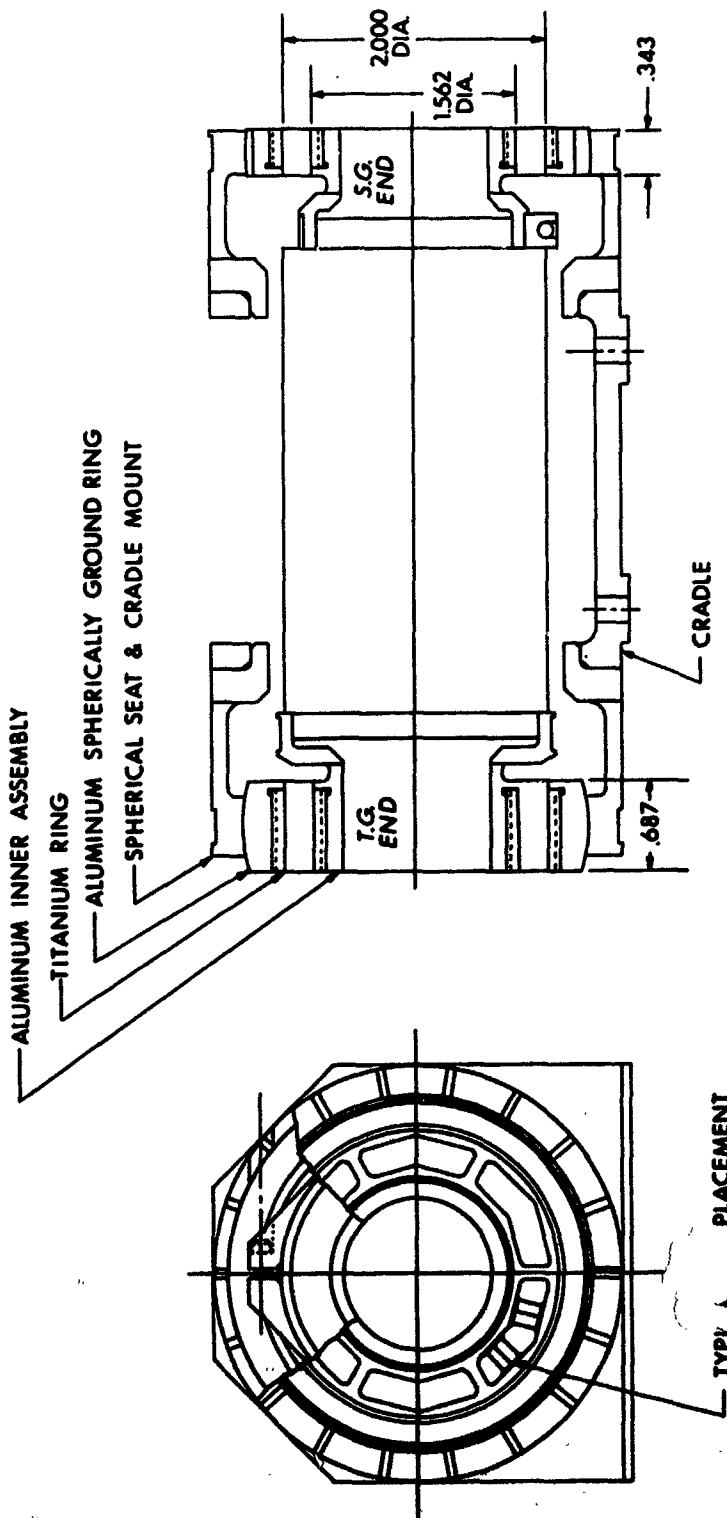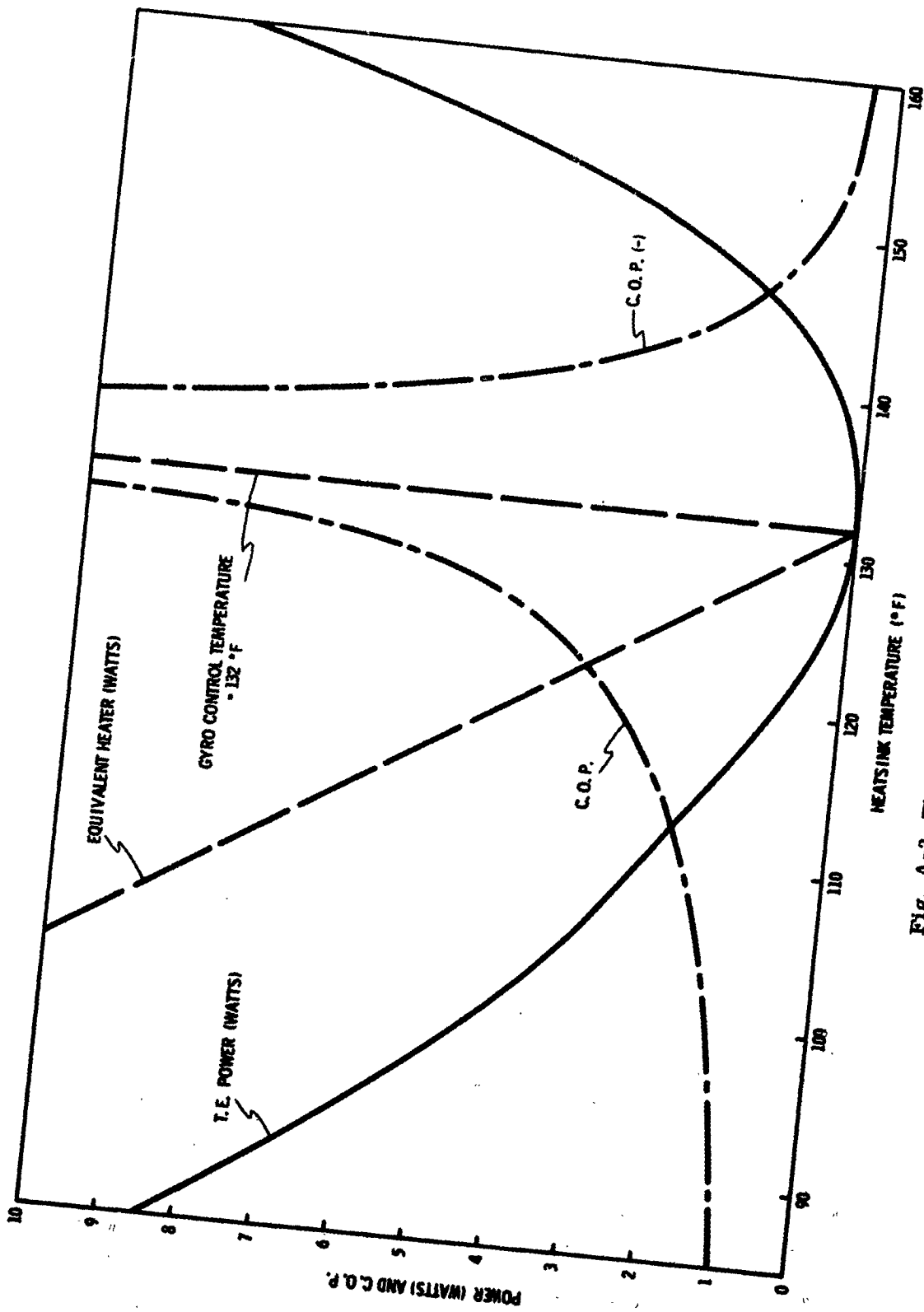
Fig. A-2   Experimental T-E Cooling Gyro Mount

Fig. A-3 Thermoelectric Experiment Results

APPENDIX B

B.1 Scope of Detailed Work.

The Ball Attitude Indicator and character capability were chosen
as the first goal for a breadboard display as being the most complex.
(Figure B-1)

Most present computer-driven displays tie up the computer with
continuing computations to produce the picture, or use a large core
memory or drum to refresh the display. It is desirable to utilize the com-
puter for its arithmetic capability and minimize its use for simple picture
refreshing.

A replaceable read-only braid memory was chosen as the basis
for picture information storage. The braid has high density, ease of man-
ufacture, changeability and is planned for use in MIT's advanced guidance
computer. In fact, the display braid could be an integral part of the com-
puter. The picture parts do not have to be computed and no mechanical
drum or tape problems are incurred.

An attempt was made to make the hardware and memory organization
as general as possible so that new kinds of pictures can be added simply
by braid changes.

Another goal was a low clock rate so that conservative, present
state - of - the - art hardware could be used. The present design per-
mits either bipolar I. C.'s or MOT arrays in most circuits.

A 5 to 7 inch diameter CRT is proposed. This size permits fast
CRT focussing and deflection, without the weight and magnetic shielding
penalties inherent in magnetic deflection. Furthermore, the smaller
tubes are more rugged, require less space and have more experience
in militarized airborne environments.

The amount of text which can be assimilated at a glance fits on a
5 inch screen, and the present ball attitude indicator is only about 3
inches in diameter. Furthermore, in a cockpit, the pilot sits so close
to the display that a large tube is simply not warranted.

Presently available CRT displays use either raster, diode function
generator curves, straight lines (vectors) or plot point-by-point. Most
computer-driven types use the latter method.

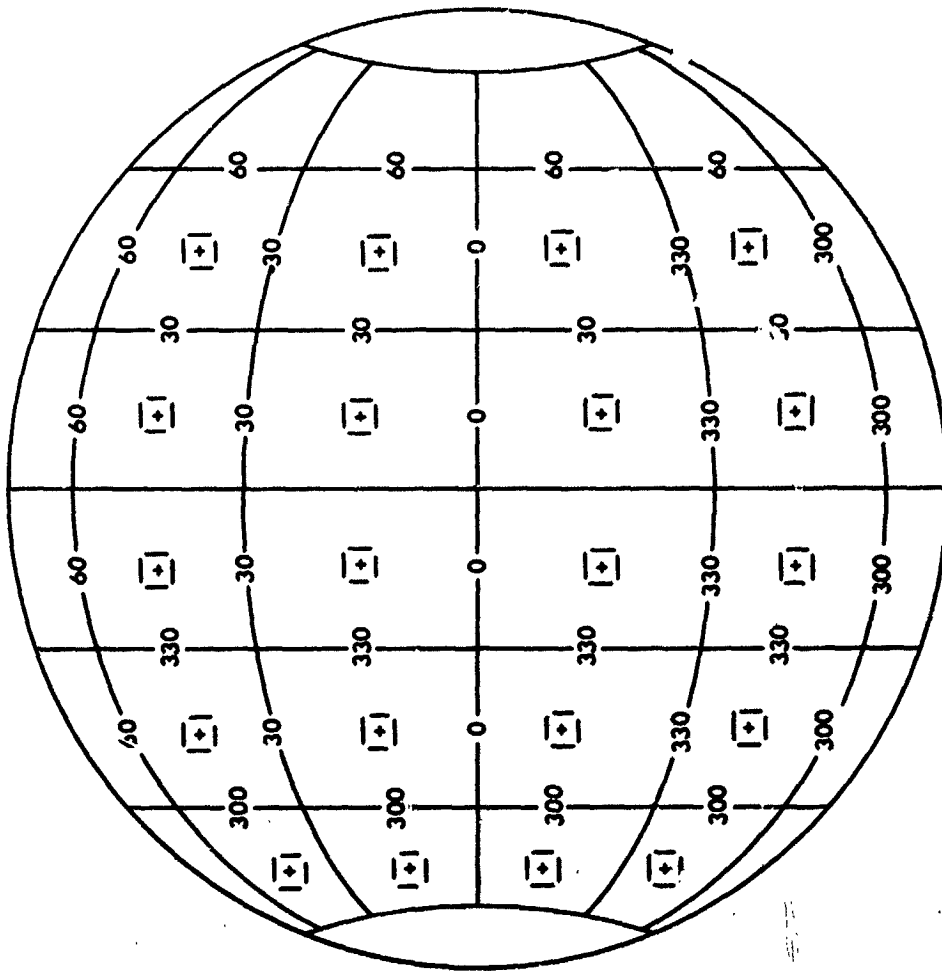One special CRT uses an internal mask to shape the beam into a
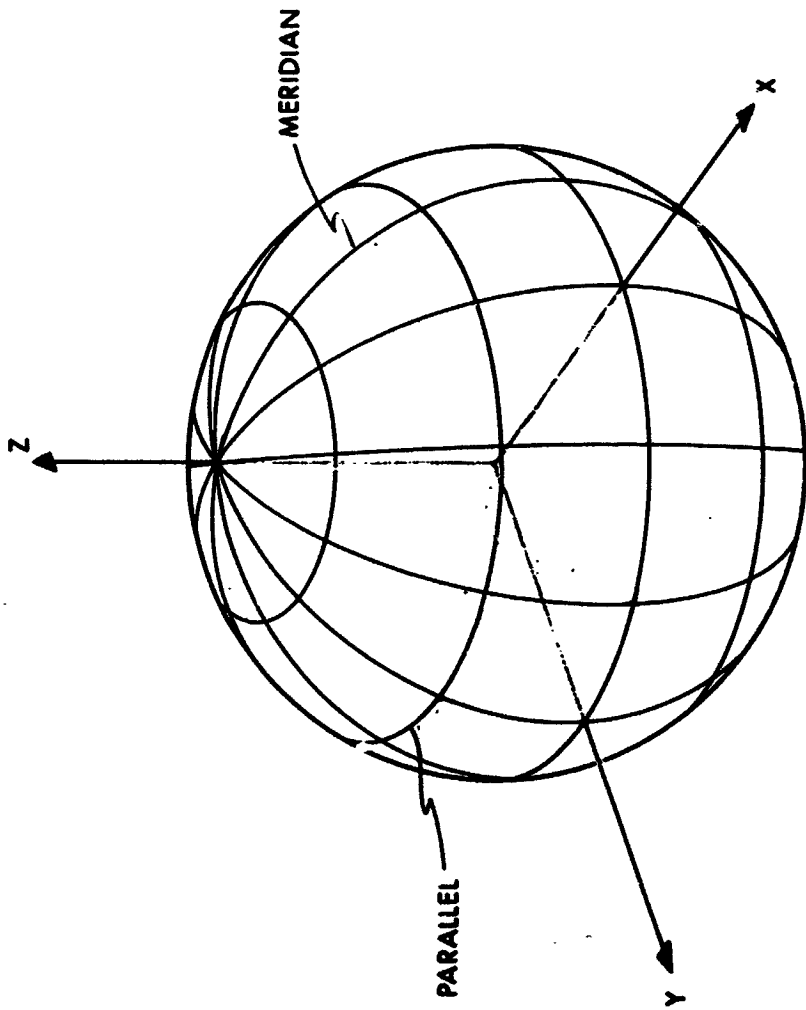
Fig. B-1 Ball Attitude Indicator.
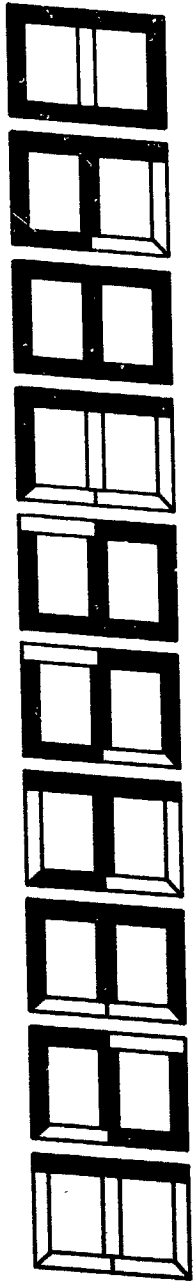
Fig. B-2 Ball Parameters.

Fig. B-3   Segment Numerics.

symbol. All desired 64 symbols must be specified before making the tube.

B.2 FDAI Display

The proposed ball display uses a circular stroke technique, a modified Lissajous generator. A circle was chosen because it is simple to generate and because it is difficult to make good circles from other stroke functions (logarithmic , parabolic, etc.). Furthermore, the ball grid is made up of circles. The stroke approach generates picture material at higher speeds than is possible with the point-by-point method. A reasonable trade-off between hardware and memory is possible because the picture to be displayed is known in advance.

Two circle types are created: Meridians (or great circles) and parallels (small circles). Electrical signals are generated in time for the X, Y, and Z coordinates. (See Figure B-2)

Meridians are produced by rotating a Y-Z plane circle around the Z-axis. Two D/A converters (8 bit DAC's) perform the rotation.

Parallels are formed by scaling an X-Y circle and translating along the Z-axis. The same DAC's perform this transformation. The DAC's are set up by words called out of memory. Finally, as the circle is swept out, the beam blanking pattern is generated by synchronously shifting a long binary number from memory to a beam control gate.

By using 7 segment numeric characters for the ball numbers, the identical meridian-parallel technique generates the numbers. (See Figure B-3)

The 3-dimensional ball described by the electronics can be displayed on a scope by feeding the X-Z voltages to the horizontal and vertical scope amplifiers. The "back" of the ball is blanked out by a simple blanking everything with a - Y coordinate voltage. The 3-dimensional effect is increased by decreasing intensity for increasing coordinate voltage. Thus outer edges are thus dimmed, appearing further away. Spot defocussing can also provide a depth cue at the outer edges. A company which makes a "3-D" scope has researched the 3-D effect and finds the degree of depth impression is proportional to the number of cues given the eye. Stereoscopy is not necessary if enough other cues are provided.

Since the actual beam is now not describing circles, but some elliptical or higher order function, continous intensity control proportional to beam speed is needed to produce nominally-even brightness.

A first-order approximation of $(X' + Z')$ for the velocity is planned. This is simple to implement in hardware and should be adequate.

The ball picture must rotate in 3-D. This fact dominated the choice of 3-dimensional electronic generation of the ball, even though only 2 dimensions are finally displayed. The 9 parameter 3-dimensional rotation matrix is already generated in the computer from the strapped-down inertial system. These 9 values can be used directly to transform the generated X, Y, and Z coordinates of a point on the fixed ball picture to a new point on a rotated ball. New parameters need only to be sent to the display when the spacecraft rotates. Nine 8-bit DAC's are required. Miniature lowcost DAC's using MOS arrays are under investigation and look promising.

B.3   Character Generation

Several character generation techniques were explored. The 5x7 dot raster is widely used by computer driven displays and produces about the minimum quality character. A 6x8 dot raster was chosen for the breadboard display.

The raster approach permits any kind of symbol in any font to be generated: upper and lower case alphabetical, numeric, mathematical, even Chinese characters. Thus information can be displayed to the astronaut in the manner with which he is most familiar and comfortable. The raster is also very compatible with the ball generation technique.

A 30 characters per line, 16 lines per frame format was chosen. This should be more than adequate. Refresh rate for the test is about 30 frames/sec.

B.4   Refresh Rate and Logic Timing

Experimentation with varying refresh and writing rates indicate refresh rates of 30-50 frames/sec produce no flicker at reasonable intensity.

Library research indicates flicker is a complex relationship of refresh rate, intensity, phosphor decay time and ambient lighting. Above 50 seems always safe.

An upper limit on phosphor decay time will be set by "smearing" at maximum spacecraft rotation rates.

A circularly polarized filter coupled with an anti-reflectance coating has enabled radar scopes to use lower intensities and thus both lengthen CRT lift and reduce flicker.

The presently proposed system results in low clock rates and a refresh rate of about 34 frames/sec. Empirical testing will determine what phosphor, intensity, and ambient light conditions will be necessary to produce a flicker-free picture with smearless rotation. The breadboard display will use a commercial X-Y oscilloscope.

All timing is derived from a synchronous time scaler which counts from 4.5 mHz to 39.1 pps. (Figure B-4)

6.25 KC is tapped off the scaler and filtered. This forms the drive for the Lissajous circle generation. Alternate + and -sin ωt provides 160 micro-second circles with an 80 micro-second set-up period between circles.

Timing control logic generates two basic time periods. One 80 μsec period reads 24 bits from memory to provide DAC and switch set-up and settling time. This period uses about 53 μsec for memory reading, and about 27 μsec for settling. The second period reads bits from memory (72 for the ball grid circles, 216 for the ball number circles) for the 160 μsec while the circle is being swept out. These bits determine the blanking pattern on the circle. Thus an entire circle is produced every 240 μsec. (Figure B-5)

For the 119 circles required to generate the ball, the result is a frame refresh rate of about 35 frames/sec.

At first glance, it would appear that 360 bits of blanking pattern storage would be needed to give the one degree resolution necessary to draw the ball numbers. But the high degree of symmetry in the ball allows a reduction to 216 bits for the numbers and 72 bits for the grid. This is accomplished by reading the blanking pattern bits from memory alternately at high and low rates, yielding high and low resolutions. Thus the ball number circles are read at 900 KC for eight 2.5 degree bits, followed by ten 1 degree bits, then four 2.5 degree bits at 900 KC. A simple 4-bit counter controls this alternating change of rate.

Therefore, only 58 x 240 = 13,920

61 x 96 = 5,856

19,775 bits of storage,

or 1236 16-bit words are required to store the ball picture.

The 24-bit set-up sequence uses 16 bits for the three 8-bit circle.

Fig. B-4 Timing Chain.

1.5 mc CLOCK → ÷2

2.25 mc 1° CIRCLE PATTERN

÷5

900 KC 2.5° CIRCLE PATTERN

÷2

450 KC CIRCLE DAC SETUP

÷2

255 KC 10° CIRCLE PATTERN

÷2

112.5 KC CHAR RASTER HORIZ

÷2

56.25 KC CHAR RASTER VERT

÷3

18.75 KC END OF CHAR

÷3

6.25 KC SQ. WAVE FOR CIRCLE GENERATION

÷27

4.17 KC CIRCLE SYNC

÷2

2.08 KC SQ. WAVE SIN ωt & COS ωt SWITCHING

÷5

417 pps MEMORY RESET

OR → TIMER RESET

417 pps CIRCLE
39.1 pps RASTER

÷10

625 pps END OF LINE

÷16
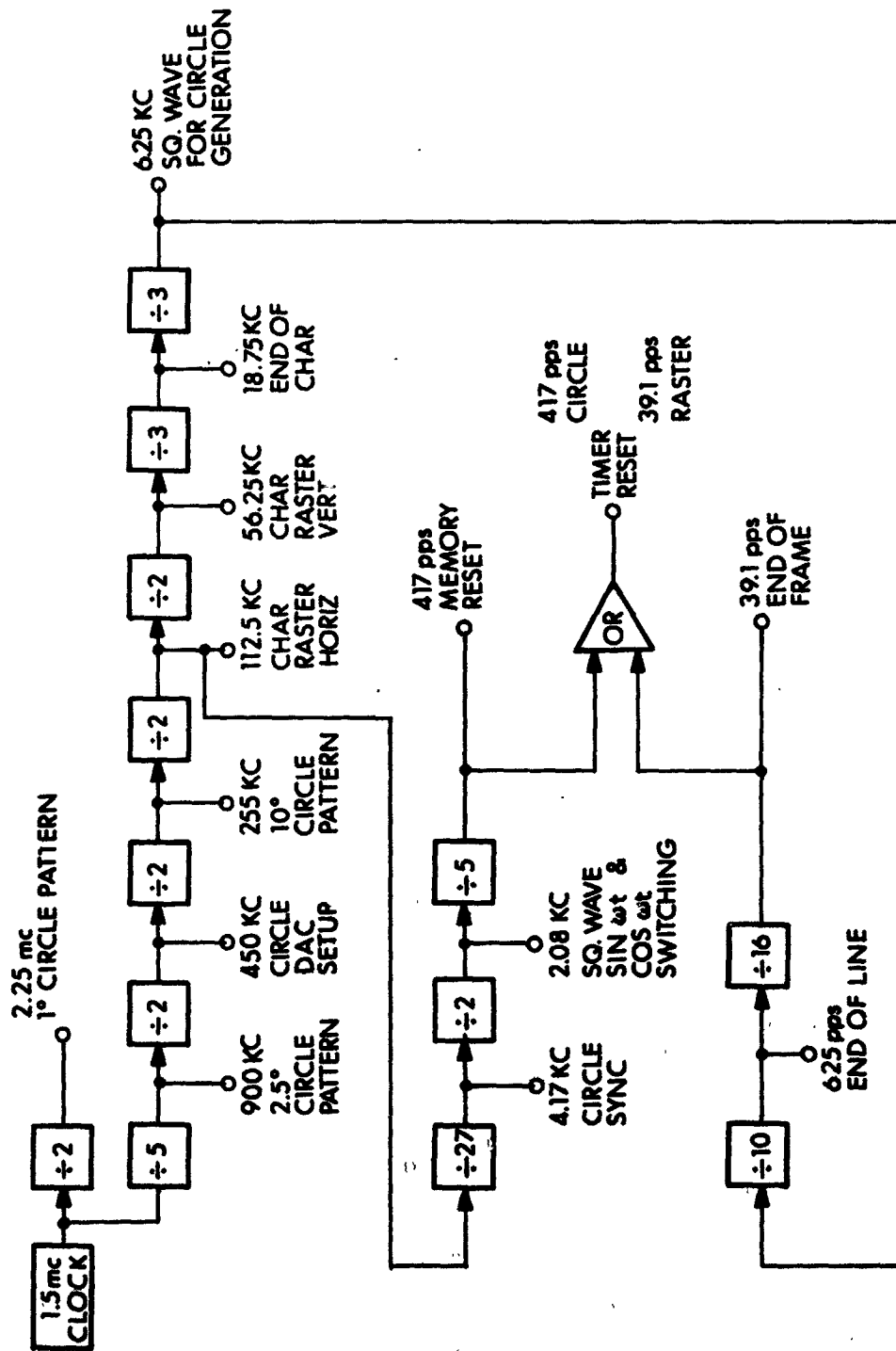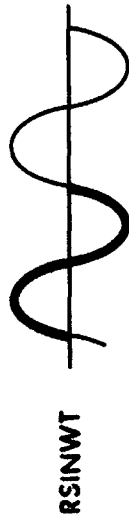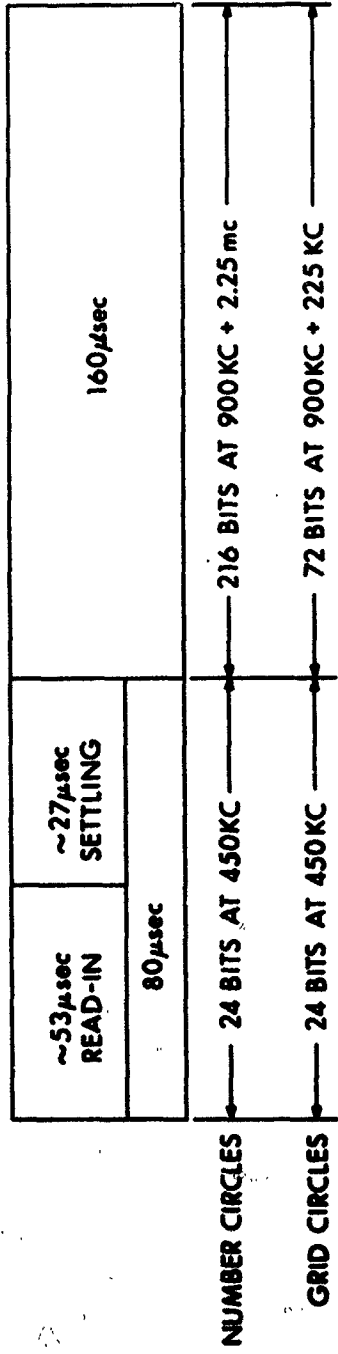
39.1 pps END OF FRAME

Fig. B-5 Timing Periods.

transformation DAC's. Of the remaining 8 bits, one indicates whether a grid or number circle is to be generated, and 7 are spare for future picture identification or control information.

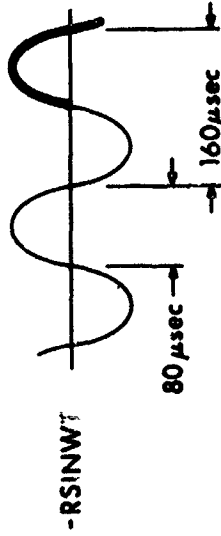The memory is read alternately into two 16-bit registers. While one is receiving data, the other shifts the previous words serially to the display under control of the timing logic. Simple digital gating switches between the 2 outputs. The present design permits memory cycle times as long as 11 micro-seconds, therefore, presenting no problem in memory speed.

In the character mode, (Figure B-6), the beam will be driven horizontally by a high speed DAC. A 56.25 KC square wave from the timing chain will be integrated to a triangular wave for the vertical character sweep, and another high speed DAC will provide vertical line spacing. 112.5 Kpps pulses step thru the horizontal characters. Every 6th step, 18.75 Kpps pulses provide the horizontal character spacing. A 625 pps pulse provides an end-of-line horizontal and vertical shift, and a 39.1 pps pulse resets the frame. (Figure B-7)

In the character mode, the raster sweeps continuously, off the timing chain. The 48-bit pattern will come from memory exactly as do the ball patterns.

The read-only memory addresses will come from a separate, serial character memory. The character memory is erasable so that 7-bit character addresses may be entered by the astronaut or computer. 480 seven bit characters require either a 3360-bit serial delay line (glass, wire, or MOS) at a 131.25 KC bit rate, or 240 sixteen bit words of erasable core-type memory.

It should be noted that by eliminating the character spacing pulses from the character generation a solid 8x96 line raster is produced. Various meter patterns, pointers, etc. can be therefore displayed simply using the character capability alone. (Figure B-8)

Figure B-9 shows a block diagram of the whole display system.

B.5   Techniques And Hardware Developed

A clock frequency of 4.5 mHz was chosen to allow the use of bipolar and MOS type integrated circuits and at the same time maintain a refresh rate of the CRT that would eliminate flicker problems.
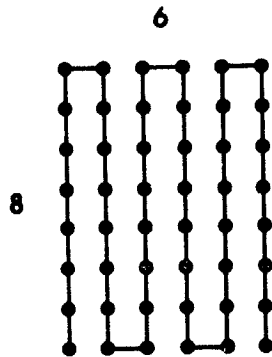
6

8

Fig. B-6 Character Raster.

56.25 KC

INTEGRATED SQUARE WAVE
(VERTICAL DRIVE VOLTAGE)

HORIZONTAL STEP PULSES
(112.5 Kpps)
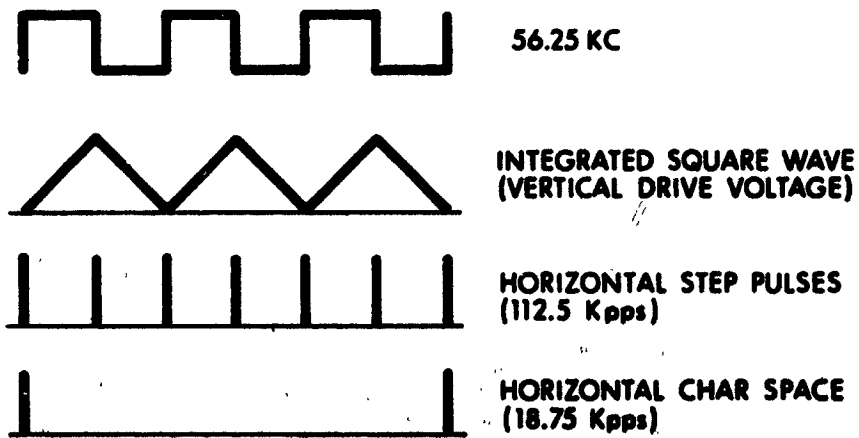
HORIZONTAL CHAR SPACE
(18.75 Kpps)

Fig. B-7 Character Timing.

The timing chain is made up of synchronous type counters to minimize delay times between the pulses and square waves being generated. All timing and control functions are derived from the timing chain which counts from 4.5 mHz to 39.1 pps. (Figure B-4)

Since the timing chain has parallel counting paths, a timer reset function is provided to continuously maintain the proper time relationships between all pulses. The use of the outputs of the timing chain will be discussed as they are used in the functional areas of the display system.

The functions of the rate and timing control circuits are to provide the gating control signals and the proper pulse train outputs to process information from memory. A description of the functions performed by these circuits in reference to the block diagram follows. (Figure B-10)

In the ball generation mode, the rate and timing control circuits produce the gating and pulse train required to generate the ball blanking pattern. A ball circle is generated every 1.5 cycles of 6.25 KC. (Figure B-11) During the first half cycle, the timing control gate C prevents the 450 KC pulses from being fed to the rate counter and logic. These pulses are allowed to be counted by the timing control counter and logic. After 24 pulses at 450 KC, a selection of a grid or number circle is made from information processed out of memory. Note that the first 24 pulses at 450 KC were sent through the raster-ball pulse selection logic to the 16-bit word counter and to the memory shift register allowing this information to be processed from memory. The remaining 12 bits at 450 KC during the first half cycle are used for settling time of the circuits receiving the information. These bits are counted by the timing control counter and logic which generates the gating signals A, B, C, and D. Gate signal D inhibits the last 12 bits at 450 KC from being passed through the raster-ball pulse selection logic. Therefore, no information is processed from memory during this time. This sequence is the same for a number of grid type circle.

During the remaining cycle at 6.25 DC, the pulse train for the blanking pattern is generated. Gate signals B and C allow the rate counter and logic as well as the rate gate generation to function during the remaining cycle. The 450 KC pulses are inhibited by these gate signals during this period. The rate counter and logic together with the rate gate generation drive the pulse steering logic allowing the correct pulse train to be generated. A number circle has 12 cycles of 10 bits at 2.25 MC and 8 bits at 900 KC. A grid circle has 12 cycles of 4 bits at 900 KC and 2 bits at 225 KC. These pulses are counted by the timing control counter and logic. The total pulses

5   6   7 (METER)

(POINTER TYPES)

(BAR METER)

6.43 VOLTS   (DIGITAL READOUT)

29.2 VOLTS   29—   (VERTICAL METER WITH DIRECTIONS)

    30—

TOO HIGH
START FAILURE CHECK ————————➤
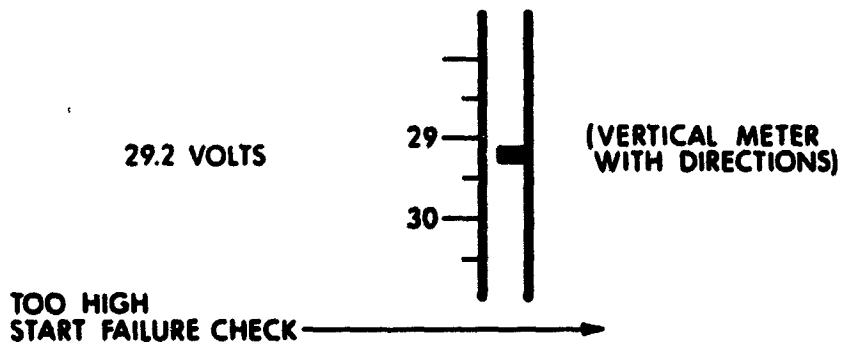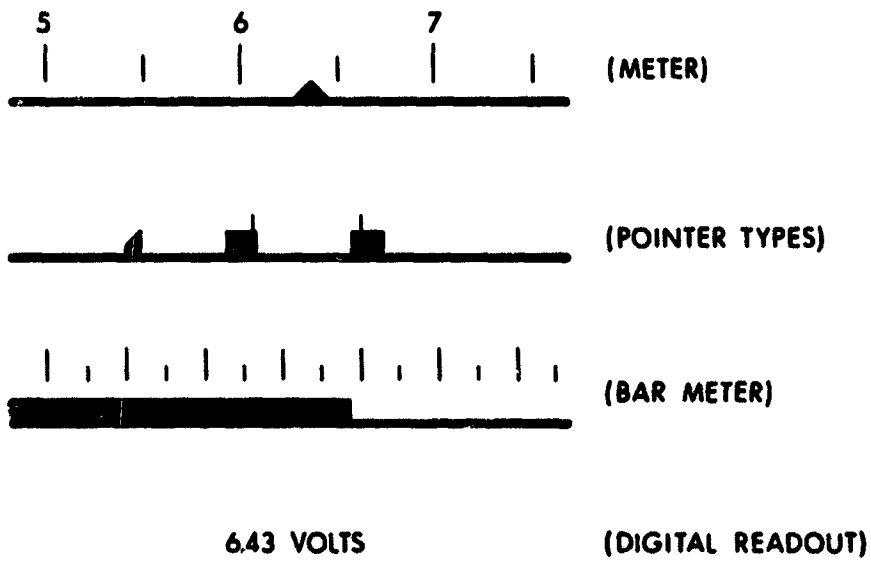
Fig. B-8 Meter Patterns.

Fig. B-9 CRT Display Block Diagram.

BALL AND CHARACTER ADDRESSES FROM COMPUTER

ADDRESS ERASABLE MEMORY

ADDRESS CONTROL COUNTER

READ ONLY MEMORY

PARALLEL-SERIAL OUTPUT REGISTERS

RT CONTROL & R CONTROL

MEMORY CONTROL

6.25 KC FILTER

$\pm R \sin \omega t$ AND $\pm R \cos \omega t$ SWITCHING

RASTER CONTROL LOGIC

TIMING CHAIN

RATE AND TIMING CONTROL LOGIC

4.5 MC CLOCK

R CONTROL

RT CONTROL

24 BIT SHIFT REG

MERIDIAN/PARALLEL ROTATION TRANSFORMATION

$V D X$

X_1 Y_1 Z_1

72 BIT ROTATION WORD FROM COMPUTER

BALL ROTATION TRANSFORMATION

X_2 Y_2 Z_2

R CONTROL

CHARACTER RASTER GENERATOR

H

V

INTENSITY BLANKING AND SWEEP CONTROL

R CONTROL & RT CONTROL

ROUTE CONTROL

BLANKING PATTERN

V

H

B-14

Fig. B-10 Rate and Timing Control Logic
          Raster Control Logic.
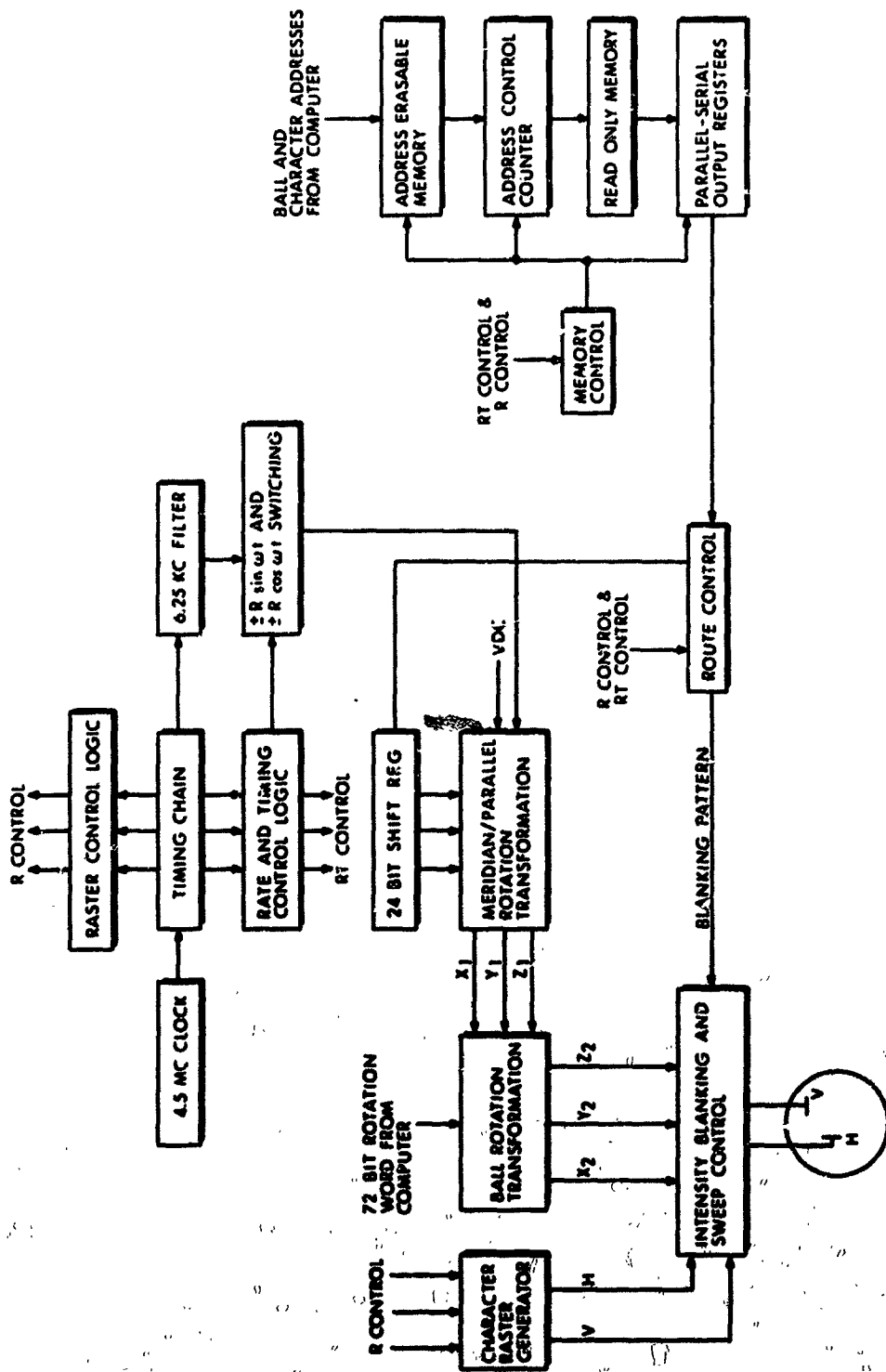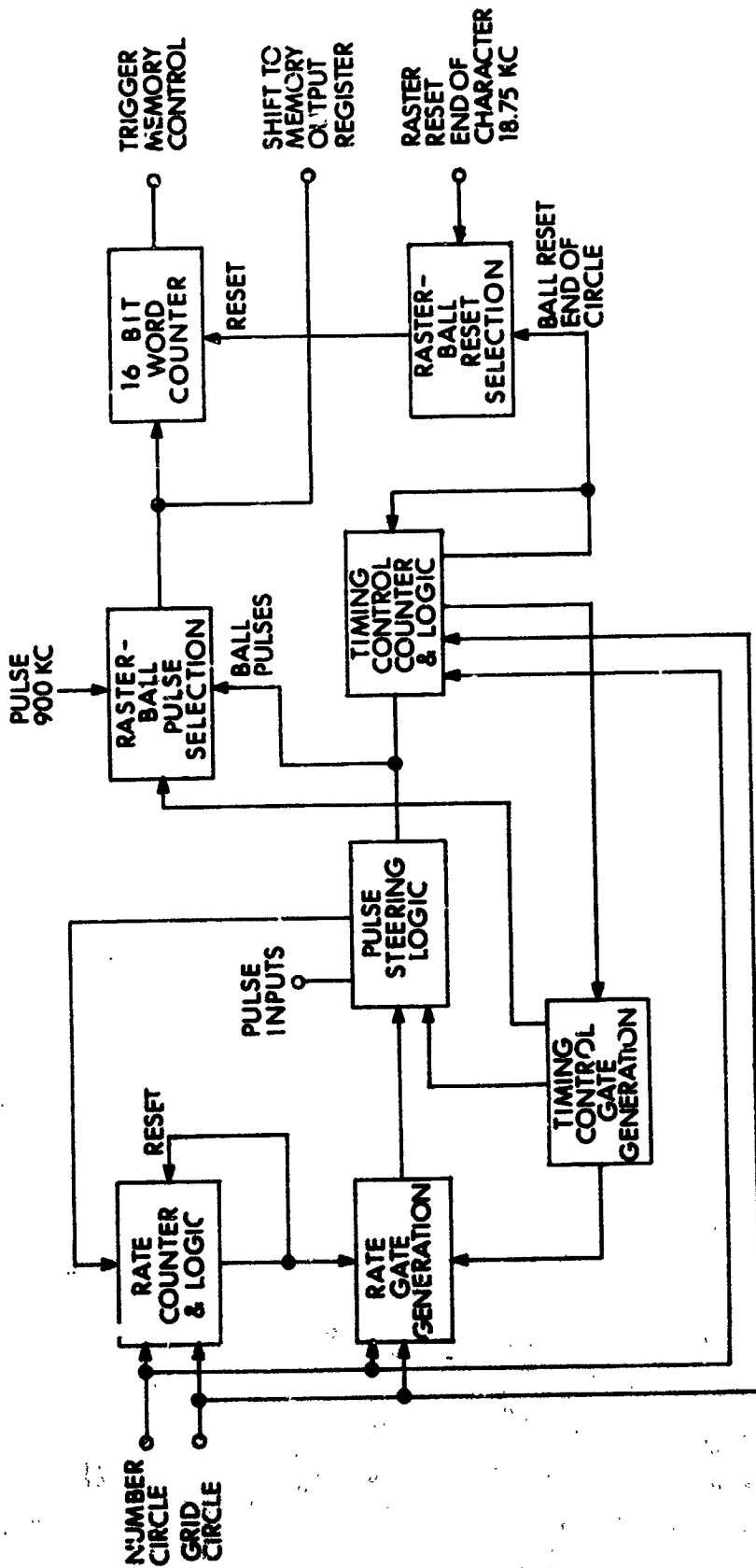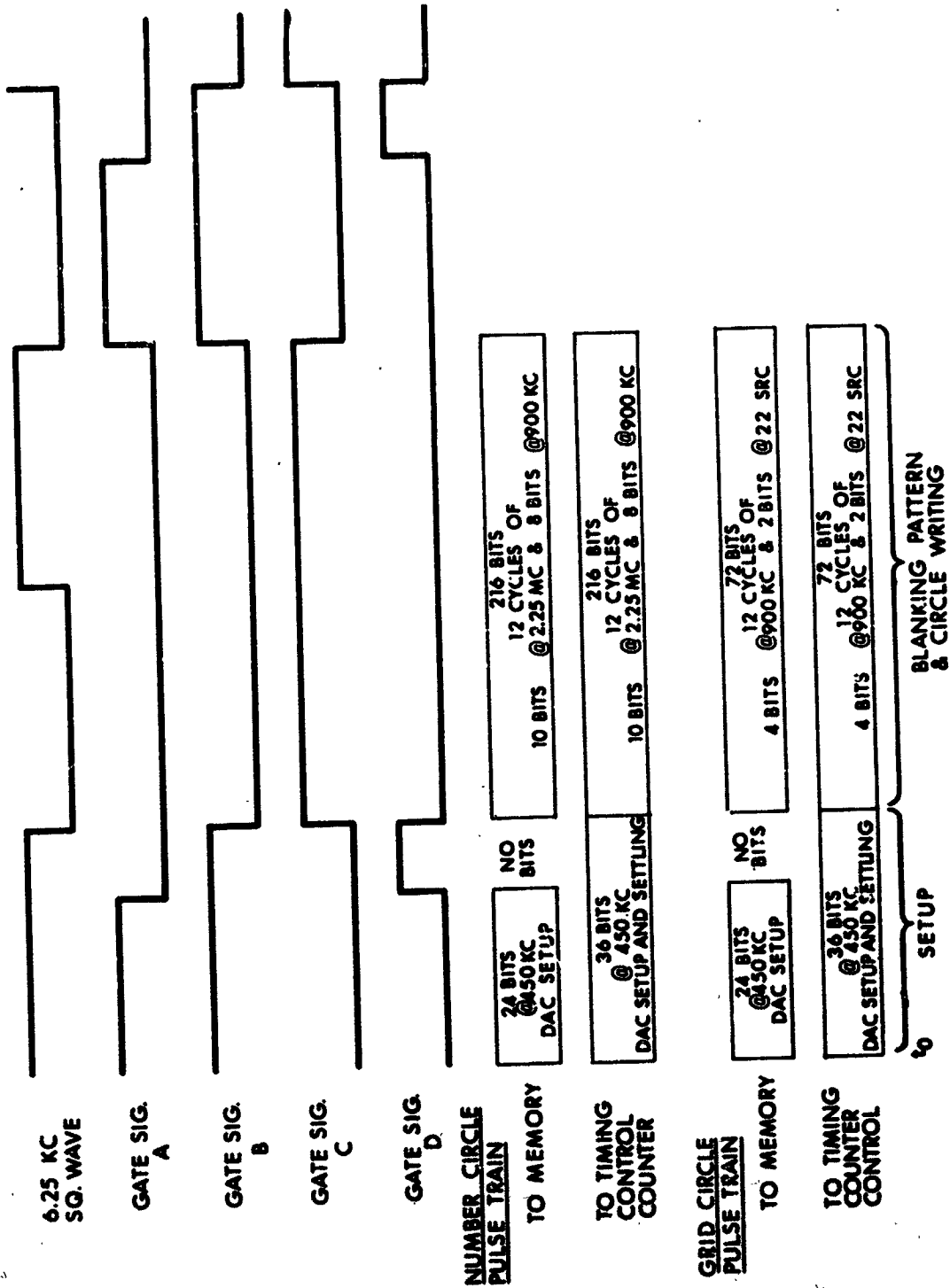
Fig. B-11 Timing Diagram; Rate and Timing Control; Ball Blanking Pattern.

counted for a number circle is 36 pulses during the first half cycle and 216 pulses in the remaining cycle for a total of 252 pulses. With the timing control counter and logic set for a number circle, the rate and timing control circuits are reset for the next circle after a count of 252 is reached. With the timing control counter and logic set for a grid circle, the rate and timing control circuits are reset for the next circle after a count of 108 is reached.

The raster-ball pulse selection passes the pulses during the remaining cycle to the 16-bit word counter and the memory output register. This transfers the blanking information for the grid or number circles to the blanking circuits of the CRT. The 16-bit word counter is reset at the end of each circle by the 4.17 KC pulse train so that the word counter will always be synchronized properly with the memory and circle sweep circuits.

When the display system is in the character raster mode, the rate and timing control circuits are not used. The only pulses required to transfer the blanking information for characters from the memory are 900 KC pulses. The raster-ball pulse selection circuit passes these 900 KC pulses to the 16-bit word counter and the memory output register. The 16-bit word counter is reset at the end of each character by the 18.75 K pulses so that the word counter will always to synchronized properly with the memory and raster sweep circuits.

B. 5. 1 Ball Circle Sweep Generation

The functions needed to generate the ball circles are $R \sin \omega t$ and $R \cos \omega t$ and a DC reference voltage for translating the parallel circles along the z axis. The generation of the sine and cosine functions are discussed with reference to Figure B-12 .

The 6.25 KC square wave is taken from the timing chain and used to generate both the sine and cosine functions. The square wave is first passed through a low pass filter to obtain a sine wave at 6.25 KC. It is then passed through an inverting amplifier with a phase shift correction adjustment. This allows the sine wave to be set at the correct phase relationship to the 6.25 KC square wave. It is then put through another inverting buffer amplifier which gives the $R \sin \omega t$ function. The $R \sin \omega t$ function is again passed through another inverting amplifier to give - $R \sin \omega t$. These two signals are selected alternately at a 2.08 KC rate through an analog switch. The $R \sin \omega t$ function is put through a unity gain integrator to obtain - $R \cos \omega t$. An inverting amplifier is used to obtain $R \cos \omega t$. Again these two signals are selected alternately at a 2.08 KC rate through an analog switch.
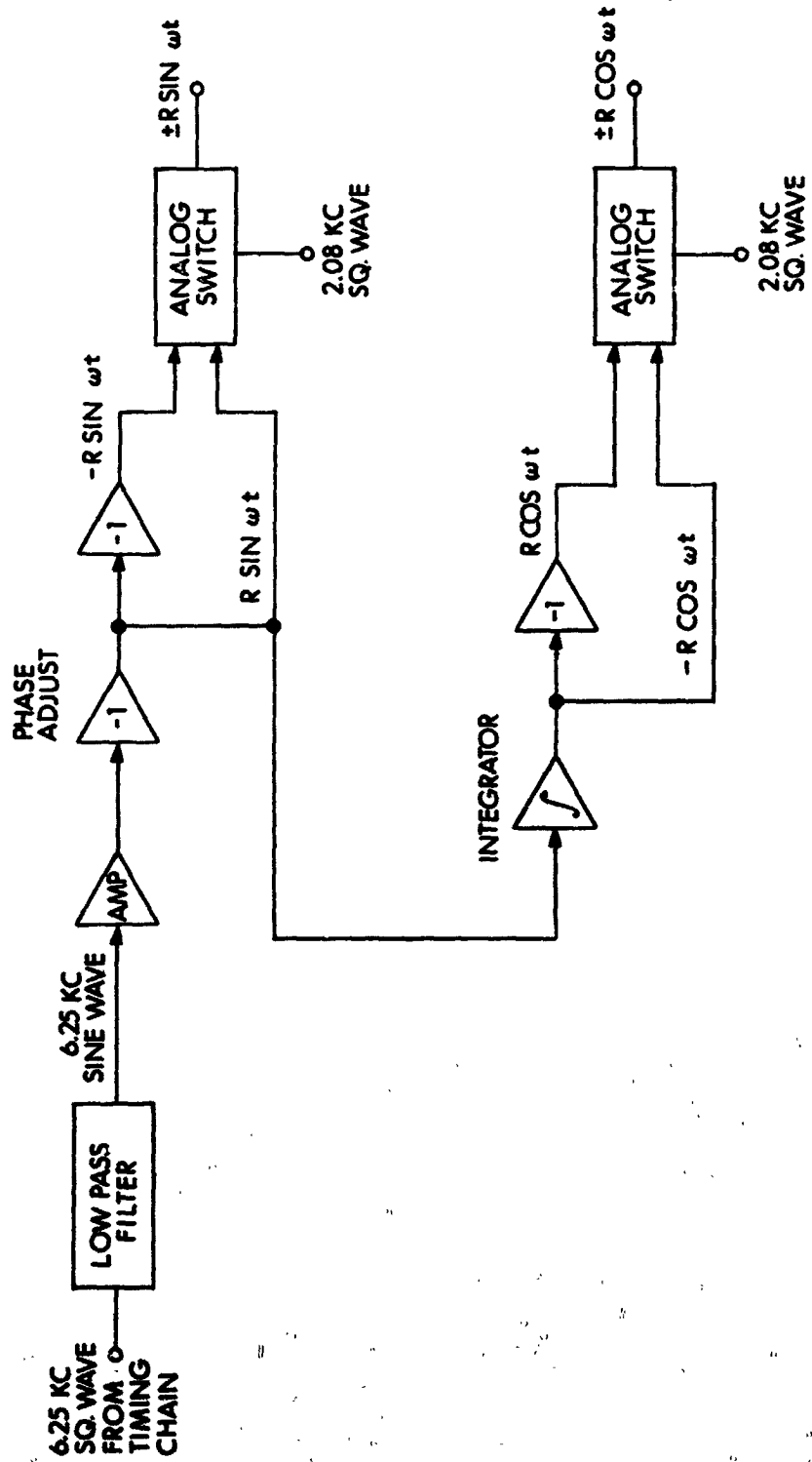
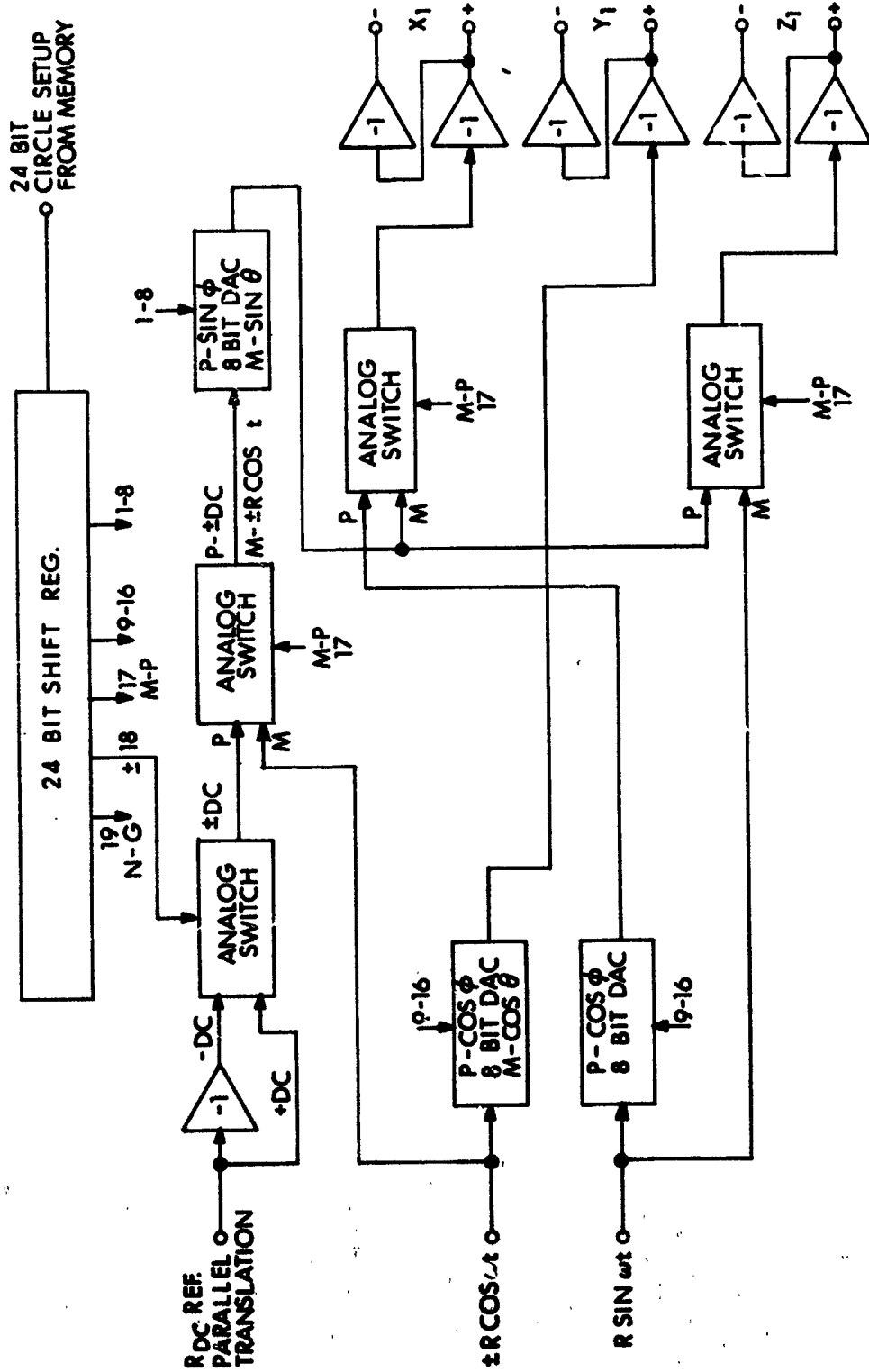**Fig. B-12** 6.25 KC Filter and ± R Sin ωt and ± R Cos ωt Amplifier 2nd Switching.

Fig. B-13   24 Bit Shift Register and Meridan - Parallel Rotation Transformation.
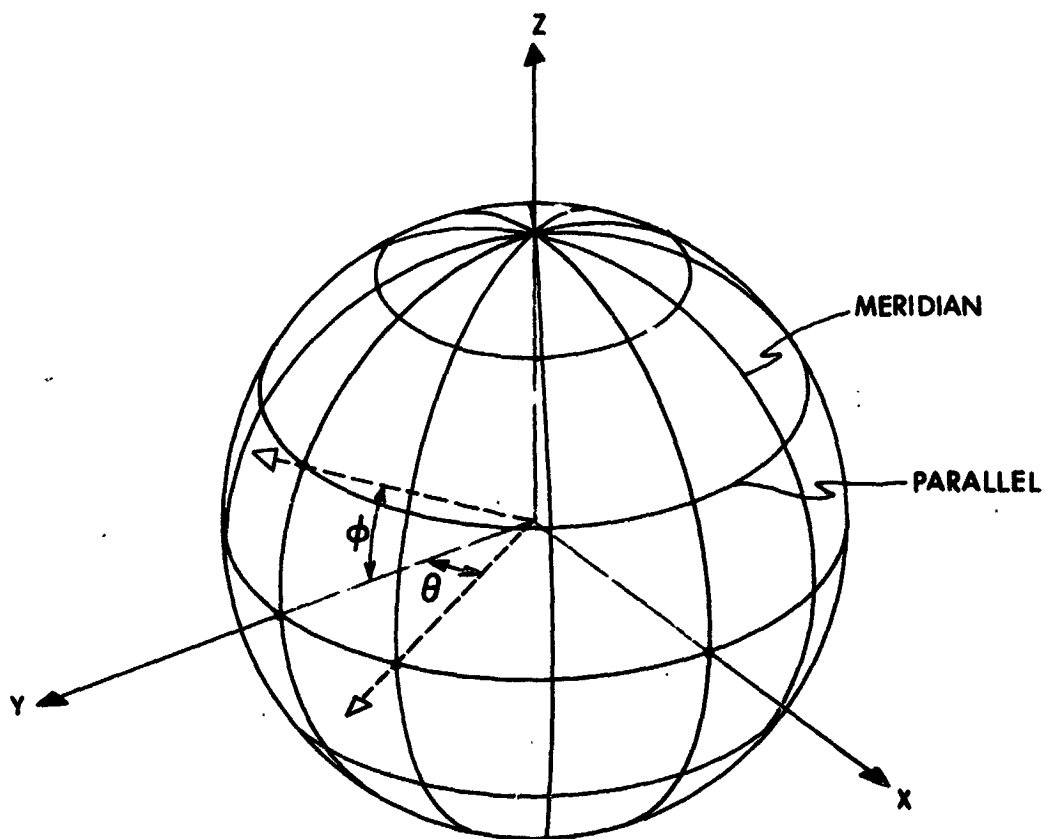
Fig. B-14 Ball Representation.

The plus and minus functions are needed alternately because a circle is complete every 1.5 cycles of the 6.25 KC signal. This allows the same phase of voltage to be used to write each circle and insures that the trace of each circle will rotate in the same direction from the starting point on the CRT. Therefore, the memory format is the same for all the ball circles.

The 24-bit shift register and meridian-parallel rotation transformation permits each ball circle to be generated in the form of three voltages X_1, Y_1, and Z_1. These voltages are proportional to the X, Y, and Z three dimensional components of the circle on the ball. (Figures B-13 and B-14) These functions are as follows:

Parallel Transformation Expressions

$$X_1 = \pm R \sin \omega t (\cos \phi)$$

$$Y_1 = \pm R \cos \omega t (\cos \phi)$$

$$Z_1 = \pm R_{DC} (\sin \phi)$$

Meridian Transformation Expressions

$$X_1 = \pm R \cos \omega t (\sin \theta)$$

$$Y_1 = \pm R \cos \omega t (\cos \theta)$$

$$Z_1 = \pm R \sin \omega t$$

This generates the ball in the fixed orientation shown.

The inputs to the meridian-parallel rotation transformation circuits are R_{DC}, $\pm R \sin \omega t$ and $\pm R \cos \omega t$. These signals are directed to amplifiers and to the 8-bit DAC's to generate the X_1, Y_1, and Z_1 outputs. These outputs described all the meridians and the parallel circles in three dimensions. The DAC's are set up before each circle is drawn by information transferred from memory. The 24-bit shift register received information from memory and sets the switches and DAC's to generate a meridian grid or number circle or a parallel grid or number circle. The 1-8 bits of the register are used to set the parallel - $\sin \phi$ or meridian - $\sin \theta$ scale factor DAC. The 9 - 16 bits are used to set two DAC's, the parallel - $\cos \phi$ or meridian - $\cos \theta$ scale factor and the parallel - $\cos \phi$ scale factor. The 17th bit sets the analog switches to the meridian or parallel position depending on the type of circle to be drawn. The 18th bit sets an analog switch for plus or minus translation of parallels along the z axis. The 19th bit is sent to the rate and timing control circuit to set up the pulse train for a grid or number circle as described previously. The 20 - 24 bits in the register are spares for future control bits if they are required. (Figure B-15)
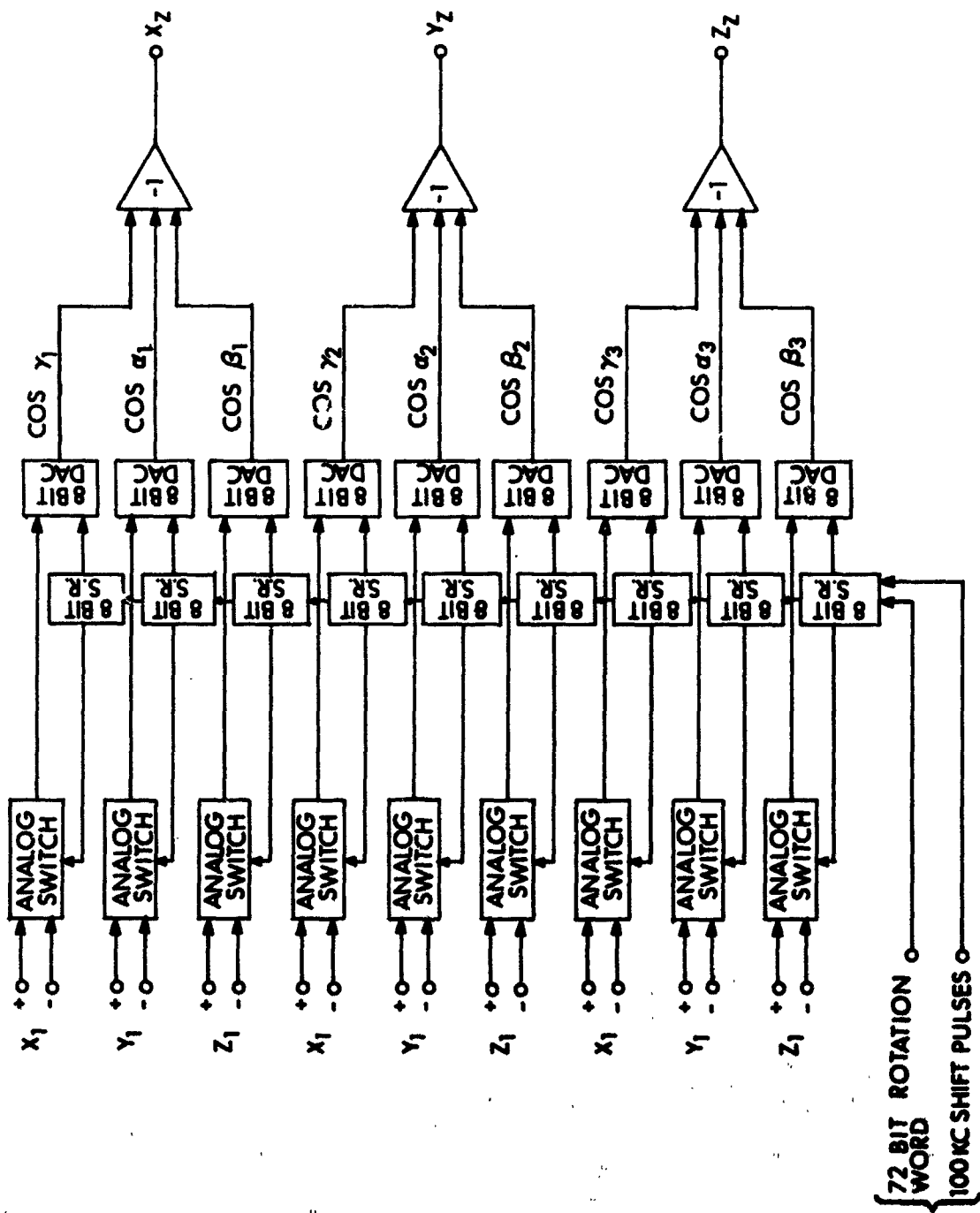
Fig. B-15 Ball Rotation Transformation

The output amplifiers provide $\pm X_1$, $\pm Y_1$, and $\pm Z_1$ which are required by the ball rotation circuits.

The ball rotation transformation circuits take the fixed ball picture generated by the ball sweep generation circuits and rotates it to any position in three dimensions upon command of the computer. This simulates the movements of the ball attitude indicator.

The functions performed by these circuits are as follows:
(Figure B-16)

$$X_2 = \cos \gamma_1 X_1 + \cos \alpha_1 Y_1 + \cos \beta_1 Z_1$$

$$Y_2 = \cos \gamma_2 X_1 + \cos \alpha_2 Y_1 + \cos \beta_2 Z_1$$

$$Z_2 = \cos \gamma_3 X_1 + \cos \alpha_3 Y_1 + \cos \beta_3 Z_1$$

where:

direction cosine	from axis	to axis
$\cos \gamma_1$	X_1	X_2
$\cos \alpha_1$	Y_1	X_2
$\cos \beta_1$	Z_1	X_2
$\cos \gamma_2$	X_1	Y_2
$\cos \alpha_2$	Y_1	Y_2
$\cos \beta_2$	Z_1	Y_2
$\cos \gamma_3$	X_1	Z_2
$\cos \alpha_3$	Y_1	Z_2
$\cos \beta_3$	Z_1	Z_2

The direction cosine information is obtained from the computer and shifted into a series of nine 8 bit shift registers. Each one of these registers contains a sign bit and 7 magnitude bits of the direction cosine. The sign bits control the analog switches which pass either plus or minus X_1, Y_1, and Z_1 components to the 8-bit DAC's The remaining 7 bits set up these DAC's. The outputs of these DAC's are summed appropriately to give X_2, Y_2, and Z_2 as shown in the equations. These outputs are then sent to the intensity, blanking and sweep control circuits.

B.5.2 Character Raster Generator

The character raster generator produces the staircase and triangular waveforms necessary for displaying alphabetical and numerical symbols
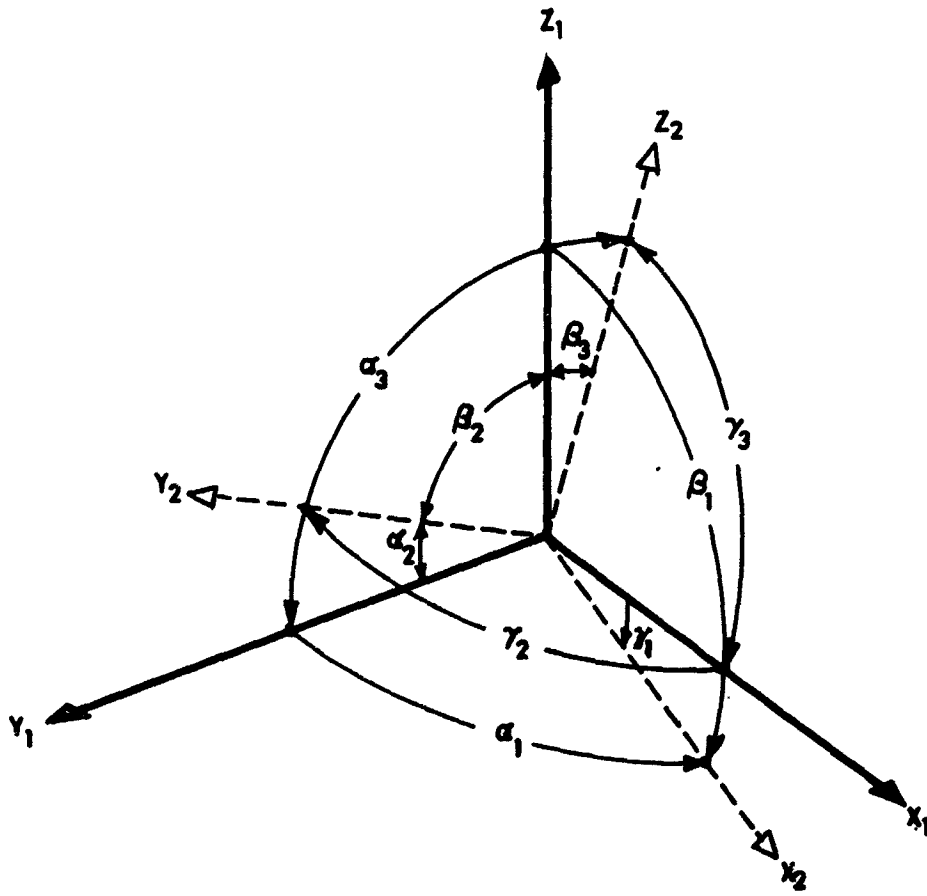
Fig. B-16   Ball Rotation Transformation
Direction Angles.

in any form desired. The inputs are pulses and square waves which are
converted into a horizontal staircase sweep, and a vertical staircase-tri-
angular wave sweep. (Figures B-17 and B-18)

The horizontal sweep is generated by pulsing an 8-bit counter with
pulses at a 112.5 KC rate which produces the character line space incre-
ments equal to a 1 count. The counter is driven with pulses at 18.75 KC
to give the character space increments equal to a 2 count. The counter is
reset by 625 cycle pulses which zero the counter at the end of every 30
character text line. If a straight raster is desired without character spaces,
the 18.75 KC pulses may be inhibited. This digital information is converted
to the staircase waveform in Figure B-18 by an 8-bit high speed DAC. The
output of the DAC is passed through a unity gain buffer amplifier before
being sent to the intensity, blanking, and sweep control circuits.

The vertical sweep is generated by pulsing a 4-bit counter with pulses
at 625 pps. This produces text line space increments equal to a count of 1.
The counter is reset by 39.1. The counter is reset by 39.1 cycle pulses which
zero the counter at the end of every 16 text lines or frame. This digital
information is converted to a staircase waveform by a 4-bit high-speed DAC.
A square wave at 56.25 KC is passed through an integrator to generate the
triangular wave character sweep. The triangular wave and staircase are
summed in a buffer amplifier to give the complete vertical sweep shown
in Figure B-18. If it is desired to eliminate the text line space to produce
a continuous vertical raster, the amplitude of the triangular wave may be
increased by gain adjustment in the buffer amplifier or the DAC DC ref-
erence voltage may be attenuated to accomplish this result. This output
is sent to the intensity, blanking, and sweep control circuits.

B. 6   Read Only Memory and Control

The read only memory provides the storage of all fixed information
such as the ball picture; numeric, alphabetic and symbolic characters;
and any other fixed pattern desired. The control section processes any in-
formation desired from memory in synchronization with other functions
in the display system. (Figure B-19)

The memory constructed has 16-bit words which are processed se-
quentially to give the setup information or blanking pattern desired. The
output of the 16-bit word counter drives the memory control circuits, which
perform the following functions:

Fig. B-17 Character Raster Generator.

V

6 CHARACTER LINES/CHARACTER

30 CHARACTERS/TEXT LINE

CHARACTER
SPACE

CHARACTER   CHARACTER LINE
WIDTH   SPACE

T

1
CHARACTER

1 TEXT LINE   END OF TEXT LINE

HORIZONTAL SWEEP

V

16 TEXT LINES/FRAME

TEXT LINE   CHARACTER
SPACE   HEIGHT

T

1 TEXT
LINE

1 FRAME   END OF FRAME

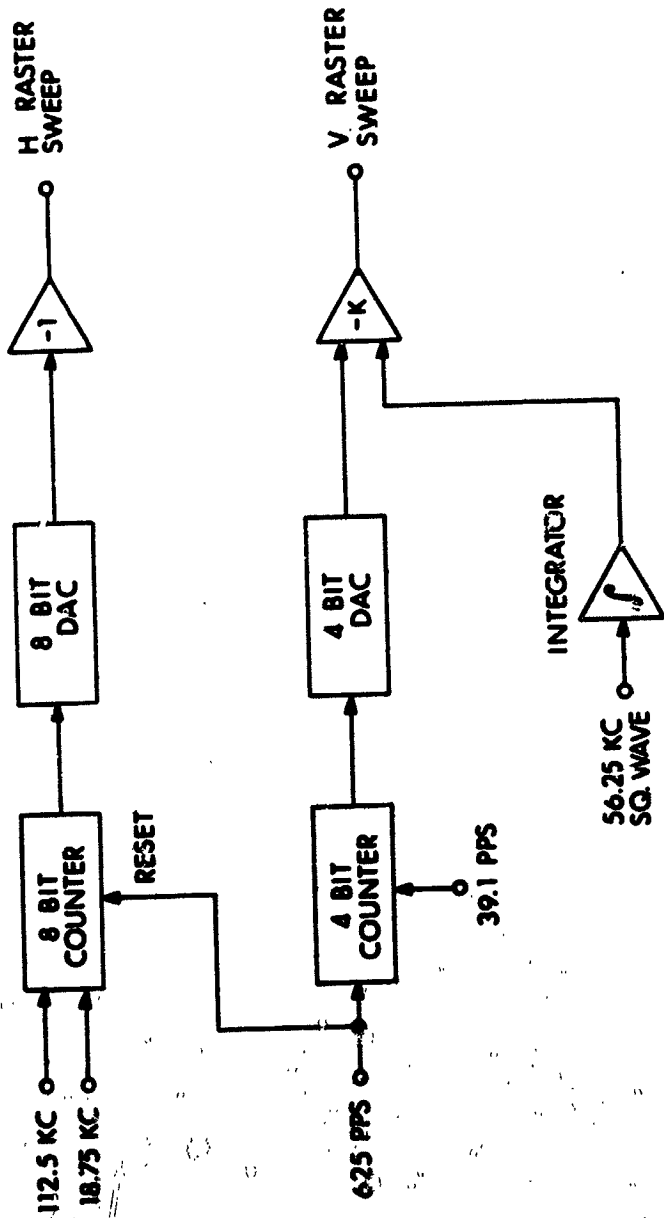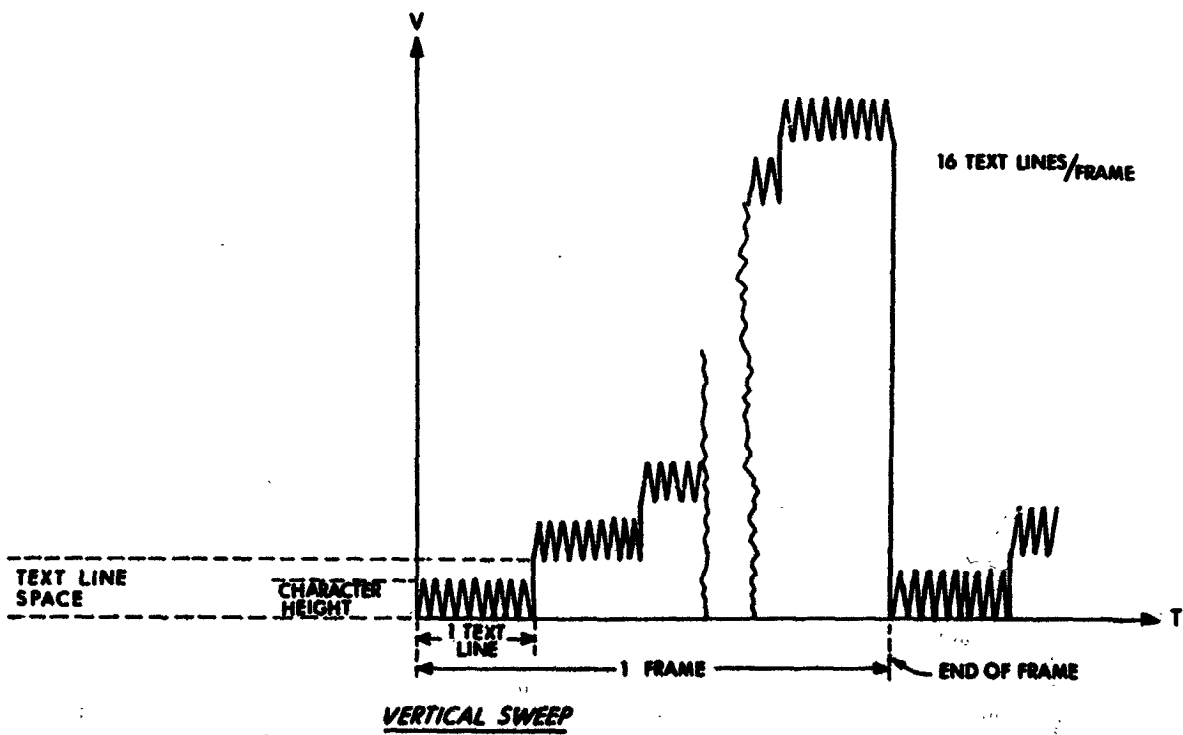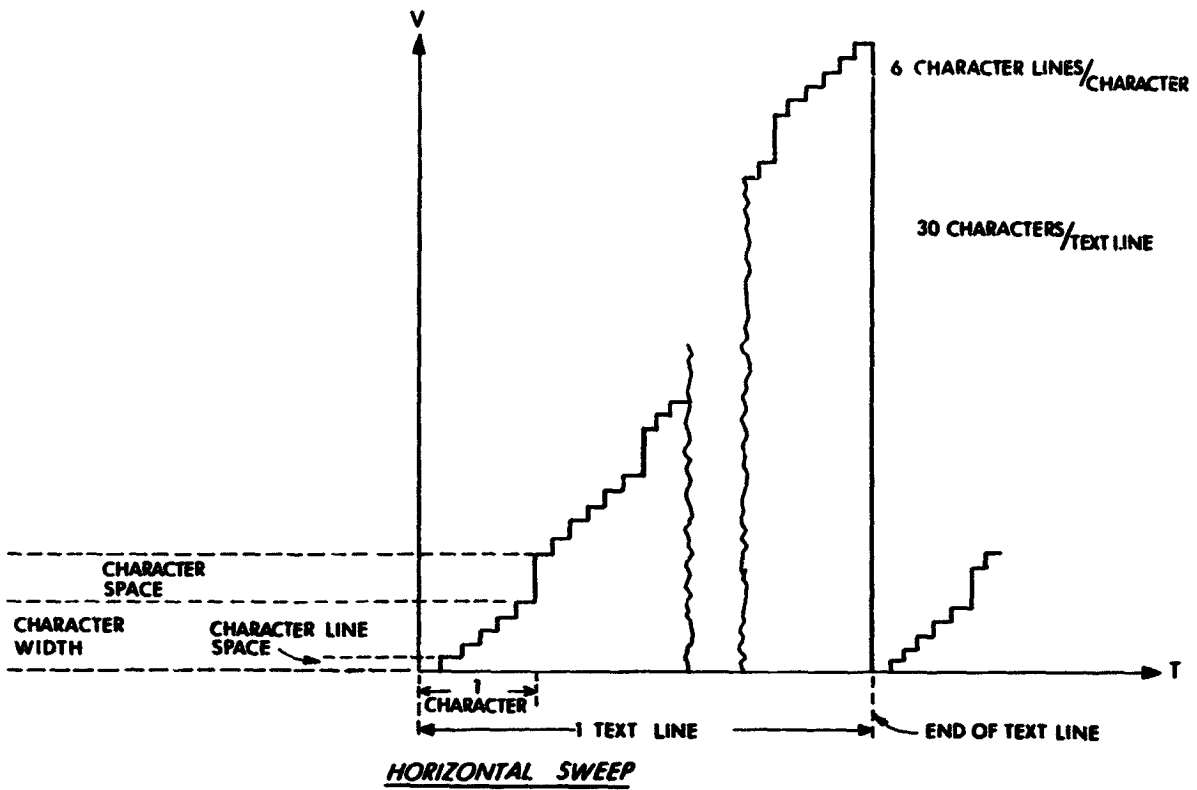*VERTICAL SWEEP*

Fig. B-18   Raster Sweeps.

1) Transfers the dual readout gates so that the next word may be read from memory;

2) Transfers the dual output register so that one register is ready for read-out information while the other is being shifted to the route control circuits;

3) Transfers the shift pulses from the rate and timing control circuits to the shift register transferring information to route control;

4) Advances the address control counter to the next desired word address;

5) Provides a read pulse to transfer the selected word to the second register set up to receive this information.

After each 16-bit word is processed, this memory control cycle is repeated. The addresses for the words to be processed from memory come from an erasable address memory. This memory is set up by the computer with the addresses of the presentation desired.

B.6.1 Route Control

The route control circuits steer the information from memory to the meridian-parallel shift register or to the blanking control circuits. In the ball mode the first 24 bits from memory are gated by gate signal A to the meridan-parallel shift register. This is the information used for set up purposes as described in the rate and timing control circuits. (Figures B-11 and B-20) The 72 bits for the grid circles or the 2.6 bits for the number circles are gated by gate signal C to the blanking control circuits. This gives the desired blanking pattern for the circle being drawn.

In the raster mode, all the bits from memory are gated continuously to the blanking control circuits.

B.6.2 Intensity, Blanking and Sweep Control

The functions of these circuits are to direct the ball and raster sweep voltages, the memory blanking signal, and the intensity modulation signal to the appropriate inputs of the oscilloscope. The ball-raster gating signal allows a selection of the ball picture or the character raster picture. (Figure B-21)

With the gating circuits in the ball mode, three analog switches allow the X_2, Y_2, and Z_2 ball signals from the ball rotation transformation circuits

B-28

BALL AND CONTROLLER ADDRESS FROM COMPUTER

ADDRESS ERASABLE MEMORY

ADDRESS CONTROL COUNTER

MEMORY DRIVE CIRCUITS

READ ONLY MEMORY

DUAL TRANSFER GATES

1 DUAL 16 BIT PARALLEL IN SERIAL OUT REGISTER

MEMORY OUTPUT TO ROUTE CONTROL

MEMORY CONTROL

OUTPUT FROM 16 BIT WORD COUNTER

SHIFT PULSES FROM TIMING AND RATE CONTROL LOGIC AND RASTER CONTROL LOGIC

Fig. B-19   Read Only Memory and Control.

MEMORY
OUTPUT

SHIFT REG
ROOTING

M-P ROTATION
SHIFT REG.

BALL
GATING

RASTER
GATING

BLANKING
ROOTING
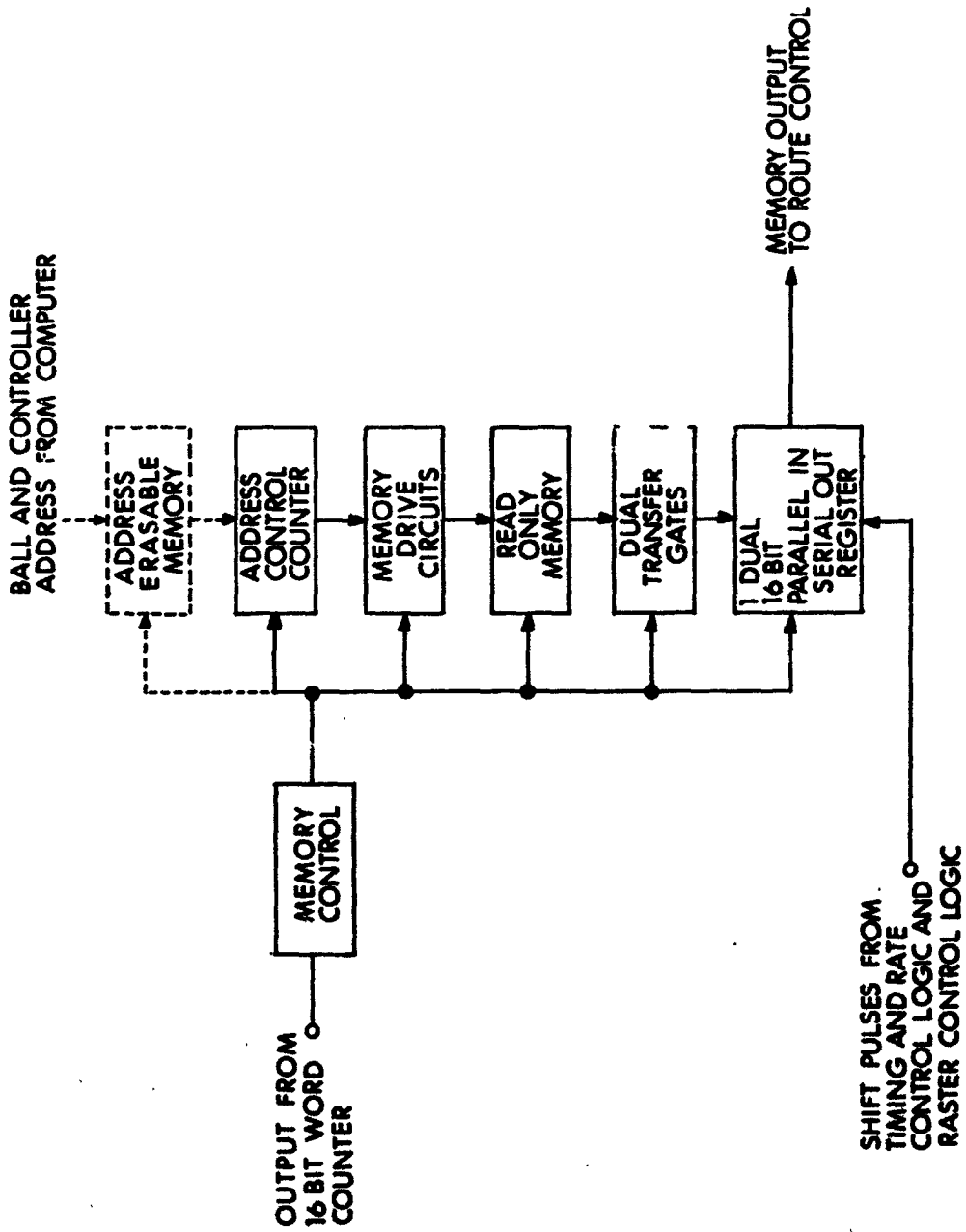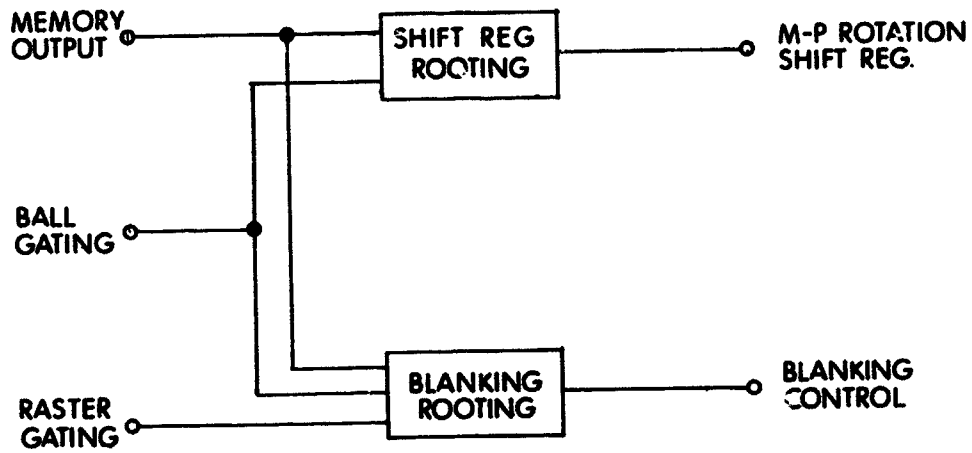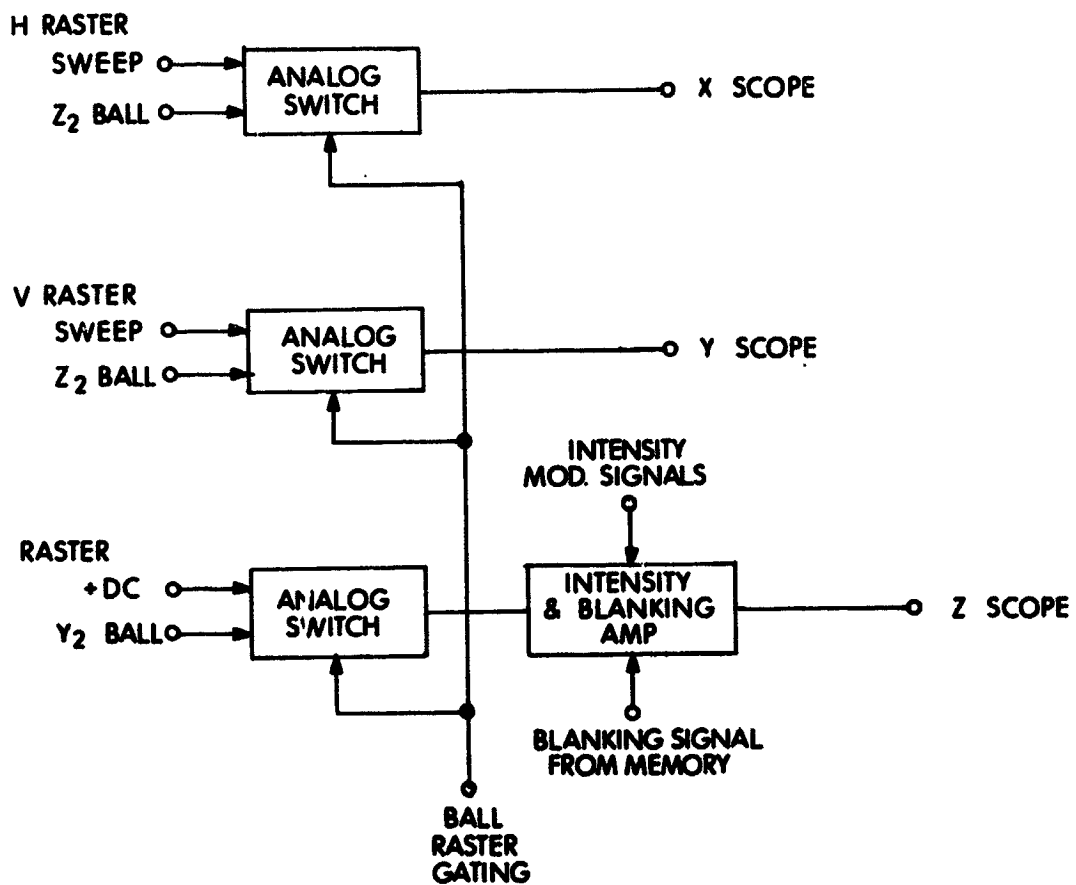
BLANKING
CONTROL

Fig. B-20 Route Control

Fig. B-21 Intensity Blanking and Sweep Control.

to be sent to the scope. The Z_2 ball signal drives the horizontal input and X_2 signal drives the vertical input of the scope. The Y_2 input drives a Schmitt trigger circuit used as a zero crossing detector. The square wave produced blanks the scope during all minus values of Y_2 and unblanks it during all positive values of Y_2. This prevents the undesired back face of the ball presentation from being displayed. The Schmitt trigger signal and the blanking pattern from memory are passed through an OR gate which allows blanking of the scope if either signal is in the blanking state. The blanking signal from the OR gate is then sent to a buffer amplifier where the intensity modulation signal is summed with the blanking signal. The output of this amplifier is sent to the Z axis of the scope.

With the gating circuits in the raster mode, the three analog switches allow the raster sweep signals to be sent to the scope. The horizontal raster sweep drives the horizontal input and the vertical raster sweep drives the vertical input of the scope. A positive DC voltage drives the Schmitt trigger circuit which produces a continuous unblanking signal to the OR gate. This allows the blanking signal from memory to be the single control of the blanking pattern. The blanking signal from the OR gate is summed with the intensity modulation signal, if it is desired, in the buffer amplifier. The output of the amplifier is sent to the Z axis of the scope.

B. 7 Progress, Conclusions and Recommendations

The development of the display system is in its final stages. The design and the evaluation of the circuits discussed are nearly complete. The ball rotation transformation circuits remain to be constructed on the plug-in cards being used for the system. The system interconnecting wiring and the rack assembly are the main construction work left to be completed.

The timing chain, rate and timing control logic, and raster control logic have been finalized and are functioning correctly. The ball sweep circuits have been completely evaluated with final plug-in card construction remaining to be done. The raster sweep circuits are in the final evaluation stage. The requirement of a very high speed DAC with an accuracy of better than 0.5% has required extensive development work. The latest configuration investigated appears to have the speed and accuracy desired. Further tests and evaluations are being made to verify that it will function properly. The memory system, route control circuits, and intensity, blanking, and sweep control circuits have been completely evaluated and constructed. The ball rotation transformation circuits have not been constructed at this time but the circuits are identical to those evaluated for the ball sweep circuits.

An oscilloscope and the Core Rope Simulator were obtained to be used in the initial as well as advanced phases of the study. The development of the CRT sweep circuits would replace the scope in future study phases. The Core Rope Simulator will be used as a large fixed memory element to replace the small memory being used presently.

Since the initial study phase has not been completed, any overall conclusions for the performance of this type of display system can not be presented here. But, some conclusions can be drawn from the evaluations already completed.

The development of the circuits described has shown that bipolar and MOS integrated circuits presently available can perform the functions desired. There are many circuits where MOS arrays are used which would require many times the volume if bipolar integrated circuits had to be used. With future development of these devices, further savings in space and weight can be accomplished.

With the development of these circuits, the feasibility of a CRT Display System which has the capability of presenting a wide variety of information is practically assured. With our circuit evaluations nearly completed, the performance in all cases indicates that the display system will meet the requirements and objectives originally stated.

The completion of the initial study phase of this program requires the construction of a few circuit boards and the assembly and wiring of the display rack. The information to be gained from this CRT Display System will be of great value in directing future development of similar types of displays. If an advanced study is initiated, the development of a memory to handle fixed as well as variable information and the computer control functions could be accomplished by the addition of the Core Rope Simulator and other equipment to the present display system.

Considering the investment already put into this study and the knowledge that will be gained by future investment, the recommendations are as follows:

1) The initial study phase of the CRT Display System be completed as soon as possible.

2) Based on the information gained from this study, an advanced study be considered for the development of a display system applicable to future spacecraft use.

VOL. I

REFERENCES

1.   North American Rockwell, Space Division Staff, Final Report,
        Contract NAS-8-18025, A Study of Manned Planetary Flyby Missions
        Based on Saturn/Apollo Systems, August 1967.

2.   The Boeing Company, Aerospace Group Staff, Phase 1 Briefing
        Report, Integrated Manned Interplanetary Spacecraft Concept
        Definition, 18 April 1967.

3.   Informal Data Exchange, W. Clarke Covington, ET23, NASA
        Manned Spacecraft Center, Houston, Texas, 24 August 1967.

4.   Battin, R. H., Astronautical Guidance, McGraw Hill Book
        Company, Inc., New York, 1964.

5.   Battin, R. H., "A New Approach to Lambert's Problem", to appear.

6.   Martin, F. H., "Closed Loop Near Optimal Steering for Class of
        Space Missions", MIT ScD Thesis, May 1965.

7.   Philliou, P. J., "Translunar Injection from Earth Parking Orbit",
        MIT Instrumentation Laboratory Guidance Performance Analysis
        Memo 504 #2-67, 10 January 1967.

8.   Kriegsman, B. A., "Radar-Updated Inertial Navigation of a Continu-
        ously Powered Space Vehicle", IEEE Aerospace Systems Conference,
        Seattle, Washington, July 1966.

9.   Battin, R. H., Class notes for Course 16.46, MIT Department of
        Aeronautics and Astronautics.

10.   Goodyear, W. H., "A General Method for the Computation of Cartesian Coordinates and Partial Derivatives of the Two-Body Problem", NASA CR-522, September 1966.

11.   Potter, J. E. and Fraser, D. C., "A Formula for Updating the Determinant of the Covariance Matrix", AIAA Journal, July 1967.

12.   Karthas, G., "Final List of Navigational Stars", MIT Instrumentation Laboratory, O&N Memo #45, November 1965.

13.   Bryson, A. E. and Johansen, D. E., "Linear Filtering for Time Varying Systems Using Measurements Containing Colored Noise", IEEE J. Automatic Control, January 1965.

14.   Bryson, A. E. and Henrikson, L. J., "Estimation Using Sampled Data Containing Sequentially Correlated Noise", AIAA Guidance, Control and Flight Dynamics Conference, Huntsville, Alabama, August 1967.

15.   Alonso, R. L., Hopkins, A. L., Jr., and Thaler, H. A., "A Multi-Processing Structure", MIT Instrumentation Laboratory Report E-2097, March 1967.

16.   Morth, R., "Reentry Guidance for Apollo", MIT Instrumentation Laboratory Report R-532, January 1966.
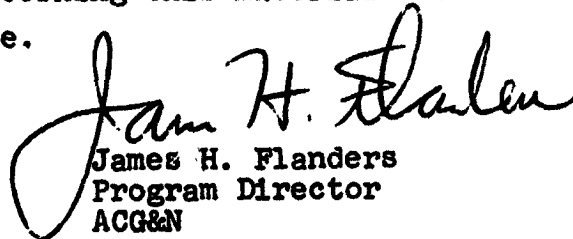
C. S. DRAPER
DIRECTOR

ASL 9-68

18 July 1968

TO: Distribution

FROM: James H. Flanders

SUBJECT: Supplement to R-600, Control Guidance and
           Navigation for Advanced Manned Missions,
           Volume I, Systems, (Ref. NAS-9-6823)

The enclosed material represents supplementary data
extracted from the basic study described on pages 1-16
thru 1-44 of the referenced volume. It is aimed at
indicating tradeoffs between fuel consumption and
guidance and navigation characteristics.

Comments or questions concerning this material should
be directed to this office.

                                James H. Flanders
                                Program Director
                                ACG&N

JHF/jdg
Distribution: Identical to R-600,
               Volume I

Encl: R-600, Control, Guidance, and   ))
       Navigation for Advanced Manned
       Missions (Final Report on Task II
       of Contract NAS 9-6823)
            Supplement I

R-600

CONTROL, GUIDANCE AND NAVIGATION FOR
ADVANCED MANNED MISSIONS

(Final Report on Task II of Contract NAS 9-6823)

Vol. I Systems

Supplement 1

INTRODUCTION

The purpose of this supplement is to provide more detailed information about fuel requirements for the interplanetary missions used as examples in MIT Instrumentation Laboratory Report R-600, Volume I. This information is provided here in three parts: 1) Tabular data for two missions, 2) Corresponding time lines of the velocity corrections, 3) Discussion and interpretation of the results. The two cases considered here are the first legs of the 1979 Mars flyby and 1977 triple-planet flyby missions mentioned in R-600. A brief description of the algorithm used to generate the data precedes the presentation of results.

THE VELOCITY CORRECTION ALGORITHM

As described in R-600, the guidance-navigation requirements study was an entirely statistical error analysis procedure. This also applies to the velocity-correction scheduling approach and the corresponding results - all data presented here should be interpreted as one-sigma values.

A simple, physically motivated approach was used to determine the timing and size of the velocity corrections - no attempt was made to optimize the results. These results should thus be interpreted as the approximate fuel requirements for making midcourse corrections on the interplanetary trips used as examples. The scheme consists of the following steps:

1. Divide the mission into an arbitrary number of decision points.

2. At each decision point calculate:
   a. The mean-squared value of the velocity correction which FTA guidance would dictate at this time.

   Call it $\overline{\Delta V^2}$ *

---

*A method for computing these quantities is given in Battin, R. H., Astronautical Guidance, McGraw Hill Book Co., New York 1964.

1

b. The variance of this estimate of $\overline{\Delta V^2}$: call it $(\sigma_V)^2$. This is a measure of our ability to determine the velocity correction based upon the available navigational information.

c. The mean-squared value of the error in implementing a velocity correction; call it $(\sigma_i)^2$. This is a measure of the uncertainty in implementing the velocity correction by thrusting.

3. Form the ratios:

$$\frac{(\sigma_V)^2}{(\Delta V)^2} = R_1$$

$$\frac{(\sigma_i)^2}{(\Delta V)^2} = R_2$$

4. If R_1 and R_2 are less than pre-specified values, a velocity correction of mean-squared value $\overline{\Delta V^2}$ is made. If either R_1 or R_2 are greater than these values, no correction is made at that particular decision point.

DISCUSSION OF RESULTS

Tables I through III and Figs. 1 through 3 give velocity-correction data for the first legs of the 1979 Mars flyby and 1977 triple-planet flyby used as examples in R-600. The following is a list of comments aimed at aiding in the interpretation of these results.

1. The runs were deliberately terminated shortly before arrival at the destination planet. Had these runs been terminated closer to the planet better accuracies could have been obtained. This, of course, was achieved in the subsequent hyperbolic flyby of the planet.

2. The perfect-sextant cases do not result in zero-error because sextant inaccuracy is only one source of navigational errors. The others, which remain even when a perfect sextant is assumed, are the various phenomena errors discussed in R-600.

3. The size of the FTA and VTA terminal errors are a function of the time of the last velocity correction. By making this velocity correction later, these errors could be reduced. Theoretically, the error could be reduced to the size of the final position-estimation uncertainty (which is also given). In practice, of course, this could require considerable amounts of fuel.

4. The algorithm for scheduling the velocity corrections outlined above seems to be a good one for selecting all but the final correction. Partial evidence of this is detectable in the accompanying data by examining the spread of values in the final correction compared to the others. The velocity required to cancel terminal-position errors increases extremely rapidly as the terminal point is approached. The selection scheme used here is not sensitive enough to carefully balance the fuel requirements against the terminal-position errors - a more optimal scheme is necessary in this region.

5. The initial velocity correction which consistently occurs at the same time is a result of the scheme making a correction to take out injection errors. At this point enough measurements have been made to determine the injection errors well enough to cancel them with a midcourse velocity correction. Note that the size of the first correction increases as the sextant becomes more accurate. This is because the better sextant provides a means of determining a more accurate extimate of the injection errors; hence, more of the error can be taken out by making a larger velocity correction.

6. Note that there is an approximate general trend toward a wider, more even spacing of the velocity corrections as the sextant accuracy degrades. This is a result of the fact that with the less accurate sextant it takes longer to obtain a good enough estimate of position and velocity errors to justify a velocity correction. An associated observation on the spacing of these corrections is the tendency for the impulses to bunch up at the two ends of the mission as the sextant becomes more accurate. In this case, when it doesn't take long to obtain an accurate estimate of the required correction, corrections group at the beginning to take out injection errors and at the end to cancel terminal errors. Little activity is required in-between to obtain these objectives.

7. Figure 1 and Table I show the results of a survey to determine the effect of the arbitrary ratios R_1 and R_2 on the velocity-correction schedule. Note that, as these ratios increase, the velocity corrections increase in frequency and total number. These are two reasons for this: 1) A less-accurate estimate of the velocity correction is required before one is scheduled - R_1 is larger, 2) A larger-percentage implementation inaccuracy is permitted - R_2 is larger.

If a straight edge is placed vertically on Fig. 1 any place but near the right end (see comment 4 above), it becomes clear that there is an approximate trend for the sum of the velocity corrections to increase at a given time as the ratios increase. The reason for this is that the relaxation of the accuracy demands as these ratios increase permits more of the early corrections to be wasted - making a velocity correction at the beginning with some uncertainty in it can lead to the necessity of having to cancel this uncertainty with another correction later when more information is available.

4

TABLE I

FIRST LEG OF 1979 MARS TWILIGHT FLYBY*
Fuel Consumption Table for Fig. 1

Vel. Corr. No.	Time (days)	Vel. Corr. (ft/sec)	Total ΔV (ft/sec)
R = .1			
1	0.4	18.4	18.4
2	45	5.2	23.6
3	71	2.6	26.2
4	108	2.5	28.7
5	139.5	68.6	97.5
FTA Error = 173.8 mi			
VTA Error = 164.7 mi			
Pos. Unc. = 111.3 mi			
R = .2			
1	0.4	18.4	18.4
2	38	4.4	22.8
3	56	2.5	25.3
4	77	1.8	27.1
5	103	1.8	28.9
6	129	3.4	32.6
FTA Error = 307.8 mi			
VTA Error = 288.6 mi			
Pos. Unc. = 111.3 mi			
R = .4			
1	0.4	18.4	18.4
2	30	3.5	21.9
3	45	2.6	24.5
4	56	1.8	26.3
5	68	1.4	27.7
6	81	1.2	28.9
7	95	1.3	30.2
8	107	1.2	31.4
9	120	1.5	32.9
10	138	10.8	43.7
FTA Error = 217.9 mi			
VTA Error = 207.6 mi			

*140-Day Leg; Run Stopped 168,000 mi from Mars.

TABLE II
FIRST LEG OF 1979 MARS TWILIGHT FLYBY*
Fuel Consumption Table for Fig. 2

Vel. Corr. No. Perfect Sextant	Time (days)	Vel. Corr. (ft/sec)	Total ΔV (ft/sec)
1	0.4	18.5	18.5
2	1.1	2.4	20.9
3	36	1.8	22.7
4	92	1.8	24.5
5	119	1.8	26.3
6	131	1.8	28.1
7	136	1.8	29.9
8	133.3	1.8	31.7
9	139.3	1.8	33.6
10	139.7	1.8	35.9

FTA Error = 3.9 mi; VTA Error = 3.2 mi; and Pos. Unc. = .48 mi.

1-Arc-sec Sextant			
1	0.4	18.5	18.5
2	3	2.4	20.9
3	34	1.8	22.7
4	64	1.8	24.5
5	103	1.8	26.3
6	123	1.8	28.1
7	133	2.0	30.4

FTA Error = 127.2 mi; VTA Error = 113.1 mi; and Pos. Unc. = 52.3 mi.

3-Arc-sec Sextant			
1	0.4	18.4	18.4
2	38	4.4	22.8
3	56	2.5	25.3
4	77	1.8	27.1
5	103	1.8	28.9
6	129	3.4	32.6

FTA Error = 307.8 mi; VTA Error = 288.6 mi; and Pos. Unc. = 111.3 mi.

10-Arc-sec Sextant			
1	0.4	18.0	18.0
2	50	9.3	27.3
3	74	5.8	33.1
4	109	5.6	38.7
5	139.6	191.6	230.6

FTA Error = 516.8 mi; VTA Error = 489.9 mi; and Pos. Unc. = 325.6 mi.

*140-Day Leg; Run stopped at 168,000 mi from Mars.

TABLE III
FIRST LEG OF 1977 TRIPLE PLANET FLYBY*
Fuel Consumption Table for Fig. 3

Vel. Corr. No. Perfect Sextant	Time (days)	Vel. Corr. (ft/sec)	Total ΔV (ft/sec)
1	0.4	18.4	18.4
2	1.2	2.7	21.1
3	28	1.8	22.9
4	69	1.8	24.7
5	94	1.8	26.5
6	106	2.0	28.5
7	111	2.1	30.6
8	112.7	1.8	32.4
9	113.5	2.0	34.8

FTA Error = 6.6 mi; VTA Error = 5.3 mi; and Pos. Unc. = .53 mi.

1-Arc-sec Sextant			
1	0.4	18.3	18.3
2	6	2.8	21.1
3	25	1.8	22.9
4	66	1.8	24.7
5	92	1.8	26.5
6	105	1.9	28.4
7	110	1.8	30.2
8	112.2	1.8	32.0
9	113.5	1.8	34.2

FTA Error = 12.3 mi; VTA Error = 10 mi; and Pos. Unc. = 6.1 mi.

3-Arc-sec Sextant			
1	0.4	17.9	17.9
2	10	4.2	22.1
3	18	2.0	24.1
4	43	1.8	25.9
5	75	1.8	27.7
6	96	1.9	29.6
7	106	1.8	31.4
8	111	2.2	33.6
9	112.5	1.8	35.8

FTA Error = 27.6 mi; VTA Error = 22.3 mi; and Pos. Unc. = 16.0 mi.

10-Arc-sec Sextant			
1	0.4	17.4	17.3
2	17	7.5	24.9
3	29	3.6	28.5
4	50	2.5	31.0
5	74	2.2	33.2
6	91	2.1	35.3
7	103	2.3	37.6
8	112	6.5	44.4

FTA Error = 90.8 mi; VTA Error = 68.3 mi; and Pos. Unc. = 48.4 mi.

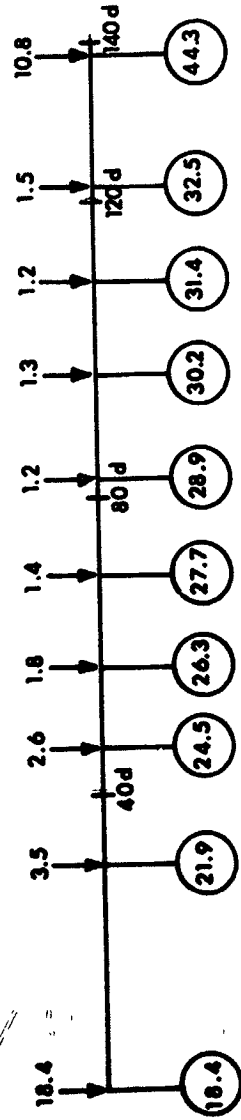*114-Day Leg, Earth-Venus; Run stopped 105,000 mi from Venus.

Uncircled Numbers Above Line are Individual Velocity Corrections (ft/sec)

Circled Numbers Below Line are Sums of Velocity Corrections to the Point Marked (ft/sec)
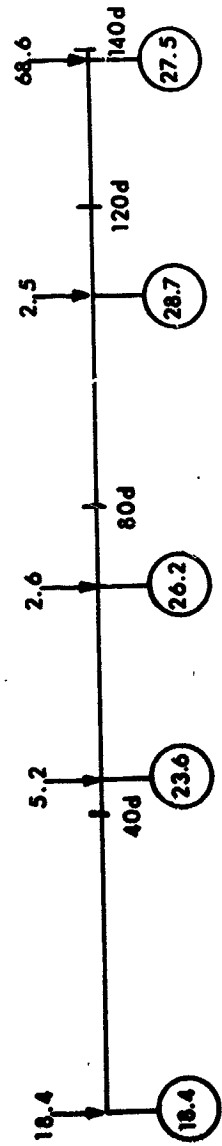
$R_1 = R_2 = 0.1$

FTA Error = 173.8 mi
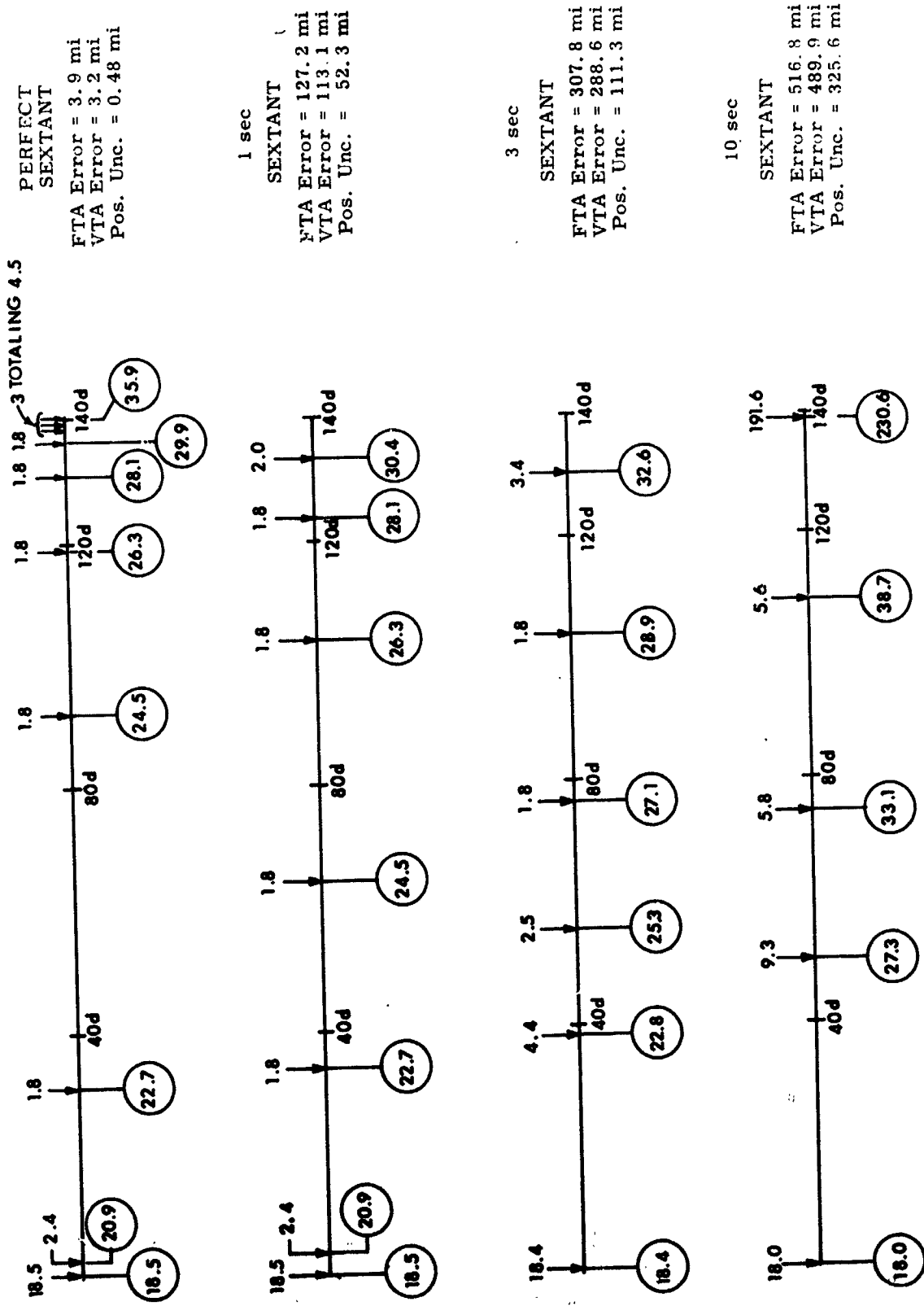VTA Error = 164.7 mi
Pos. Unc. = 111.3 mi
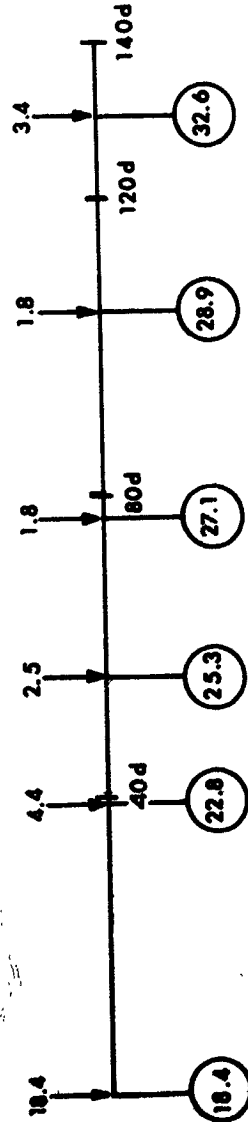
$R_1 = R_2 = 0.2$

FTA Error = 307.8 mi
VTA Error = 288.6 mi
Pos. Unc. = 111.3 mi

$R_1 = R_2 = 0.4$

FTA Error = 217.9 mi
VTA Error = 207.6 mi
Pos. Unc. = 111.3 mi

Fig. 1 First Leg of 1979 Mars Flyby

Uncircled Numbers Above Line are Individual Velocity Corrections (ft/sec)
Circled Numbers Below Line are Sums of Velocity Corrections to the Point Marked (ft/sec)

PERFECT
SEXTANT

FTA Error = 3.9 mi
VTA Error = 3.2 mi
Pos. Unc. = 0.48 mi

1 sec
SEXTANT

FTA Error = 127.2 mi
VTA Error = 113.1 mi
Pos. Unc. = 52.3 mi

3 sec
SEXTANT

FTA Error = 307.8 mi
VTA Error = 288.6 mi
Pos. Unc. = 111.3 mi

10 sec
SEXTANT

FTA Error = 516.8 mi
VTA Error = 489.9 mi
Pos. Unc. = 325.6 mi
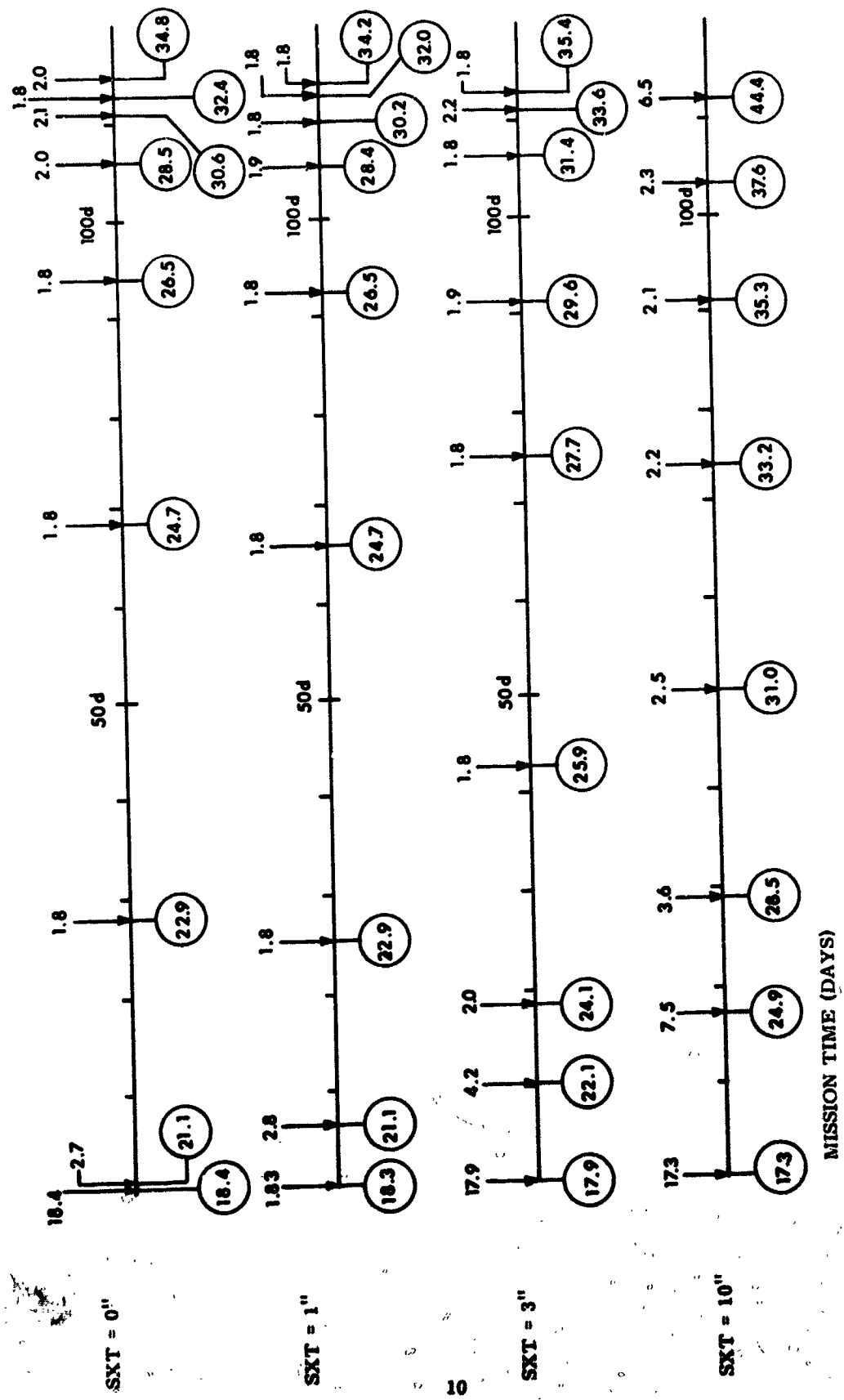
Fig. 2 First Leg of 1979 Mars Flyby

Fig. 3 Fuel Consumption Pattern for First Leg (Earth-Venus) of Triple-Planet Flyby